

650 AF

A TWO-DIMENSIONAL HYDRODYNAMIC MODEL USING A
FINITE-VOLUME APPROACH

By

JOAQUIM JOSÉ AREIAS CAPITÃO

A THESIS PRESENTED TO THE GRADUATE SCHOOL
OF THE UNIVERSITY OF FLORIDA IN
PARTIAL FULFILLMENT OF THE REQUIREMENTS
FOR THE DEGREE OF MASTER OF SCIENCE

UNIVERSITY OF FLORIDA

1989

ACKNOWLEDGEMENTS

I would like to express my gratitude to Dr. Peter Sheng, my advisor and committee chairman, for his guidance and support during the time I was studying at the University of Florida, and to Dr. Robert Dean and Dr. Max Sheppard for serving on my committee and for their comments about this work.

The support of all my fellow students and the several postdoctoral associates from whom I have learned so much during my stay in Gainesville was also deeply appreciated. Dr. Pei-Fang Wang was particularly helpful, not only for his effort in providing me all the elements I needed during this work but also for his unwavering support at the most difficult times. The help of Mr. Yuming Liu and Mr. Hyekeun Lee was also essential to the development of this work. I would also like to thank Mr. Subarna Malakar for his support when dealing with the strong-willed computers used in this work.

I must thank Dr. António Melo Baptista for all the great advice and timely encouragement I have received from him in the last seven and one-half years. His friendship is greatly appreciated.

I would also like to express my appreciation for the support from the Luso-American Educational Commission in Lisbon (administering the Fulbright Program in Portugal) and from the Institute of International Education (offices in New York, Atlanta and Houston) who, as agents of the Fulbright Program, promptly gave me all the support I needed before and during my stay in the United States.

My gratitude must also be extended to my employer in Portugal, Laboratório Nacional de Engenharia Civil, for allowing me to come to the United States for an academic program.

Last but not least, I would like to thank my family and friends in Portugal and in the United States for the support I received from them, without which none of this would have been possible.

TABLE OF CONTENTS

ACKNOWLEDGEMENTS	ii
LIST OF FIGURES	vi
ABSTRACT	vii
CHAPTERS	
1 INTRODUCTION	1
2 BRIEF REVIEW	4
3 THE NUMERICAL MODEL	7
3.1 Governing Equations	7
3.2 The Computational Grid	9
3.3 The Fractional Step Method	13
3.4 The Advection Step	15
3.5 The Diffusion Step	19
3.6 The Coriolis Step	25
3.7 The Propagation Step	26
3.8 The Boundary Conditions	37
3.9 Numerical Stability	38
4 APPLICATIONS	40
4.1 Comparison with Analytical Solution	40
4.2 Square Basin with Constant Slope	41
4.3 Square Basin with V-Shaped Bottom	53
4.4 Lake Okeechobee with Constant Wind	53
4.5 Lake Okeechobee with Sinusoidal Wind	75

5 CONCLUSIONS	79
BIBLIOGRAPHY	81
BIOGRAPHICAL SKETCH	83

LIST OF FIGURES

3.1	Physical domain vs. computational domain	9
3.2	Contravariant and covariant directions	10
3.3	Basic computational cell	13
4.1	Skewed grid for a square basin with uniform depth	42
4.2	Comparison with analytical solution	43
4.3	Skewed grid for a square basin with uniform bottom slope	44
4.4	Velocity results with constant slope - present model	45
4.5	Velocity results with constant slope - CH3D	46
4.6	Surface elevation with constant slope - present model	47
4.7	Surface elevation with constant slope - CH3D	48
4.8	Time series results at points A and B - present model	49
4.9	Time series results at points C and D - present model	50
4.10	Time series results at points A and B - CH3D	51
4.11	Time series results at points C and D - CH3D	52
4.12	Skewed grid for a square basin with V-shaped bottom	54
4.13	Velocity results with V-shaped bottom - present model	55
4.14	Velocity results with V-shaped bottom - CH3D	56
4.15	Surface elevation with V-shaped bottom - present model	57
4.16	Surface elevation with V-shaped bottom - CH3D	58
4.17	Time series results at points A and B - present model	59
4.18	Time series results at points C and D - present model	60

4.19	Time series results at points A and B - CH3D	61
4.20	Time series results at points C and D - CH3D	62
4.21	Curvilinear grid for Lake Okeechobee	63
4.22	Bottom contours for Lake Okeechobee	64
4.23	Velocity results for Lake Okeechobee - present model	65
4.24	Velocity results for Lake Okeechobee - CH3D	66
4.25	Surface elevation for Lake Okeechobee - present model	67
4.26	Surface elevation for Lake Okeechobee - CH3D	68
4.27	Time series results at points A and B - present model	69
4.28	Time series results at points C and D - present model	70
4.29	Time series results at points E and F - present model	71
4.30	Time series results at points A and B - CH3D	72
4.31	Time series results at points C and D - CH3D	73
4.32	Time series results at points E and F - CH3D	74
4.33	Long-term simulation results - points A and B	76
4.34	Long-term simulation results - points C and D	77
4.35	Long-term simulation results - points E and F	78

Abstract of Thesis Presented to the Graduate School
of the University of Florida in Partial Fulfillment of the
Requirements for the Degree of Master of Science

A TWO-DIMENSIONAL HYDRODYNAMIC MODEL USING A
FINITE-VOLUME APPROACH

By

JOAQUIM JOSÉ AREIAS CAPITÃO

December 1989

Chairman: Dr. Y. Peter Sheng
Major Department: Coastal and Oceanographic Engineering

A two-dimensional model of wind-driven circulation in a closed basin was developed using a finite-volume technique for generalized curvilinear grids and applying some of the recent developments in hydrodynamic modeling. The terms in the Navier-Stokes equations were treated separately according to the fractional step method and the propagation step, including the continuity equation and the pressure and stress terms in the momentum equations, was solved using a conjugate gradient method.

The model was then applied to a number of test cases to examine the feasibility of the approach used by comparing with results obtained with the two-dimensional version of the three-dimensional model CH3D. These included a square basin with constant slope and with a V-shaped bottom and Lake Okeechobee, in South Florida. To evaluate the long-term numerical stability of the model, a ten-day model simulation with varying wind was also run for Lake Okeechobee.

CHAPTER 1 INTRODUCTION

Water is as essential to any kind of human activity as the air we breathe. Ever since the first human settlements, their location has been dependent on the presence of water. Big cities have naturally developed around important rivers or lakes, or by the ocean, where water for drinking, irrigation and, since the industrial revolution, cooling of industrial plants, is easily accessible.

Unfortunately, water bodies have been considered as infinite sources of fresh water and, at the same time, infinite dump sites for urban, agricultural and industrial waste. Only in the last few years have we started to become aware of the limits to this source and the effect of using it as a dump site. Entire seas, like the Mediterranean, have reached dangerous levels of pollution. Rivers and lakes all over the world are so polluted, chemically and bacteriologically, that their water is totally unusable without previous expensive treatment.

All this has happened over a period of time and the human mind seems to be able to adapt to new conditions without fully realizing their implications. It took, therefore, well-publicized accidents like oil spills or garbage being washed ashore in popular beaches to make the general public aware of the seriousness of the problem. That public awareness has put pressure on the political establishment to find solutions and this has led to increased pressure on the scientific community to develop the knowledge of the physical, chemical and biological processes involved.

One of the basic subjects involved is the knowledge of hydrodynamic circulation in shallow water, where the problem is more pressing. The research in this field has traditionally used three different tools to reach the same objective, a better

knowledge of circulation patterns in any given area:

1. field measurements;
2. scale models; and
3. numerical models.

Field measurements are in a class by themselves and even the strongest supporters of scale or numerical models will accept the need for some amount of field data to support their modeling effort. The continuous development of new instrumentation and the increase in computer speed when processing the data has made field measurements an important part of any study concerned with the knowledge of circulation patterns in any shallow water area. However, field measurements are still expensive and must be used sparingly.

Huge scale models for whole estuaries were common in the past, and some are still being used. However, the cost of keeping and operating such a model has increased steadily, while, at the same time, the use of ever more powerful computers has made numerical models cheaper and cheaper. Therefore, scale models seem to be, at present, more adequate for studying specific physical processes, instead of general circulation patterns for vast areas.

The evolution of computers, in terms of speed and memory, has made numerical modeling relatively cheap. But numerical models are not without problems of their own. Although the Navier-Stokes equations are accepted as a good representation of the physics involved, for instantaneous, three-dimensional circulation, from a practical point of view they must be integrated over a finite period of time, giving rise to problems like turbulence closure.

This thesis presents a new numerical model of hydrodynamic circulation, using a finite volume technique to solve the two-dimensional, vertically integrated, Navier-

Stokes equations in a curvilinear grid, and using a fractional step method to solve the different terms in the equations separately.

Chapter 2 consists of a brief review of work done in the past on numerical modeling of hydrodynamics, mainly those models which, in some way, influenced the way the present model was developed.

In Chapter 3 the finite volume equations are derived from the two-dimensional vertically averaged Navier-Stokes equations.

In Chapter 4 a number of test cases are presented and Chapter 5 contains the conclusions of the present work and some ideas about possible future developments on the present numerical model.

CHAPTER 2 BRIEF REVIEW

A large number of numerical models of hydrodynamic circulation have been developed over the last few decades, and most of them use finite difference or finite element methods in the solution of the Navier-Stokes equations. The finite-element methods have traditionally been considered to have a better ability to deal with complex geometries, since they can use non-rectangular grid cells. The need for rectangular grid cells was, therefore, the main limitation of finite-difference methods like the one developed by Leendertse (1967), which, on the other hand, have always been much more intuitive in their development and, therefore, easier to modify.

Although the developers of finite difference models were not ready to move into finite element modeling, they would recognize the limitations associated with their own technique, which was a first step into overcoming those limitations. One approach was the coupling of models using a sparse grid far from the boundary and a much denser grid near the boundary, as in Sheng (1976). Another possible approach utilizes the grid generation techniques presented in Thompson et al. (1985) to resolve the physical domain with a boundary-fitted curvilinear grid. Spaulding (1984) developed the equations of motion in generalized curvilinear coordinates, in terms of the cartesian components of the dependent variables (the velocity components), while Sheng (1986) derived the equations of motion in terms of the contravariant components of the dependent variables.

The approach used in this thesis is the same followed by Sheng (1986) and Sheng et al. (1988) which consists of transforming not only the independent variables but also the dependent variables and, therefore, working with equations in terms of

contravariant components of velocity.

Another problem associated with finite difference methods is the non-conservative nature of the discretized equations in curvilinear grids due to the use of differential equations. This problem is usually taken care of by treating the geometric terms more precisely. An alternative to this is to develop the numerical model equations starting with the integral equations instead of the differential equations. This is done in finite-volume techniques, and a comparison between the two approaches is presented by Vinokur (1986). A more detailed explanation of a model using a finite volume method is presented in Rosenfeld et al. (1988).

When numerical schemes are developed to solve complicated equations, special care must be taken to guarantee numerical stability and consistency. This usually involves an option between more elaborate numerical schemes and very small spatial and temporal resolutions. The fractional step method, presented in Yanenko (1971) is a convenient way to get around these limitations by breaking each time step into a series of intermediate steps, with a number of terms in the equations being solved at each time step. Each intermediate step can then be solved using the more convenient numerical scheme for the specific terms involved, and having only the limitations in terms of temporal and spatial resolution imposed by those terms. In this model, the fractional step method is used, breaking the Navier-Stokes equations into four separate equations, each one to be solved at a different intermediate step. In the advection step, only the non-linear terms in the momentum equations are used. The diffusion step solves for the horizontal turbulent diffusion terms and the Coriolis terms are solved in the Coriolis step. Finally, a propagation step solves the remaining terms in the momentum equations, pressure terms, wind stress and bottom friction, together with the continuity equation.

The propagation step was solved using a conjugate gradient procedure detailed in Hauguel (1979) and used before, among others, in the cartesian grid, finite difference circulation model developed by Liu (1988).

CHAPTER 3
THE NUMERICAL MODEL

3.1 Governing Equations

The equations describing the two-dimensional, vertically-integrated flow in shallow water can be obtained from the three-dimensional Navier-Stokes equations, assuming a hydrostatic vertical pressure distribution and, in this case, a constant and uniform density. The turbulence closure problem was solved using a constant and uniform eddy viscosity coefficient, and the final two-dimensional equations are, in a cartesian coordinate system,

$$\frac{\partial \zeta}{\partial t} = -\frac{\partial U_C}{\partial x} - \frac{\partial V_C}{\partial y} \quad (3.1)$$

$$\begin{aligned} \frac{\partial U_C}{\partial t} = & -\frac{\partial}{\partial x} \left(\frac{U_C U_C}{H} \right) - \frac{\partial}{\partial y} \left(\frac{U_C V_C}{H} \right) + A_H \frac{\partial^2 U_C}{\partial x^2} + A_H \frac{\partial^2 U_C}{\partial y^2} \\ & + f V_C - g H \frac{\partial \zeta}{\partial x} + \frac{1}{\rho} (\tau_{wx} - \tau_{bx}) \end{aligned} \quad (3.2)$$

$$\begin{aligned} \frac{\partial V_C}{\partial t} = & -\frac{\partial}{\partial x} \left(\frac{U_C V_C}{H} \right) - \frac{\partial}{\partial y} \left(\frac{V_C V_C}{H} \right) + A_H \frac{\partial^2 V_C}{\partial x^2} + A_H \frac{\partial^2 V_C}{\partial y^2} \\ & - f U_C - g H \frac{\partial \zeta}{\partial y} + \frac{1}{\rho} (\tau_{wy} - \tau_{by}) \end{aligned} \quad (3.3)$$

where t is time, x and y are the cartesian spatial coordinates, $U_C(x, y, t)$ and $V_C(x, y, t)$ are the cartesian components of the vertically-integrated velocity in the x and y directions, $H(x, y, t)$ is the total water depth, A_H is the eddy viscosity coefficient, f is the Coriolis parameter, g is the acceleration of gravity, ρ is the

water density, $\tau_{wx}(x, y, t)$ and $\tau_{wy}(x, y, t)$ are the x and y components of the surface wind stress and $\tau_{bx}(x, y, t)$ and $\tau_{by}(x, y, t)$ are the x and y components of the bottom stress.

The bottom stress was modeled, as in Liu (1988) by

$$\tau_{bx} = \frac{\rho g U_C \sqrt{U_C^2 + V_C^2}}{C^2 H^2} \quad (3.4)$$

$$\tau_{by} = \frac{\rho g V_C \sqrt{U_C^2 + V_C^2}}{C^2 H^2} \quad (3.5)$$

where C is the Chézy bottom friction coefficient given, in the C.G.S. system ($cm^{1/2}/sec$) by

$$C = 8.21 \frac{R^{1/6}}{n} \quad (3.6)$$

and n is the Manning coefficient. The hydraulic radius, R is given by the ratio between the water cross-section and the wetted perimeter,

$$R = \frac{Hb}{2H + b} \quad (3.7)$$

In lakes and estuaries, the width of the basin is usually much larger than its depth, and the hydraulic radius is approximately equal to the depth H .

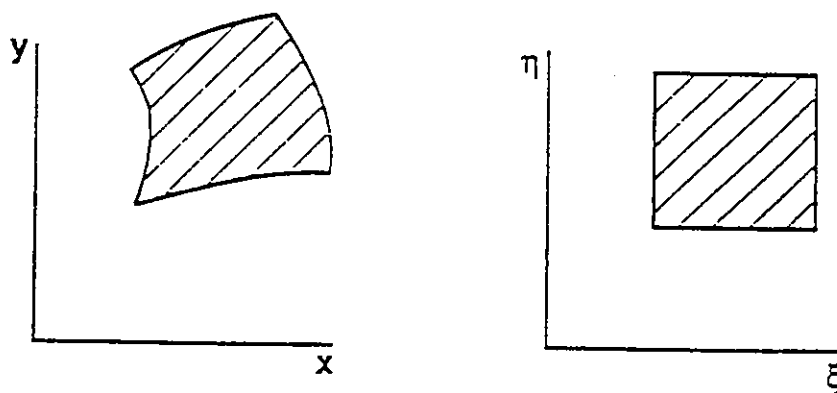


Figure 3.1: Physical domain vs. computational domain

3.2 The Computational Grid

Because of the extreme difficulty in generating an orthogonal curvilinear grid, the equations above have to be solved in a generic curvilinear grid, not necessarily orthogonal (figure 3.1). For that purpose, a different coordinate system, (ξ, η) is defined for the computational domain such that each curvilinear cell in the physical grid is mapped into a rectangular cell in the computational grid. For sake of simplicity, all sides of the computational cell have length $\Delta\xi = \Delta\eta = 1$.

Changing from the (x, y) cartesian coordinate system to the (ξ, η) curvilinear coordinate system involves defining a number of geometric quantities. First of all, we need to define contravariant and covariant directions (figure 3.2). A contravariant base vector is perpendicular to a line along which its coordinate remains unchanged. A covariant vector is tangent to a line along which only the other coordinate changes.

If the curvilinear grid is orthogonal, the two coordinate axis will be perpendicular to each other at every point and, therefore, the contravariant and covariant directions coincide, since a vector perpendicular to one of the coordinate axis is also tangent to the other coordinate axis.

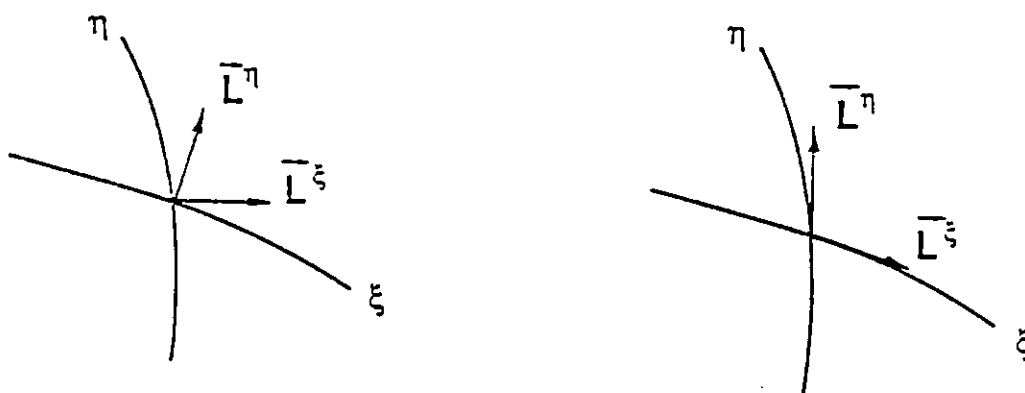


Figure 3.2: Contravariant and covariant directions

Contravariant length vectors can be defined at the center of each side of a cell, parallel to the contravariant base vectors defined above, with magnitude equal to the length of the side:

$$\vec{L}^\xi = y_\eta \vec{i} - x_\eta \vec{j} \quad (3.8)$$

$$\vec{L}^\eta = -y_\xi \vec{i} + x_\xi \vec{j} \quad (3.9)$$

where \vec{i} and \vec{j} are the base vectors in the cartesian coordinate system and the subscripts denote partial derivatives.

Since the equations will be written in terms of contravariant fluxes, these must be defined with relation to the cartesian vertically-integrated velocities used in equations 3.1 to 3.3. The contravariant flux components are obtained by performing the dot product of the contravariant length vectors and the vertically-integrated velocity vector $\vec{U} = U_C \vec{i} + V_C \vec{j}$:

$$U^\xi = y_\eta U_C - x_\eta V_C \quad (3.10)$$

$$U^\eta = -y_\xi U_C + x_\xi V_C \quad (3.11)$$

Following the procedure used by Rosenfeld et al. (1988) for their three-dimensional model, the velocity vector can also be written in terms of the covariant directions as

$$\vec{U} = \vec{L}_\xi U^\xi + \vec{L}_\eta U^\eta \quad (3.12)$$

$$\begin{aligned} u^\xi (\vec{L}^\xi - \vec{L}_\xi) + u^\eta (\vec{L}^\eta - \vec{L}_\eta) &= \vec{0} \\ \Rightarrow \vec{L}^\xi &= \vec{L}_\xi \quad \wedge \quad \vec{L}^\eta = \vec{L}_\eta \end{aligned}$$

To ensure the invariance of the velocity vector, the relationship between the contravariant length vectors \vec{L}^ξ and \vec{L}^η and the covariant "length" vectors \vec{L}_ξ and \vec{L}_η must be given by

$$\vec{L}^\xi \cdot \vec{L}_\xi = \vec{L}^\eta \cdot \vec{L}_\eta = 1 \quad (3.13)$$

$$\vec{L}^\xi \cdot \vec{L}_\eta = \vec{L}^\eta \cdot \vec{L}_\xi = 0 \quad (3.14)$$

which allows for the simple formulation used for the advection terms. Substituting equations 3.8 and 3.9 into equations 3.13 and 3.14 leads to

$$\vec{L}_\xi = \frac{x_\xi}{A} \vec{i} + \frac{y_\xi}{A} \vec{j} \quad (3.15)$$

$$\vec{L}_\eta = \frac{x_\eta}{A} \vec{i} + \frac{y_\eta}{A} \vec{j} \quad (3.16)$$

where A is the area of the cell surrounding the point where the vectors are defined, and also the Jacobian of the transformation, given by

$$A = x_\xi y_\eta - x_\eta y_\xi \quad (3.17)$$

To get the results in a more easily understandable form, the reverse conversion also needs to be done, from contravariant flux components to cartesian vertically-integrated velocity components, using the following relationships:

$$U_C = \frac{x_\xi}{A} U^\xi + \frac{x_\eta}{A} U^\eta \quad (3.18)$$

$$V_C = \frac{y_\xi}{A} U^\xi + \frac{y_\eta}{A} U^\eta \quad (3.19)$$

The basic computational cell is defined in figure 3.3. The computed surface elevation is an average value over the cell. In terms of physical representation, it is assumed to be the value at the center of the cell, and is denoted by (i, j) . The contravariant flux components are solved at the right face of the cell, $(i + \frac{1}{2}, j)$ for U^ξ and at the top face, $(i, j + \frac{1}{2})$ for U^η . Once again, when it comes to a physical representation, these flux components through the cell faces are converted into cartesian vertically-integrated velocity components at the center point of each face of the computational cell.

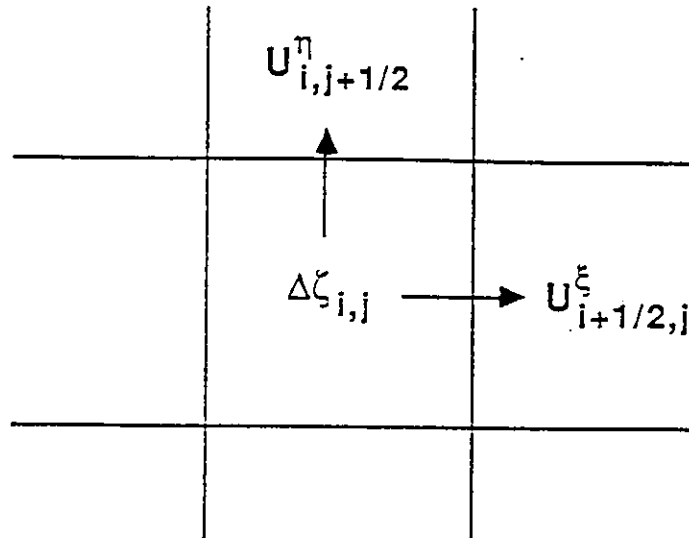


Figure 3.3: Basic computational cell

3.3 The Fractional Step Method

Following the procedure detailed in Yanenko (1971), the equations of motion (eqs. 3.1 to 3.3) were broken into a series of intermediate steps, for advection, diffusion, Coriolis and propagation. A formal consistency analysis for this approach has not yet been made for the full non-linear Navier-Stokes equations. However, it has been used successfully in a number of hydrodynamic models, like Liu (1988) or Benqué et al. (1982) and, depending on the validation of this particular model, is worth trying.

Denoting the intermediate results with one, two and three stars, after the advection step, the diffusion step and the Coriolis step, respectively, the equations for the advection step can be written as

$$\frac{U_C^* - U_C^n}{\Delta t} = -\frac{\partial}{\partial x} \left(\frac{U_C U_C}{H} \right) - \frac{\partial}{\partial y} \left(\frac{U_C V_C}{H} \right) \quad (3.20)$$

$$\frac{V_C^* - V_C^n}{\Delta t} = -\frac{\partial}{\partial x} \left(\frac{U_C V_C}{H} \right) - \frac{\partial}{\partial y} \left(\frac{V_C V_C}{H} \right) \quad (3.21)$$

For the diffusion step, only the diffusion terms are retained,

$$\frac{U_C^{**} - U_C^*}{\Delta t} = A_H \frac{\partial^2 U_C}{\partial x^2} + A_H \frac{\partial^2 U_C}{\partial y^2} \quad (3.22)$$

$$\frac{V_C^{**} - V_C^*}{\Delta t} = A_H \frac{\partial^2 V_C}{\partial x^2} + A_H \frac{\partial^2 V_C}{\partial y^2} \quad (3.23)$$

and the Coriolis step is

$$\frac{U_C^{***} - U_C^{**}}{\Delta t} = fV_C \quad (3.24)$$

$$\frac{V_C^{***} - V_C^{**}}{\Delta t} = -fU_C \quad (3.25)$$

The propagation step includes the continuity equation and the remaining terms in the momentum equations, pressure, wind stress and bottom friction terms:

$$\frac{\zeta^{n+1} - \zeta^n}{\Delta t} = -\frac{\partial U_C}{\partial x} - \frac{\partial V_C}{\partial y} \quad (3.26)$$

$$\frac{U_C^{n+1} - U_C^{***}}{\Delta t} = -gH \frac{\partial \zeta}{\partial x} + \tau_{wx} - \tau_{bx} \quad (3.27)$$

$$\frac{V_C^{n+1} - V_C^{***}}{\Delta t} = -gH \frac{\partial \zeta}{\partial y} + \tau_{wy} - \tau_{by} \quad (3.28)$$

The contravariant equations for each of these intermediate steps will be the object of each of the next four sections.

3.4 The Advection Step

The contravariant form of the equations for each of the intermediate steps will always be written in the form

$$A \frac{\Delta U^\xi}{\Delta t} = \vec{L}^\xi \cdot \vec{F} \quad (3.29)$$

$$A \frac{\Delta U^\eta}{\Delta t} = \vec{L}^\eta \cdot \vec{F} \quad (3.30)$$

where \vec{F} depends on the specific step being solved.

The advection terms in the momentum equations deal with the advection of the vertically-integrated velocity vector through a computational cell. Writing the vertically-integrated velocity vector as a function of the covariant "length" vectors, as in equation 3.12, \vec{F} is defined as

$$\vec{F} = \frac{\partial}{\partial \xi} \left(-\frac{U^\xi U^\xi}{H} \vec{L}_\xi - \frac{U^\xi U^\eta}{H} \vec{L}_\eta \right) + \frac{\partial}{\partial \eta} \left(-\frac{U^\xi U^\eta}{H} \vec{L}_\xi - \frac{U^\eta U^\eta}{H} \vec{L}_\eta \right) \quad (3.31)$$

Substituting \vec{F} in equations 3.29 and 3.30 we get the contravariant equations for the advection step

$$\begin{aligned} \frac{U^{\xi*} - U^{\xi n}}{\Delta t} &= -\frac{y_\eta}{A} \frac{\partial}{\partial \xi} \left(\frac{x_\xi U^\xi U^\xi}{A H} \right) - \frac{y_\eta}{A} \frac{\partial}{\partial \xi} \left(\frac{x_\eta U^\xi U^\eta}{A H} \right) \\ &\quad - \frac{y_\eta}{A} \frac{\partial}{\partial \eta} \left(\frac{x_\xi U^\xi U^\eta}{A H} \right) - \frac{y_\eta}{A} \frac{\partial}{\partial \eta} \left(\frac{x_\eta U^\eta U^\eta}{A H} \right) \\ &\quad + \frac{x_\eta}{A} \frac{\partial}{\partial \xi} \left(\frac{y_\xi U^\xi U^\xi}{A H} \right) + \frac{x_\eta}{A} \frac{\partial}{\partial \xi} \left(\frac{y_\eta U^\xi U^\eta}{A H} \right) \end{aligned}$$

$$+ \frac{x_\eta}{A} \frac{\partial}{\partial \eta} \left(\frac{y_\xi U^\xi U^\eta}{A H} \right) + \frac{x_\eta}{A} \frac{\partial}{\partial \eta} \left(\frac{y_\eta U^\eta U^\eta}{A H} \right) \quad (3.32)$$

$$\begin{aligned} \frac{U^{\eta^*} - U^{\eta^n}}{\Delta t} &= \frac{y_\xi}{A} \frac{\partial}{\partial \xi} \left(\frac{x_\xi U^\xi U^\xi}{A H} \right) + \frac{y_\xi}{A} \frac{\partial}{\partial \xi} \left(\frac{x_\eta U^\xi U^\eta}{A H} \right) \\ &+ \frac{y_\xi}{A} \frac{\partial}{\partial \eta} \left(\frac{x_\xi U^\xi U^\eta}{A H} \right) + \frac{y_\xi}{A} \frac{\partial}{\partial \eta} \left(\frac{x_\eta U^\eta U^\eta}{A H} \right) \\ &- \frac{x_\xi}{A} \frac{\partial}{\partial \xi} \left(\frac{y_\xi U^\xi U^\xi}{A H} \right) - \frac{x_\xi}{A} \frac{\partial}{\partial \xi} \left(\frac{y_\eta U^\xi U^\eta}{A H} \right) \\ &- \frac{x_\xi}{A} \frac{\partial}{\partial \eta} \left(\frac{y_\xi U^\xi U^\eta}{A H} \right) - \frac{x_\xi}{A} \frac{\partial}{\partial \eta} \left(\frac{y_\eta U^\eta U^\eta}{A H} \right) \end{aligned} \quad (3.33)$$

Since the ξ and η derivatives are totally separable, each of these equations can still be broken into a ξ -sweep equation and a η -sweep equation to be solved sequentially. If U^{ξ^*} and U^{η^*} denote the intermediate flux components after the ξ -sweep,

$$\begin{aligned} \frac{U^{\xi^*} - U^{\xi^n}}{\Delta t} &= -\frac{y_\eta}{A} \frac{\partial}{\partial \xi} \left(\frac{x_\xi U^\xi U^\xi}{A H} \right) - \frac{y_\eta}{A} \frac{\partial}{\partial \xi} \left(\frac{x_\eta U^\xi U^\eta}{A H} \right) \\ &+ \frac{x_\eta}{A} \frac{\partial}{\partial \xi} \left(\frac{y_\xi U^\xi U^\xi}{A H} \right) + \frac{x_\eta}{A} \frac{\partial}{\partial \xi} \left(\frac{y_\eta U^\xi U^\eta}{A H} \right) \end{aligned} \quad (3.34)$$

$$\begin{aligned} \frac{U^{\eta^*} - U^{\eta^n}}{\Delta t} &= \frac{y_\xi}{A} \frac{\partial}{\partial \xi} \left(\frac{x_\xi U^\xi U^\xi}{A H} \right) + \frac{y_\xi}{A} \frac{\partial}{\partial \xi} \left(\frac{x_\eta U^\xi U^\eta}{A H} \right) \\ &- \frac{x_\xi}{A} \frac{\partial}{\partial \xi} \left(\frac{y_\xi U^\xi U^\xi}{A H} \right) - \frac{x_\xi}{A} \frac{\partial}{\partial \xi} \left(\frac{y_\eta U^\xi U^\eta}{A H} \right) \end{aligned} \quad (3.35)$$

$$\begin{aligned} \frac{U^{\xi^*} - U^{\xi^*}}{\Delta t} &= -\frac{y_\eta}{A} \frac{\partial}{\partial \eta} \left(\frac{x_\xi U^\xi U^\eta}{A H} \right) - \frac{y_\eta}{A} \frac{\partial}{\partial \eta} \left(\frac{x_\eta U^\eta U^\eta}{A H} \right) \\ &+ \frac{x_\eta}{A} \frac{\partial}{\partial \eta} \left(\frac{y_\xi U^\xi U^\eta}{A H} \right) + \frac{x_\eta}{A} \frac{\partial}{\partial \eta} \left(\frac{y_\eta U^\eta U^\eta}{A H} \right) \end{aligned} \quad (3.36)$$

$$\begin{aligned} \frac{U^{\eta^*} - U^{\eta^*}}{\Delta t} &= \frac{y_\xi}{A} \frac{\partial}{\partial \eta} \left(\frac{x_\xi U^\xi U^\eta}{A H} \right) + \frac{y_\xi}{A} \frac{\partial}{\partial \eta} \left(\frac{x_\eta U^\eta U^\eta}{A H} \right) \\ &- \frac{x_\xi}{A} \frac{\partial}{\partial \eta} \left(\frac{y_\xi U^\xi U^\eta}{A H} \right) - \frac{x_\xi}{A} \frac{\partial}{\partial \eta} \left(\frac{y_\eta U^\eta U^\eta}{A H} \right) \end{aligned} \quad (3.37)$$

These four equations are solved explicitly, with the spatial derivatives being approximated by centered differences around the right side of each cell, where the U^ξ fluxes are computed, or around the top side of each cell, where the U^η fluxes are computed.

Denoting the center of a generic cell with the subscripts i and j , the right side face of the cell will be denoted by $i + \frac{1}{2}, j$ and the top side of the cell by $i, j + \frac{1}{2}$ (figure 3.3).

The discrete form of the ξ -sweep equations is therefore written as

$$\begin{aligned}
 U_{i+\frac{1}{2},j}^{\xi*} = & U_{i+\frac{1}{2},j}^{\xi^n} - \frac{y_{\eta_{i+\frac{1}{2},j}} \Delta t}{A_{i+\frac{1}{2},j}} \left(\frac{x_{\xi_{i+1,j}} U_{i+1,j}^{\xi^n} U_{i+1,j}^{\xi^n}}{A_{i+1,j} H_{i+1,j}^n} - \frac{x_{\xi_{i,j}} U_{i,j}^{\xi^n} U_{i,j}^{\xi^n}}{A_{i,j} H_{i,j}^n} \right) \\
 & - \frac{y_{\eta_{i+\frac{1}{2},j}} \Delta t}{A_{i+\frac{1}{2},j}} \left(\frac{x_{\eta_{i+1,j}} U_{i+1,j}^{\xi^n} U_{i+1,j}^{\eta^n}}{A_{i+1,j} H_{i+1,j}^n} - \frac{x_{\eta_{i,j}} U_{i,j}^{\xi^n} U_{i,j}^{\eta^n}}{A_{i,j} H_{i,j}^n} \right) \\
 & + \frac{x_{\eta_{i+\frac{1}{2},j}} \Delta t}{A_{i+\frac{1}{2},j}} \left(\frac{y_{\xi_{i+1,j}} U_{i+1,j}^{\xi^n} U_{i+1,j}^{\xi^n}}{A_{i+1,j} H_{i+1,j}^n} - \frac{y_{\xi_{i,j}} U_{i,j}^{\xi^n} U_{i,j}^{\xi^n}}{A_{i,j} H_{i,j}^n} \right) \\
 & + \frac{x_{\eta_{i+\frac{1}{2},j}} \Delta t}{A_{i+\frac{1}{2},j}} \left(\frac{y_{\eta_{i+1,j}} U_{i+1,j}^{\xi^n} U_{i+1,j}^{\eta^n}}{A_{i+1,j} H_{i+1,j}^n} - \frac{y_{\eta_{i,j}} U_{i,j}^{\xi^n} U_{i,j}^{\eta^n}}{A_{i,j} H_{i,j}^n} \right)
 \end{aligned} \tag{3.38}$$

$$\begin{aligned}
 U_{i,j+\frac{1}{2}}^{\eta*} = & U_{i,j+\frac{1}{2}}^{\eta^n} + \frac{y_{\xi_{i,j+\frac{1}{2}}} \Delta t}{A_{i,j+\frac{1}{2}}} \left(\frac{x_{\xi_{i+\frac{1}{2},j+\frac{1}{2}}} U_{i+\frac{1}{2},j+\frac{1}{2}}^{\xi^n} U_{i+\frac{1}{2},j+\frac{1}{2}}^{\xi^n}}{A_{i+\frac{1}{2},j+\frac{1}{2}} H_{i+\frac{1}{2},j+\frac{1}{2}}^n} \right. \\
 & \left. - \frac{x_{\xi_{i-\frac{1}{2},j+\frac{1}{2}}} U_{i-\frac{1}{2},j+\frac{1}{2}}^{\xi^n} U_{i-\frac{1}{2},j+\frac{1}{2}}^{\xi^n}}{A_{i-\frac{1}{2},j+\frac{1}{2}} H_{i-\frac{1}{2},j+\frac{1}{2}}^n} \right) \\
 & + \frac{y_{\xi_{i,j+\frac{1}{2}}} \Delta t}{A_{i,j+\frac{1}{2}}} \left(\frac{x_{\eta_{i+\frac{1}{2},j+\frac{1}{2}}} U_{i+\frac{1}{2},j+\frac{1}{2}}^{\xi^n} U_{i+\frac{1}{2},j+\frac{1}{2}}^{\eta^n}}{A_{i+\frac{1}{2},j+\frac{1}{2}} H_{i+\frac{1}{2},j+\frac{1}{2}}^n} \right. \\
 & \left. - \frac{x_{\eta_{i-\frac{1}{2},j+\frac{1}{2}}} U_{i-\frac{1}{2},j+\frac{1}{2}}^{\xi^n} U_{i-\frac{1}{2},j+\frac{1}{2}}^{\eta^n}}{A_{i-\frac{1}{2},j+\frac{1}{2}} H_{i-\frac{1}{2},j+\frac{1}{2}}^n} \right) \\
 & - \frac{x_{\xi_{i,j+\frac{1}{2}}} \Delta t}{A_{i,j+\frac{1}{2}}} \left(\frac{y_{\xi_{i+\frac{1}{2},j+\frac{1}{2}}} U_{i+\frac{1}{2},j+\frac{1}{2}}^{\xi^n} U_{i+\frac{1}{2},j+\frac{1}{2}}^{\xi^n}}{A_{i+\frac{1}{2},j+\frac{1}{2}} H_{i+\frac{1}{2},j+\frac{1}{2}}^n} \right.
 \end{aligned}$$

$$\begin{aligned}
& \frac{y_{\epsilon_{i-\frac{1}{2},j+\frac{1}{2}}} U_{i-\frac{1}{2},j+\frac{1}{2}}^{\epsilon^n} U_{i-\frac{1}{2},j+\frac{1}{2}}^{\epsilon^n}}{A_{i-\frac{1}{2},j+\frac{1}{2}} H_{i-\frac{1}{2},j+\frac{1}{2}}^n} \Bigg) \\
& - \frac{x_{\epsilon_{i,j+\frac{1}{2}}} \Delta t}{A_{i,j+\frac{1}{2}}} \left(\frac{y_{\eta_{i+\frac{1}{2},j+\frac{1}{2}}} U_{i+\frac{1}{2},j+\frac{1}{2}}^{\epsilon^n} U_{i+\frac{1}{2},j+\frac{1}{2}}^{\eta^n}}{A_{i+\frac{1}{2},j+\frac{1}{2}} H_{i+\frac{1}{2},j+\frac{1}{2}}^n} \right. \\
& \left. - \frac{y_{\eta_{i-\frac{1}{2},j+\frac{1}{2}}} U_{i-\frac{1}{2},j+\frac{1}{2}}^{\epsilon^n} U_{i-\frac{1}{2},j+\frac{1}{2}}^{\eta^n}}{A_{i-\frac{1}{2},j+\frac{1}{2}} H_{i-\frac{1}{2},j+\frac{1}{2}}^n} \right) \tag{3.39}
\end{aligned}$$

and the equations for the η -sweep become

$$\begin{aligned}
U_{i+\frac{1}{2},j}^{\epsilon^*} &= U_{i+\frac{1}{2},j}^{\epsilon^{\#}} - \frac{y_{\eta_{i+\frac{1}{2},j}} \Delta t}{A_{i+\frac{1}{2},j}} \left(\frac{x_{\epsilon_{i+\frac{1}{2},j+\frac{1}{2}}} U_{i+\frac{1}{2},j+\frac{1}{2}}^{\epsilon^{\#}} U_{i+\frac{1}{2},j+\frac{1}{2}}^{\eta^{\#}}}{A_{i+\frac{1}{2},j+\frac{1}{2}} H_{i+\frac{1}{2},j+\frac{1}{2}}^n} \right. \\
& \left. - \frac{x_{\epsilon_{i+\frac{1}{2},j-\frac{1}{2}}} U_{i+\frac{1}{2},j-\frac{1}{2}}^{\epsilon^{\#}} U_{i+\frac{1}{2},j-\frac{1}{2}}^{\eta^{\#}}}{A_{i+\frac{1}{2},j-\frac{1}{2}} H_{i+\frac{1}{2},j-\frac{1}{2}}^n} \right) \\
& - \frac{y_{\eta_{i+\frac{1}{2},j}} \Delta t}{A_{i+\frac{1}{2},j}} \left(\frac{x_{\eta_{i+\frac{1}{2},j+\frac{1}{2}}} U_{i+\frac{1}{2},j+\frac{1}{2}}^{\eta^{\#}} U_{i+\frac{1}{2},j+\frac{1}{2}}^{\eta^{\#}}}{A_{i+\frac{1}{2},j+\frac{1}{2}} H_{i+\frac{1}{2},j+\frac{1}{2}}^n} \right. \\
& \left. - \frac{x_{\eta_{i+\frac{1}{2},j-\frac{1}{2}}} U_{i+\frac{1}{2},j-\frac{1}{2}}^{\eta^{\#}} U_{i+\frac{1}{2},j-\frac{1}{2}}^{\eta^{\#}}}{A_{i+\frac{1}{2},j-\frac{1}{2}} H_{i+\frac{1}{2},j-\frac{1}{2}}^n} \right) \\
& + \frac{x_{\eta_{i+\frac{1}{2},j}} \Delta t}{A_{i+\frac{1}{2},j}} \left(\frac{y_{\epsilon_{i+\frac{1}{2},j+\frac{1}{2}}} U_{i+\frac{1}{2},j+\frac{1}{2}}^{\epsilon^{\#}} U_{i+\frac{1}{2},j+\frac{1}{2}}^{\eta^{\#}}}{A_{i+\frac{1}{2},j+\frac{1}{2}} H_{i+\frac{1}{2},j+\frac{1}{2}}^n} \right. \\
& \left. - \frac{y_{\epsilon_{i+\frac{1}{2},j-\frac{1}{2}}} U_{i+\frac{1}{2},j-\frac{1}{2}}^{\epsilon^{\#}} U_{i+\frac{1}{2},j-\frac{1}{2}}^{\eta^{\#}}}{A_{i+\frac{1}{2},j-\frac{1}{2}} H_{i+\frac{1}{2},j-\frac{1}{2}}^n} \right) \\
& + \frac{x_{\eta_{i+\frac{1}{2},j}} \Delta t}{A_{i+\frac{1}{2},j}} \left(\frac{y_{\epsilon_{i+\frac{1}{2},j+\frac{1}{2}}} U_{i+\frac{1}{2},j+\frac{1}{2}}^{\eta^{\#}} U_{i+\frac{1}{2},j+\frac{1}{2}}^{\eta^{\#}}}{A_{i+\frac{1}{2},j+\frac{1}{2}} H_{i+\frac{1}{2},j+\frac{1}{2}}^n} \right. \\
& \left. - \frac{y_{\epsilon_{i+\frac{1}{2},j-\frac{1}{2}}} U_{i+\frac{1}{2},j-\frac{1}{2}}^{\eta^{\#}} U_{i+\frac{1}{2},j-\frac{1}{2}}^{\eta^{\#}}}{A_{i+\frac{1}{2},j-\frac{1}{2}} H_{i+\frac{1}{2},j-\frac{1}{2}}^n} \right) \tag{3.40}
\end{aligned}$$

$$U_{i,j+\frac{1}{2}}^{\eta^*} = U_{i,j+\frac{1}{2}}^{\eta^{\#}} + \frac{y_{\epsilon_{i,j+\frac{1}{2}}} \Delta t}{A_{i,j+\frac{1}{2}}} \left(\frac{x_{\epsilon_{i,j+1}} U_{i,j+1}^{\epsilon^{\#}} U_{i,j+1}^{\eta^{\#}}}{A_{i,j+1} H_{i,j+1}^n} - \frac{x_{\epsilon_{i,j}} U_{i,j}^{\epsilon^{\#}} U_{i,j}^{\eta^{\#}}}{A_{i,j} H_{i,j}^n} \right)$$

$$\begin{aligned}
& + \frac{y_{\xi_{i,j+\frac{1}{2}}}\Delta t}{A_{i,j+\frac{1}{2}}} \left(\frac{x_{\eta_{i,j+1}} U_{i,j+1}^{\eta\#} U_{i,j+1}^{\eta\#}}{A_{i,j+1} H_{i,j+1}^n} - \frac{x_{\eta_{i,j}} U_{i,j}^{\eta\#} U_{i,j}^{\eta\#}}{A_{i,j} H_{i,j}^n} \right) \\
& - \frac{x_{\xi_{i,j+\frac{1}{2}}}\Delta t}{A_{i,j+\frac{1}{2}}} \left(\frac{y_{\xi_{i,j+1}} U_{i,j+1}^{\xi\#} U_{i,j+1}^{\eta\#}}{A_{i,j+1} H_{i,j+1}^n} - \frac{y_{\xi_{i,j}} U_{i,j}^{\xi\#} U_{i,j}^{\eta\#}}{A_{i,j} H_{i,j}^n} \right) \\
& - \frac{x_{\xi_{i,j+\frac{1}{2}}}\Delta t}{A_{i,j+\frac{1}{2}}} \left(\frac{y_{\xi_{i,j+1}} U_{i,j+1}^{\eta\#} U_{i,j+1}^{\eta\#}}{A_{i,j+1} H_{i,j+1}^n} - \frac{y_{\xi_{i,j}} U_{i,j}^{\eta\#} U_{i,j}^{\eta\#}}{A_{i,j} H_{i,j}^n} \right)
\end{aligned} \tag{3.41}$$

Since the U^ξ and U^η equations are solved at different positions, interpolated values of each component must be computed at the position where the other component is solved. These interpolations, like all those made in the other intermediate steps, are made by four-point averaging.

$$U_{i,j+\frac{1}{2}}^\xi = \frac{U_{i+\frac{1}{2},j}^\xi + U_{i+\frac{1}{2},j+1}^\xi + U_{i-\frac{1}{2},j+1}^\xi + U_{i-\frac{1}{2},j}^\xi}{4} \tag{3.42}$$

$$U_{i+\frac{1}{2},j}^\eta = \frac{U_{i,j+\frac{1}{2}}^\eta + U_{i,j-\frac{1}{2}}^\eta + U_{i+1,j-\frac{1}{2}}^\eta + U_{i+1,j+\frac{1}{2}}^\eta}{4} \tag{3.43}$$

3.5 The Diffusion Step

In the diffusion step, the turbulence closure problem is solved assuming a constant and uniform horizontal eddy viscosity. This makes it possible to take the eddy viscosity out of the derivatives leading to a simple definition of the \vec{F} vector in equations 3.29 and 3.30:

$$\vec{F} = A_H \nabla^2 \vec{U} \tag{3.44}$$

In the contravariant coordinate system, the Laplacian of the vertically-integrated velocity vector can be written as

$$\begin{aligned}
 \nabla^2 \vec{U} = & \frac{1}{A} \frac{\partial}{\partial \xi} \left\{ \frac{y_\eta}{A} \left[\frac{\partial}{\partial \xi} (y_\eta \vec{U}) - \frac{\partial}{\partial \eta} (y_\xi \vec{U}) \right] \right. \\
 & \left. - \frac{x_\eta}{A} \left[-\frac{\partial}{\partial \xi} (x_\eta \vec{U}) + \frac{\partial}{\partial \eta} (x_\xi \vec{U}) \right] \right\} \\
 & + \frac{1}{A} \frac{\partial}{\partial \eta} \left\{ -\frac{y_\xi}{A} \left[\frac{\partial}{\partial \xi} (y_\eta \vec{U}) - \frac{\partial}{\partial \eta} (y_\xi \vec{U}) \right] \right. \\
 & \left. + \frac{x_\xi}{A} \left[-\frac{\partial}{\partial \xi} (x_\eta \vec{U}) + \frac{\partial}{\partial \eta} (x_\xi \vec{U}) \right] \right\} \quad (3.45)
 \end{aligned}$$

Writing the vertically-integrated velocity vector \vec{U} as a function of the contravariant flux components, and performing the dot product with the length vectors, the equation for U^ξ , equation 3.29 becomes

$$\begin{aligned}
 \frac{U^{\xi''} - U^{\xi'}}{\Delta t} = & A_H \frac{y_\eta}{A^2} \frac{\partial}{\partial \xi} \left\{ \frac{y_\eta}{A} \left[\frac{\partial}{\partial \xi} \left(\frac{x_\xi y_\eta}{A} U^\xi + \frac{x_\eta y_\eta}{A} U^\eta \right) \right. \right. \\
 & \left. \left. - \frac{\partial}{\partial \eta} \left(\frac{x_\xi y_\xi}{A} U^\xi + \frac{x_\eta y_\xi}{A} U^\eta \right) \right] - \frac{x_\eta}{A} \left[-\frac{\partial}{\partial \xi} \left(\frac{x_\xi x_\eta}{A} U^\xi \right. \right. \right. \\
 & \left. \left. + \frac{x_\eta^2}{A} U^\eta \right) + \frac{\partial}{\partial \eta} \left(\frac{x_\xi^2}{A} U^\xi + \frac{x_\xi x_\eta}{A} U^\eta \right) \right] \right\} \\
 & + A_H \frac{y_\eta}{A^2} \frac{\partial}{\partial \eta} \left\{ -\frac{y_\xi}{A} \left[\frac{\partial}{\partial \xi} \left(\frac{x_\xi y_\eta}{A} U^\xi + \frac{x_\eta y_\eta}{A} U^\eta \right) \right. \right. \\
 & \left. \left. - \frac{\partial}{\partial \eta} \left(\frac{x_\xi y_\xi}{A} U^\xi + \frac{x_\eta y_\xi}{A} U^\eta \right) \right] + \frac{x_\xi}{A} \left[-\frac{\partial}{\partial \xi} \left(\frac{x_\xi x_\eta}{A} U^\xi \right. \right. \right. \\
 & \left. \left. + \frac{x_\eta^2}{A} U^\eta \right) + \frac{\partial}{\partial \eta} \left(\frac{x_\xi^2}{A} U^\xi + \frac{x_\xi x_\eta}{A} U^\eta \right) \right] \right\} \\
 & - A_H \frac{x_\eta}{A^2} \frac{\partial}{\partial \xi} \left\{ \frac{y_\eta}{A} \left[\frac{\partial}{\partial \xi} \left(\frac{y_\xi y_\eta}{A} U^\xi + \frac{y_\eta^2}{A} U^\eta \right) \right. \right. \\
 & \left. \left. - \frac{\partial}{\partial \eta} \left(\frac{y_\xi^2}{A} U^\xi + \frac{y_\xi y_\eta}{A} U^\eta \right) \right] - \frac{x_\eta}{A} \left[-\frac{\partial}{\partial \xi} \left(\frac{x_\eta y_\xi}{A} U^\xi \right. \right. \right. \\
 & \left. \left. + \frac{x_\eta y_\eta}{A} U^\eta \right) + \frac{\partial}{\partial \eta} \left(\frac{x_\xi y_\xi}{A} U^\xi + \frac{x_\xi y_\eta}{A} U^\eta \right) \right] \right\}
 \end{aligned}$$

$$\begin{aligned}
& -A_H \frac{x_\eta}{A^2} \frac{\partial}{\partial \eta} \left\{ -\frac{y_\xi}{A} \left[\frac{\partial}{\partial \xi} \left(\frac{y_\xi y_\eta}{A} U^\xi + \frac{y_\eta^2}{A} U^\eta \right) \right. \right. \\
& \left. \left. - \frac{\partial}{\partial \eta} \left(\frac{y_\xi^2}{A} U^\xi + \frac{y_\xi y_\eta}{A} U^\eta \right) \right] + \frac{x_\xi}{A} \left[-\frac{\partial}{\partial \xi} \left(\frac{x_\eta y_\xi}{A} U^\xi \right. \right. \right. \\
& \left. \left. \left. + \frac{x_\eta y_\eta}{A} U^\eta \right) + \frac{\partial}{\partial \eta} \left(\frac{x_\xi y_\xi}{A} U^\xi + \frac{x_\xi y_\eta}{A} U^\eta \right) \right] \right\} \quad (3.46)
\end{aligned}$$

Equation 3.30, for U^η , becomes

$$\begin{aligned}
\frac{U^{\eta**} - U^\eta}{\Delta t} &= -A_H \frac{y_\xi}{A^2} \frac{\partial}{\partial \xi} \left\{ \frac{y_\eta}{A} \left[\frac{\partial}{\partial \xi} \left(\frac{x_\xi y_\eta}{A} U^\xi + \frac{x_\eta y_\eta}{A} U^\eta \right) \right. \right. \\
& \left. \left. - \frac{\partial}{\partial \eta} \left(\frac{x_\xi y_\xi}{A} U^\xi + \frac{x_\eta y_\xi}{A} U^\eta \right) \right] - \frac{x_\eta}{A} \left[-\frac{\partial}{\partial \xi} \left(\frac{x_\xi x_\eta}{A} U^\xi \right. \right. \right. \\
& \left. \left. \left. + \frac{x_\eta^2}{A} U^\eta \right) + \frac{\partial}{\partial \eta} \left(\frac{x_\xi^2}{A} U^\xi + \frac{x_\xi x_\eta}{A} U^\eta \right) \right] \right\} \\
& -A_H \frac{y_\xi}{A^2} \frac{\partial}{\partial \eta} \left\{ -\frac{y_\xi}{A} \left[\frac{\partial}{\partial \xi} \left(\frac{x_\xi y_\eta}{A} U^\xi + \frac{x_\eta y_\eta}{A} U^\eta \right) \right. \right. \\
& \left. \left. - \frac{\partial}{\partial \eta} \left(\frac{x_\xi y_\xi}{A} U^\xi + \frac{x_\eta y_\xi}{A} U^\eta \right) \right] + \frac{x_\xi}{A} \left[-\frac{\partial}{\partial \xi} \left(\frac{x_\xi x_\eta}{A} U^\xi \right. \right. \right. \\
& \left. \left. \left. + \frac{x_\eta^2}{A} U^\eta \right) + \frac{\partial}{\partial \eta} \left(\frac{x_\xi^2}{A} U^\xi + \frac{x_\xi x_\eta}{A} U^\eta \right) \right] \right\} \\
& +A_H \frac{x_\xi}{A^2} \frac{\partial}{\partial \xi} \left\{ \frac{y_\eta}{A} \left[\frac{\partial}{\partial \xi} \left(\frac{y_\xi y_\eta}{A} U^\xi + \frac{y_\eta^2}{A} U^\eta \right) \right. \right. \\
& \left. \left. - \frac{\partial}{\partial \eta} \left(\frac{y_\xi^2}{A} U^\xi + \frac{y_\xi y_\eta}{A} U^\eta \right) \right] - \frac{x_\eta}{A} \left[-\frac{\partial}{\partial \xi} \left(\frac{x_\eta y_\xi}{A} U^\xi \right. \right. \right. \\
& \left. \left. \left. + \frac{x_\eta y_\eta}{A} U^\eta \right) + \frac{\partial}{\partial \eta} \left(\frac{x_\xi y_\xi}{A} U^\xi + \frac{x_\xi y_\eta}{A} U^\eta \right) \right] \right\} \\
& +A_H \frac{x_\xi}{A^2} \frac{\partial}{\partial \eta} \left\{ -\frac{y_\xi}{A} \left[\frac{\partial}{\partial \xi} \left(\frac{y_\xi y_\eta}{A} U^\xi + \frac{y_\eta^2}{A} U^\eta \right) \right. \right. \\
& \left. \left. - \frac{\partial}{\partial \eta} \left(\frac{y_\xi^2}{A} U^\xi + \frac{y_\xi y_\eta}{A} U^\eta \right) \right] + \frac{x_\xi}{A} \left[-\frac{\partial}{\partial \xi} \left(\frac{x_\eta y_\xi}{A} U^\xi \right. \right. \right. \\
& \left. \left. \left. + \frac{x_\eta y_\eta}{A} U^\eta \right) + \frac{\partial}{\partial \eta} \left(\frac{x_\xi y_\xi}{A} U^\xi + \frac{x_\xi y_\eta}{A} U^\eta \right) \right] \right\} \quad (3.47)
\end{aligned}$$

To make things simpler, auxiliary variables B , C , D and E were defined as follows:

$$B = \frac{y_\eta}{A} \left[\frac{\partial}{\partial \xi} \left(\frac{x_\xi y_\eta}{A} U^\xi + \frac{x_\eta y_\eta}{A} U^\eta \right) - \frac{\partial}{\partial \eta} \left(\frac{x_\xi y_\xi}{A} U^\xi + \frac{x_\eta y_\xi}{A} U^\eta \right) \right] - \frac{x_\eta}{A} \left[-\frac{\partial}{\partial \xi} \left(\frac{x_\xi x_\eta}{A} U^\xi + \frac{x_\eta^2}{A} U^\eta \right) + \frac{\partial}{\partial \eta} \left(\frac{x_\xi^2}{A} U^\xi + \frac{x_\xi x_\eta}{A} U^\eta \right) \right] \quad (3.48)$$

$$C = -\frac{y_\xi}{A} \left[\frac{\partial}{\partial \xi} \left(\frac{x_\xi y_\eta}{A} U^\xi + \frac{x_\eta y_\eta}{A} U^\eta \right) - \frac{\partial}{\partial \eta} \left(\frac{x_\xi y_\xi}{A} U^\xi + \frac{x_\eta y_\xi}{A} U^\eta \right) \right] + \frac{x_\xi}{A} \left[-\frac{\partial}{\partial \xi} \left(\frac{x_\xi x_\eta}{A} U^\xi + \frac{x_\eta^2}{A} U^\eta \right) + \frac{\partial}{\partial \eta} \left(\frac{x_\xi^2}{A} U^\xi + \frac{x_\xi x_\eta}{A} U^\eta \right) \right] \quad (3.49)$$

$$D = \frac{y_\eta}{A} \left[\frac{\partial}{\partial \xi} \left(\frac{y_\xi y_\eta}{A} U^\xi + \frac{y_\eta^2}{A} U^\eta \right) - \frac{\partial}{\partial \eta} \left(\frac{y_\xi^2}{A} U^\xi + \frac{y_\xi y_\eta}{A} U^\eta \right) \right] - \frac{x_\eta}{A} \left[-\frac{\partial}{\partial \xi} \left(\frac{x_\eta y_\xi}{A} U^\xi + \frac{x_\eta y_\eta}{A} U^\eta \right) + \frac{\partial}{\partial \eta} \left(\frac{x_\xi y_\xi}{A} U^\xi + \frac{x_\xi y_\eta}{A} U^\eta \right) \right] \quad (3.50)$$

$$E = -\frac{y_\xi}{A} \left[\frac{\partial}{\partial \xi} \left(\frac{y_\xi y_\eta}{A} U^\xi + \frac{y_\eta^2}{A} U^\eta \right) - \frac{\partial}{\partial \eta} \left(\frac{y_\xi^2}{A} U^\xi + \frac{y_\xi y_\eta}{A} U^\eta \right) \right] + \frac{x_\xi}{A} \left[-\frac{\partial}{\partial \xi} \left(\frac{x_\eta y_\xi}{A} U^\xi + \frac{x_\eta y_\eta}{A} U^\eta \right) + \frac{\partial}{\partial \eta} \left(\frac{x_\xi y_\xi}{A} U^\xi + \frac{x_\xi y_\eta}{A} U^\eta \right) \right] \quad (3.51)$$

Equations 3.46 and 3.47 then become

$$\frac{U^{\xi**} - U^{\xi*}}{\Delta t} = A_H \frac{y_\eta}{A^2} \frac{\partial B}{\partial \xi} + A_H \frac{y_\eta}{A^2} \frac{\partial C}{\partial \eta} - A_H \frac{x_\eta}{A^2} \frac{\partial D}{\partial \xi} - A_H \frac{x_\eta}{A^2} \frac{\partial E}{\partial \eta} \quad (3.52)$$

$$\frac{U^{\eta**} - U^{\eta*}}{\Delta t} = -A_H \frac{y_\xi}{A^2} \frac{\partial B}{\partial \xi} - A_H \frac{y_\xi}{A^2} \frac{\partial C}{\partial \eta} + A_H \frac{x_\xi}{A^2} \frac{\partial D}{\partial \xi} + A_H \frac{x_\xi}{A^2} \frac{\partial E}{\partial \eta} \quad (3.53)$$

The diffusion equations are then solved explicitly, with the spatial derivatives being approximated by centered differences. Equations 3.52 and 3.53 become

$$\begin{aligned}
U_{i+\frac{1}{2},j}^{\xi^{**}} &= U_{i+\frac{1}{2},j}^{\xi^*} + A_H \frac{y_{\eta_{i+\frac{1}{2},j}} \Delta t}{A_{i+\frac{1}{2},j}^2} (B_{i+1,j} - B_{i,j}) \\
&+ A_H \frac{y_{\eta_{i+\frac{1}{2},j}} \Delta t}{A_{i+\frac{1}{2},j}^2} (C_{i+\frac{1}{2},j+\frac{1}{2}} - C_{i+\frac{1}{2},j-\frac{1}{2}}) - A_H \frac{x_{\eta_{i+\frac{1}{2},j}} \Delta t}{A_{i+\frac{1}{2},j}^2} (D_{i+1,j} - D_{i,j}) \\
&- \textcircled{A_H} \frac{x_{\eta_{i+\frac{1}{2},j}} \Delta t}{A_{i+\frac{1}{2},j}^2} (E_{i+\frac{1}{2},j+\frac{1}{2}} - E_{i+\frac{1}{2},j-\frac{1}{2}}) \quad (3.54)
\end{aligned}$$

$$\begin{aligned}
U_{i,j+\frac{1}{2}}^{\eta^{**}} &= U_{i,j+\frac{1}{2}}^{\eta^*} - A_H \frac{y_{\xi_{i,j+\frac{1}{2}}} \Delta t}{A_{i,j+\frac{1}{2}}^2} (B_{i+\frac{1}{2},j+\frac{1}{2}} - B_{i-\frac{1}{2},j+\frac{1}{2}}) \\
&- A_H \frac{y_{\xi_{i,j+\frac{1}{2}}} \Delta t}{A_{i,j+\frac{1}{2}}^2} (C_{i,j+1} - C_{i,j}) + A_H \frac{x_{\xi_{i,j+\frac{1}{2}}} \Delta t}{A_{i,j+\frac{1}{2}}^2} (D_{i+\frac{1}{2},j+\frac{1}{2}} - D_{i-\frac{1}{2},j+\frac{1}{2}}) \\
&+ A_H \frac{x_{\xi_{i,j+\frac{1}{2}}} \Delta t}{A_{i,j+\frac{1}{2}}^2} (E_{i,j+1} - E_{i,j}) \quad (3.55)
\end{aligned}$$

The discrete form of the auxiliary variables is

$$\begin{aligned}
B_{i,j} &= \frac{y_{\eta_{i,j}}}{A_{i,j}} \left(\frac{x_{\xi_{i+\frac{1}{2},j}} y_{\eta_{i+\frac{1}{2},j}} U_{i+\frac{1}{2},j}^{\xi^*}}{A_{i+\frac{1}{2},j}} - \frac{x_{\xi_{i-\frac{1}{2},j}} y_{\eta_{i-\frac{1}{2},j}} U_{i-\frac{1}{2},j}^{\xi^*}}{A_{i-\frac{1}{2},j}} \right. \\
&+ \frac{x_{\eta_{i+\frac{1}{2},j}} y_{\eta_{i+\frac{1}{2},j}} U_{i+\frac{1}{2},j}^{\eta^*}}{A_{i+\frac{1}{2},j}} - \frac{x_{\eta_{i-\frac{1}{2},j}} y_{\eta_{i-\frac{1}{2},j}} U_{i-\frac{1}{2},j}^{\eta^*}}{A_{i-\frac{1}{2},j}} - \frac{x_{\xi_{i,j+\frac{1}{2}}} y_{\xi_{i,j+\frac{1}{2}}} U_{i,j+\frac{1}{2}}^{\xi^*}}{A_{i,j+\frac{1}{2}}} \\
&+ \left. \frac{x_{\xi_{i,j-\frac{1}{2}}} y_{\xi_{i,j-\frac{1}{2}}} U_{i,j-\frac{1}{2}}^{\xi^*}}{A_{i,j-\frac{1}{2}}} - \frac{x_{\eta_{i,j+\frac{1}{2}}} y_{\xi_{i,j+\frac{1}{2}}} U_{i,j+\frac{1}{2}}^{\eta^*}}{A_{i,j+\frac{1}{2}}} + \frac{x_{\eta_{i,j-\frac{1}{2}}} y_{\xi_{i,j-\frac{1}{2}}} U_{i,j-\frac{1}{2}}^{\eta^*}}{A_{i,j-\frac{1}{2}}} \right) \\
&- \frac{x_{\eta_{i,j}}}{A_{i,j}} \left(- \frac{x_{\xi_{i+\frac{1}{2},j}} x_{\eta_{i+\frac{1}{2},j}} U_{i+\frac{1}{2},j}^{\xi^*}}{A_{i+\frac{1}{2},j}} + \frac{x_{\xi_{i-\frac{1}{2},j}} x_{\eta_{i-\frac{1}{2},j}} U_{i-\frac{1}{2},j}^{\xi^*}}{A_{i-\frac{1}{2},j}} - \frac{x_{\eta_{i+\frac{1}{2},j}}^2 U_{i+\frac{1}{2},j}^{\eta^*}}{A_{i+\frac{1}{2},j}} \right. \\
&+ \frac{x_{\eta_{i-\frac{1}{2},j}}^2 U_{i-\frac{1}{2},j}^{\eta^*}}{A_{i-\frac{1}{2},j}} + \frac{x_{\xi_{i,j+\frac{1}{2}}}^2 U_{i,j+\frac{1}{2}}^{\xi^*}}{A_{i,j+\frac{1}{2}}} - \frac{x_{\xi_{i,j-\frac{1}{2}}}^2 U_{i,j-\frac{1}{2}}^{\xi^*}}{A_{i,j-\frac{1}{2}}} \\
&+ \frac{x_{\xi_{i,j+\frac{1}{2}}} x_{\eta_{i,j+\frac{1}{2}}} U_{i,j+\frac{1}{2}}^{\eta^*}}{A_{i,j+\frac{1}{2}}} \\
&\left. - \frac{x_{\xi_{i,j-\frac{1}{2}}} x_{\eta_{i,j-\frac{1}{2}}} U_{i,j-\frac{1}{2}}^{\eta^*}}{A_{i,j-\frac{1}{2}}} \right) \quad (3.56)
\end{aligned}$$

$$\begin{aligned}
& + \frac{x_{\eta_{i-\frac{1}{2},j}} y_{\xi_{i-\frac{1}{2},j}} U^{\xi^*}}{A_{i-\frac{1}{2},j}} - \frac{x_{\eta_{i+\frac{1}{2},j}} y_{\xi_{i+\frac{1}{2},j}} U^{\eta^*}}{A_{i+\frac{1}{2},j}} + \frac{x_{\eta_{i-\frac{1}{2},j}} y_{\xi_{i+\frac{1}{2},j}} U^{\eta^*}}{A_{i-\frac{1}{2},j}} \\
& + \frac{x_{\xi_{i,j+\frac{1}{2}}} y_{\xi_{i,j+\frac{1}{2}}} U^{\xi^*}}{A_{i,j+\frac{1}{2}}} - \frac{x_{\xi_{i,j-\frac{1}{2}}} y_{\xi_{i,j-\frac{1}{2}}} U^{\xi^*}}{A_{i,j-\frac{1}{2}}} + \frac{x_{\xi_{i,j+\frac{1}{2}}} y_{\eta_{i,j+\frac{1}{2}}} U^{\eta^*}}{A_{i,j+\frac{1}{2}}} \\
& - \frac{x_{\xi_{i,j-\frac{1}{2}}} y_{\eta_{i,j-\frac{1}{2}}} U^{\eta^*}}{A_{i,j-\frac{1}{2}}} \Big) \tag{3.59}
\end{aligned}$$

As in the advection step, when information is needed at positions different from where they are computed, four-point interpolation is used.

3.6 The Coriolis Step

The \vec{F} vector in the Coriolis step is given by

$$\vec{F} = Af(\vec{U} \times \vec{k}) \tag{3.60}$$

which, after replacing \vec{U} with the contravariant flux components and taking the dot product with the contravariant length vectors leads to

$$\frac{U^{\xi^{***}} - U^{\xi^{**}}}{\Delta t} = f \frac{x_{\xi} x_{\eta} + y_{\xi} y_{\eta}}{A} U^{\xi} + f \frac{x_{\eta}^2 + y_{\eta}^2}{A} U^{\eta} \tag{3.61}$$

$$\frac{U^{\eta^{***}} - U^{\eta^{**}}}{\Delta t} = -f \frac{x_{\xi}^2 + y_{\xi}^2}{A} U^{\xi} - f \frac{x_{\xi} x_{\eta} + y_{\xi} y_{\eta}}{A} U^{\eta} \tag{3.62}$$

Equation 3.61 is solved first, implicitly in terms of U^{ξ} , and using, in the right hand side, the last known values for the other component, $U^{\eta^{**}}$.

$$\begin{aligned}
U_{i+\frac{1}{2},j}^{\xi^{***}} &= U_{i+\frac{1}{2},j}^{\xi^{**}} + f\Delta t \frac{x_{\xi_{i+\frac{1}{2},j}} x_{\eta_{i+\frac{1}{2},j}} + y_{\xi_{i+\frac{1}{2},j}} y_{\eta_{i+\frac{1}{2},j}}}{A_{i+\frac{1}{2},j}} U_{i+\frac{1}{2},j}^{\xi^{***}} \\
&\quad + f\Delta t \frac{x_{\eta_{i+\frac{1}{2},j}}^2 + y_{\eta_{i+\frac{1}{2},j}}^2}{A_{i+\frac{1}{2},j}} U_{i+\frac{1}{2},j}^{\eta^{**}}
\end{aligned} \tag{3.63}$$

Since the two flux components are being computed at different positions, the computed values for U^n after the diffusion steps must be interpolated in order to be used in the Coriolis step. As in the previous cases, a four-point interpolation scheme was used.

After getting new values for U^ξ , they are also interpolated to be used in equation 3.62, which, once again, is solved implicitly in terms of U^n .

$$\begin{aligned}
U_{i,j+\frac{1}{2}}^{\eta^{***}} &= U_{i,j+\frac{1}{2}}^{\eta^{**}} - f\Delta t \frac{x_{\xi_{i,j+\frac{1}{2}}}^2 + y_{\xi_{i,j+\frac{1}{2}}}^2}{A_{i,j+\frac{1}{2}}} U_{i,j+\frac{1}{2}}^{\xi^{***}} \\
&\quad - f\Delta t \frac{x_{\xi_{i,j+\frac{1}{2}}} x_{\eta_{i,j+\frac{1}{2}}} + y_{\xi_{i,j+\frac{1}{2}}} y_{\eta_{i,j+\frac{1}{2}}}}{A_{i,j+\frac{1}{2}}} U_{i,j+\frac{1}{2}}^{\eta^{***}}
\end{aligned} \tag{3.64}$$

3.7 The Propagation Step

The propagation step includes not only the remaining terms in the momentum equations but also the continuity equation. Equations for $U^{\xi^{n+1}}$ and $U^{\eta^{n+1}}$ are first derived from the momentum equations and substituted in the continuity equation to get an equation on ζ than can be solved using a conjugate gradient method. The new values for ζ are then used to compute U^ξ and U^η .

Going back again to equations 3.29 and 3.30, the vector \vec{F} is given, in the propagation step, by

$$\vec{F} = -gH \frac{\partial}{\partial \xi} (\zeta \vec{L}^\xi) - gh \frac{\partial}{\partial \eta} (\zeta \vec{L}^\eta) + \frac{A}{\rho} (\vec{\tau}_w - \vec{\tau}_b) \quad (3.65)$$

The continuity equation, reflecting the mass balance over each computational cell is given, in the contravariant coordinate system, by

$$A \frac{\partial \zeta}{\partial t} = - \frac{\partial U^\xi}{\partial \xi} - \frac{\partial U^\eta}{\partial \eta} \quad (3.66)$$

The bottom friction formulation used is outlined in section 3.1. Note that, for a contravariant coordinate system, the flux magnitude term, which, in the cartesian coordinate system is given by

$$S = \sqrt{U_C^2 + V_C^2} \quad (3.67)$$

becomes

$$S = \frac{\sqrt{(x_\xi^2 + y_\xi^2) U^{\xi^2} + (x_\eta^2 + y_\eta^2) U^{\eta^2} + 2(x_\xi x_\eta + y_\xi y_\eta) U^\xi U^\eta}}{A} \quad (3.68)$$

The bottom friction components to be used in the momentum equations can, therefore, be written as

$$\tau_{b\xi} = \frac{\rho g U^\xi S}{C^2 H^2} \quad (3.69)$$

$$\tau_{b\eta} = \frac{\rho g U^\eta S}{C^2 H^2} \quad (3.70)$$

All three equations in this step are solved implicitly. However, a number of problems arise from that. First, the bottom friction terms are non-linear, and, to be solved implicitly, must be linearized. This is done by always using the flux magnitude value given by equation 3.68 after the Coriolis step, and solving implicitly only for the other occurrence of one of the flux components. The total depth is also taken after the last time step (since the depth is changed only at the propagation step, these are the last known depth values):

$$\tau_{b\xi}^{n+1} = \frac{\rho g U^{\xi^{n+1}} S^{***}}{C^{n^2} H^{n^2}} \quad (3.71)$$

$$\tau_{b\eta}^{n+1} = \frac{\rho g U^{\eta^{n+1}} S^{***}}{C^{n^2} H^{n^2}} \quad (3.72)$$

The other problem is that, to use the conjugate gradient as presented by Hauguel (1979), the η derivative terms in the U^ξ equation and the ξ derivative terms in the U^η equation must be treated explicitly, so that the ξ derivative terms and the η derivative terms in the final ζ equation can be solved separately.

Defining a coefficient β given by

$$\beta = 1 + \frac{gS\Delta t}{AC^2H^2} \quad (3.73)$$

the following equations are obtained for U^ξ and U^η :

$$\begin{aligned}
U^{\xi^{n+1}} = & \frac{U^{\xi^{***}}}{\beta^{***}} - \frac{gH^n \Delta t}{\beta^{***} A} y_\eta \frac{\partial}{\partial \xi} (y_\eta \zeta^{n+1}) - \frac{gH^n \Delta t}{\beta^{***} A} x_\eta \frac{\partial}{\partial \xi} (x_\eta \zeta^{n+1}) \\
& + \frac{gH^n \Delta t}{\beta^{***} A} y_\eta \frac{\partial}{\partial \eta} (y_\xi \zeta^n) + \frac{gH^n \Delta t}{\beta^{***} A} x_\eta \frac{\partial}{\partial \eta} (x_\xi \zeta^n) + \frac{\Delta t}{\beta^{***} \rho} y_\eta \tau_{wz} \\
& - \frac{\Delta t}{\beta^{***} \rho} x_\eta \tau_{wy}
\end{aligned} \tag{3.74}$$

$$\begin{aligned}
U^{\eta^{n+1}} = & \frac{U^{\eta^{***}}}{\beta^{***}} + \frac{gH^n \Delta t}{\beta^{***} A} y_\xi \frac{\partial}{\partial \xi} (y_\eta \zeta^n) + \frac{gH^n \Delta t}{\beta^{***} A} x_\xi \frac{\partial}{\partial \xi} (x_\eta \zeta^n) \\
& - \frac{gH^n \Delta t}{\beta^{***} A} y_\xi \frac{\partial}{\partial \eta} (y_\xi \zeta^{n+1}) - \frac{gH^n \Delta t}{\beta^{***} A} x_\xi \frac{\partial}{\partial \eta} (x_\xi \zeta^{n+1}) \\
& - \frac{\Delta t}{\beta^{***} \rho} y_\xi \tau_{wz} + \frac{\Delta t}{\beta^{***} \rho} x_\xi \tau_{wy}
\end{aligned} \tag{3.75}$$

Substituting these into the continuity equation 3.66 and replacing all occurrences of ζ^{n+1} with $\zeta^n + \Delta \zeta$, a single equation was derived, where $\Delta \zeta$ is the only unknown, that can be solved using the conjugate gradient method:

$$\begin{aligned}
\frac{\Delta \zeta}{\Delta t} = & \frac{g \Delta t}{A} \frac{\partial}{\partial \xi} \left\{ \frac{H^n}{\beta^{***} A} \left[y_\eta \frac{\partial}{\partial \xi} (y_\eta \Delta \zeta) + x_\eta \frac{\partial}{\partial \xi} (x_\eta \Delta \zeta) \right] \right\} \\
& - \frac{g \Delta t}{A} \frac{\partial}{\partial \eta} \left\{ \frac{H^n}{\beta^{***} A} \left[y_\xi \frac{\partial}{\partial \eta} (y_\xi \Delta \zeta) + x_\xi \frac{\partial}{\partial \eta} (x_\xi \Delta \zeta) \right] \right\} \\
= & - \frac{1}{A} \frac{\partial}{\partial \xi} \left(\frac{U^{\xi^{***}}}{\beta^{***}} \right) + \frac{g \Delta t}{A} \frac{\partial}{\partial \xi} \left\{ \frac{H^n}{\beta^{***} A} \left[y_\eta \frac{\partial}{\partial \xi} (y_\eta \zeta^n) \right. \right. \\
& \left. \left. + x_\eta \frac{\partial}{\partial \xi} (x_\eta \zeta^n) \right] \right\} - \frac{g \Delta t}{A} \frac{\partial}{\partial \xi} \left\{ \frac{H^n}{\beta^{***} A} \left[y_\eta \frac{\partial}{\partial \eta} (y_\xi \zeta^n) \right. \right. \\
& \left. \left. + x_\eta \frac{\partial}{\partial \eta} (x_\xi \zeta^n) \right] \right\} - \frac{\Delta t}{A} \frac{\partial}{\partial \xi} \left[\frac{1}{\beta^{***} \rho} (y_\eta \tau_{wz} - x_\eta \tau_{wy}) \right] \\
& - \frac{1}{A} \frac{\partial}{\partial \eta} \left(\frac{U^{\eta^{***}}}{\beta^{***}} \right) - \frac{g \Delta t}{A} \frac{\partial}{\partial \eta} \left\{ \frac{H^n}{\beta^{***} A} \left[y_\xi \frac{\partial}{\partial \xi} (y_\eta \zeta^n) \right. \right. \\
& \left. \left. + x_\xi \frac{\partial}{\partial \xi} (x_\eta \zeta^n) \right] \right\} + \frac{g \Delta t}{A} \frac{\partial}{\partial \eta} \left\{ \frac{H^n}{\beta^{***} A} \left[y_\xi \frac{\partial}{\partial \eta} (y_\xi \zeta^n) \right. \right. \\
& \left. \left. + x_\xi \frac{\partial}{\partial \eta} (x_\xi \zeta^n) \right] \right\} + \frac{\Delta t}{A} \frac{\partial}{\partial \eta} \left[\frac{1}{\beta^{***} \rho} (y_\xi \tau_{wz} - x_\xi \tau_{wy}) \right]
\end{aligned} \tag{3.76}$$

Since none of the implicit terms contains any cross derivatives, the same procedure followed by Liu (1988) can be followed, breaking this equation in two, one for the ξ derivative terms and the other for the η derivative terms:

$$\begin{aligned} \frac{A}{2g(\Delta t)^2} \Delta \zeta_1 &= \frac{\partial}{\partial \xi} \left\{ \frac{H^n}{\beta^{***} A} \left[y_\eta \frac{\partial}{\partial \xi} (y_\eta \Delta \zeta_1) + x_\eta \frac{\partial}{\partial \xi} (x_\eta \Delta \zeta_1) \right] \right\} \\ &= -\frac{1}{g \Delta t} \frac{\partial}{\partial \xi} \left(\frac{U^{\epsilon^{***}}}{\beta^{***}} \right) + \frac{\partial}{\partial \xi} \left\{ \frac{H^n}{\beta^{***} A} \left[y_\eta \frac{\partial}{\partial \xi} (y_\eta S^n) \right. \right. \\ &\quad \left. \left. + x_\eta \frac{\partial}{\partial \xi} (x_\eta S^n) \right] \right\} - \frac{\partial}{\partial \xi} \left\{ \frac{H^n}{\beta^{***} A} \left[y_\eta \frac{\partial}{\partial \eta} (y_\epsilon S^n) \right. \right. \\ &\quad \left. \left. + x_\eta \frac{\partial}{\partial \eta} (x_\epsilon S^n) \right] \right\} - \frac{1}{g} \frac{\partial}{\partial \xi} \left[\frac{1}{\beta^{***}} (y_\eta \tau_{wx} - x_\eta \tau_{wy}) \right] - q \quad (3.77) \end{aligned}$$

$$\begin{aligned} \frac{A}{2g(\Delta t)^2} \Delta \zeta_2 &= \frac{\partial}{\partial \eta} \left\{ \frac{H^n}{\beta^{***} A} \left[y_\epsilon \frac{\partial}{\partial \eta} (y_\epsilon \Delta \zeta_2) + x_\epsilon \frac{\partial}{\partial \eta} (x_\epsilon \Delta \zeta_2) \right] \right\} \\ &= -\frac{1}{g \Delta t} \frac{\partial}{\partial \eta} \left(\frac{U^{\eta^{***}}}{\beta^{***}} \right) - \frac{\partial}{\partial \eta} \left\{ \frac{H^n}{\beta^{***} A} \left[y_\epsilon \frac{\partial}{\partial \xi} (y_\eta S^n) \right. \right. \\ &\quad \left. \left. + x_\epsilon \frac{\partial}{\partial \xi} (x_\eta S^n) \right] \right\} + \frac{\partial}{\partial \eta} \left\{ \frac{H^n}{\beta^{***} A} \left[y_\epsilon \frac{\partial}{\partial \eta} (y_\epsilon S^n) \right. \right. \\ &\quad \left. \left. + x_\epsilon \frac{\partial}{\partial \eta} (x_\epsilon S^n) \right] \right\} + \frac{1}{g} \frac{\partial}{\partial \eta} \left[\frac{1}{\beta^{***}} (y_\epsilon \tau_{wx} - x_\epsilon \tau_{wy}) \right] + q \quad (3.78) \end{aligned}$$

$$\Delta \zeta_1 = \Delta \zeta_2 \quad (3.79)$$

The spatial derivatives are approximated by centered differences, leading to the following discrete equations:

$$\begin{aligned} \left[\frac{A_{i,j}}{2g(\Delta t)^2} + \frac{H_{i+\frac{1}{2},j}^n}{\beta_{i+\frac{1}{2},j}^{***} A_{i+\frac{1}{2},j}} \left(y_{\eta_{i+\frac{1}{2},j}} y_{\eta_{i,j}} + x_{\eta_{i+\frac{1}{2},j}} x_{\eta_{i,j}} \right) \right. \\ \left. + \frac{H_{i-\frac{1}{2},j}^n}{\beta_{i-\frac{1}{2},j}^{***} A_{i-\frac{1}{2},j}} \left(y_{\eta_{i-\frac{1}{2},j}} y_{\eta_{i,j}} + x_{\eta_{i-\frac{1}{2},j}} x_{\eta_{i,j}} \right) \right] \Delta \zeta_{1,i,j} \end{aligned}$$

$$\begin{aligned}
& -\frac{H_{i-\frac{1}{2},j}^n}{\beta_{i-\frac{1}{2},j}^{***} A_{i-\frac{1}{2},j}} \left(y_{n_{i-\frac{1}{2},j}} y_{n_{i-1,j}} + x_{n_{i-\frac{1}{2},j}} x_{n_{i-1,j}} \right) \Delta \zeta_{1_{i-1,j}} \\
& -\frac{H_{i+\frac{1}{2},j}^n}{\beta_{i+\frac{1}{2},j}^{***} A_{i+\frac{1}{2},j}} \left(y_{n_{i+\frac{1}{2},j}} y_{n_{i+1,j}} + x_{n_{i+\frac{1}{2},j}} x_{n_{i+1,j}} \right) \Delta \zeta_{1_{i+1,j}} \\
= & -\frac{1}{g \Delta t} \left(\frac{U_{i+\frac{1}{2},j}^{\xi^{***}}}{\beta_{i+\frac{1}{2},j}^{***}} - \frac{U_{i-\frac{1}{2},j}^{\xi^{***}}}{\beta_{i-\frac{1}{2},j}^{***}} \right) + \frac{H_{i+\frac{1}{2},j}^n}{\beta_{i+\frac{1}{2},j}^{***} A_{i+\frac{1}{2},j}} \left(y_{n_{i+\frac{1}{2},j}} y_{n_{i+1,j}} \zeta_{i+1,j}^n \right. \\
& \left. - y_{n_{i+\frac{1}{2},j}} y_{n_{i,j}} \zeta_{i,j}^n + x_{n_{i+\frac{1}{2},j}} x_{n_{i+1,j}} \zeta_{i+1,j}^n - x_{n_{i+\frac{1}{2},j}} x_{n_{i,j}} \zeta_{i,j}^n \right) \\
& -\frac{H_{i-\frac{1}{2},j}^n}{\beta_{i-\frac{1}{2},j}^{***} A_{i-\frac{1}{2},j}} \left(y_{n_{i-\frac{1}{2},j}} y_{n_{i,j}} \zeta_{i,j}^n - y_{n_{i-\frac{1}{2},j}} y_{n_{i-1,j}} \zeta_{i-1,j}^n \right. \\
& \left. + x_{n_{i-\frac{1}{2},j}} x_{n_{i,j}} \zeta_{i,j}^n - x_{n_{i-\frac{1}{2},j}} x_{n_{i-1,j}} \zeta_{i-1,j}^n \right) \\
& -\frac{H_{i+\frac{1}{2},j}^n}{\beta_{i+\frac{1}{2},j}^{***} A_{i+\frac{1}{2},j}} \left(y_{n_{i+\frac{1}{2},j}} y_{\epsilon_{i+\frac{1}{2},j+\frac{1}{2}}} \zeta_{i+\frac{1}{2},j+\frac{1}{2}}^n \right. \\
& \left. - y_{n_{i+\frac{1}{2},j}} y_{\epsilon_{i+\frac{1}{2},j-\frac{1}{2}}} \zeta_{i+\frac{1}{2},j-\frac{1}{2}}^n + x_{n_{i+\frac{1}{2},j}} x_{\epsilon_{i+\frac{1}{2},j+\frac{1}{2}}} \zeta_{i+\frac{1}{2},j+\frac{1}{2}}^n \right. \\
& \left. - x_{n_{i+\frac{1}{2},j}} x_{\epsilon_{i+\frac{1}{2},j-\frac{1}{2}}} \zeta_{i+\frac{1}{2},j-\frac{1}{2}}^n \right) \\
& +\frac{H_{i-\frac{1}{2},j}^n}{\beta_{i-\frac{1}{2},j}^{***} A_{i-\frac{1}{2},j}} \left(y_{n_{i-\frac{1}{2},j}} y_{\epsilon_{i-\frac{1}{2},j+\frac{1}{2}}} \zeta_{i-\frac{1}{2},j+\frac{1}{2}}^n \right. \\
& \left. - y_{n_{i-\frac{1}{2},j}} y_{\epsilon_{i-\frac{1}{2},j-\frac{1}{2}}} \zeta_{i-\frac{1}{2},j-\frac{1}{2}}^n + x_{n_{i-\frac{1}{2},j}} x_{\epsilon_{i-\frac{1}{2},j+\frac{1}{2}}} \zeta_{i-\frac{1}{2},j+\frac{1}{2}}^n \right. \\
& \left. - x_{n_{i-\frac{1}{2},j}} x_{\epsilon_{i-\frac{1}{2},j-\frac{1}{2}}} \zeta_{i-\frac{1}{2},j-\frac{1}{2}}^n \right) - \frac{1}{g} \left[\frac{1}{\beta_{i+\frac{1}{2},j}^{***}} \left(y_{n_{i+\frac{1}{2},j}} \tau_{wx_{i+\frac{1}{2},j}} \right. \right. \\
& \left. - x_{n_{i+\frac{1}{2},j}} \tau_{wy_{i+\frac{1}{2},j}} \right) - \frac{1}{\beta_{i-\frac{1}{2},j}^{***}} \left(y_{n_{i-\frac{1}{2},j}} \tau_{wx_{i-\frac{1}{2},j}} \right. \\
& \left. - x_{n_{i-\frac{1}{2},j}} \tau_{wy_{i-\frac{1}{2},j}} \right) \Big] - q_{i,j} \tag{3.80}
\end{aligned}$$

$$\begin{aligned}
& \left[\frac{A_{i,j}}{2g (\Delta t)^2} + \frac{H_{i,j+\frac{1}{2}}^n}{\beta_{i,j+\frac{1}{2}}^{***} A_{i,j+\frac{1}{2}}} \left(y_{n_{i,j+\frac{1}{2}}} y_{n_{i,j}} + x_{n_{i,j+\frac{1}{2}}} x_{n_{i,j}} \right) \right. \\
& \left. + \frac{H_{i,j-\frac{1}{2}}^n}{\beta_{i,j-\frac{1}{2}}^{***} A_{i,j-\frac{1}{2}}} \left(y_{n_{i,j-\frac{1}{2}}} y_{n_{i,j}} + x_{n_{i,j-\frac{1}{2}}} x_{n_{i,j}} \right) \right] \Delta \zeta_{2_{i,j}} \\
& -\frac{H_{i,j-\frac{1}{2}}^n}{\beta_{i,j-\frac{1}{2}}^{***} A_{i,j-\frac{1}{2}}} \left(y_{n_{i,j-\frac{1}{2}}} y_{n_{i,j-1}} + x_{n_{i,j-\frac{1}{2}}} x_{n_{i,j-1}} \right) \Delta \zeta_{2_{i,j-1}} ? \\
& -\frac{H_{i,j+\frac{1}{2}}^n}{\beta_{i,j+\frac{1}{2}}^{***} A_{i,j+\frac{1}{2}}} \left(y_{n_{i,j+\frac{1}{2}}} y_{n_{i,j+1}} + x_{n_{i,j+\frac{1}{2}}} x_{n_{i,j+1}} \right) \Delta \zeta_{2_{i,j+1}}
\end{aligned}$$

$$\begin{aligned}
&= -\frac{1}{g\Delta t} \left(\frac{U_{i,j+\frac{1}{2}}^{n***}}{\beta_{i,j+\frac{1}{2}}^{***}} - \frac{U_{i,j-\frac{1}{2}}^{n***}}{\beta_{i,j-\frac{1}{2}}^{***}} \right) \\
&\quad - \frac{H_{i,j+\frac{1}{2}}^n}{\beta_{i,j+\frac{1}{2}}^{***} A_{i,j+\frac{1}{2}}} \left(y_{\epsilon_{i,j+\frac{1}{2}}} y_{\eta_{i+\frac{1}{2},j+\frac{1}{2}}} \zeta_{i+\frac{1}{2},j+\frac{1}{2}}^n \right. \\
&\quad \left. - y_{\epsilon_{i,j+\frac{1}{2}}} y_{\eta_{i-\frac{1}{2},j+\frac{1}{2}}} \zeta_{i-\frac{1}{2},j+\frac{1}{2}}^n + x_{\epsilon_{i,j+\frac{1}{2}}} x_{\eta_{i+\frac{1}{2},j+\frac{1}{2}}} \zeta_{i+\frac{1}{2},j+\frac{1}{2}}^n \right. \\
&\quad \left. - x_{\epsilon_{i,j+\frac{1}{2}}} x_{\eta_{i-\frac{1}{2},j+\frac{1}{2}}} \zeta_{i-\frac{1}{2},j+\frac{1}{2}}^n \right) \\
&\quad + \frac{H_{i,j-\frac{1}{2}}^n}{\beta_{i,j-\frac{1}{2}}^{***} A_{i,j-\frac{1}{2}}} \left(y_{\epsilon_{i,j-\frac{1}{2}}} y_{\eta_{i+\frac{1}{2},j-\frac{1}{2}}} \zeta_{i+\frac{1}{2},j-\frac{1}{2}}^n \right. \\
&\quad \left. - y_{\epsilon_{i,j-\frac{1}{2}}} y_{\eta_{i-\frac{1}{2},j-\frac{1}{2}}} \zeta_{i-\frac{1}{2},j-\frac{1}{2}}^n + x_{\epsilon_{i,j-\frac{1}{2}}} x_{\eta_{i+\frac{1}{2},j-\frac{1}{2}}} \zeta_{i+\frac{1}{2},j-\frac{1}{2}}^n \right. \\
&\quad \left. - x_{\epsilon_{i,j-\frac{1}{2}}} x_{\eta_{i-\frac{1}{2},j-\frac{1}{2}}} \zeta_{i-\frac{1}{2},j-\frac{1}{2}}^n \right) + \frac{H_{i,j+\frac{1}{2}}^n}{\beta_{i,j+\frac{1}{2}}^{***} A_{i,j+\frac{1}{2}}} \left(y_{\epsilon_{i,j+\frac{1}{2}}} y_{\epsilon_{i,j+1}} \zeta_{i,j+1}^n \right. \\
&\quad \left. - y_{\epsilon_{i,j+\frac{1}{2}}} y_{\epsilon_{i,j}} \zeta_{i,j}^n + x_{\epsilon_{i,j+\frac{1}{2}}} x_{\epsilon_{i,j+1}} \zeta_{i,j+1}^n - x_{\epsilon_{i,j+\frac{1}{2}}} x_{\epsilon_{i,j}} \zeta_{i,j}^n \right) \\
&\quad - \frac{H_{i,j-\frac{1}{2}}^n}{\beta_{i,j-\frac{1}{2}}^{***} A_{i,j-\frac{1}{2}}} \left(y_{\epsilon_{i,j-\frac{1}{2}}} y_{\epsilon_{i,j}} \zeta_{i,j}^n - y_{\epsilon_{i,j-\frac{1}{2}}} y_{\epsilon_{i,j-1}} \zeta_{i,j-1}^n \right. \\
&\quad \left. + x_{\epsilon_{i,j-\frac{1}{2}}} x_{\epsilon_{i,j}} \zeta_{i,j}^n - x_{\epsilon_{i,j-\frac{1}{2}}} x_{\epsilon_{i,j-1}} \zeta_{i,j-1}^n \right) \\
&\quad + \frac{1}{g} \left[\frac{1}{\beta_{i,j+\frac{1}{2}}^{***}} \left(y_{\epsilon_{i,j+\frac{1}{2}}} \tau_{wx_{i,j+\frac{1}{2}}} - x_{\epsilon_{i,j+\frac{1}{2}}} \tau_{wy_{i,j+\frac{1}{2}}} \right) \right. \\
&\quad \left. - \frac{1}{\beta_{i,j-\frac{1}{2}}^{***}} \left(y_{\epsilon_{i,j-\frac{1}{2}}} \tau_{wx_{i,j-\frac{1}{2}}} - x_{\epsilon_{i,j-\frac{1}{2}}} \tau_{wy_{i,j-\frac{1}{2}}} \right) \right] + q_{i,j} \quad (3.81)
\end{aligned}$$

These equations can be written, in matricial form, as

$$M\Delta\zeta = f - N^T q \quad (3.82)$$

$$\equiv \begin{cases} N\Delta\zeta = 0 \\ \Delta\zeta_1 = \Delta\zeta_2 \end{cases} \quad (3.83)$$

where

$$\Rightarrow N \left(M^{-1} \right) - M^{-1} N^T q = 0 \quad (3.84)$$

$$M = \begin{bmatrix} M_1 & 0 \\ 0 & M_2 \end{bmatrix} \quad (3.84)$$

$$N = \begin{bmatrix} N_1 & 0 \\ 0 & N_2 \end{bmatrix} \quad (3.85)$$

The partial matrices M_1 and M_2 are tridiagonal matrices that contain the left hand side of equations 3.77 and 3.78 respectively, while, in this case, and since $\Delta\zeta_1$ and $\Delta\zeta_2$ are computed in the same positions, N_1 is an identity matrix and $N_2 = -N_1$.

The right hand side vector f is defined as

$$f = \begin{bmatrix} f_1 \\ f_2 \end{bmatrix} \quad (3.86)$$

where f_1 and f_2 contain the right hand side terms (except for q) in equations 3.77 and 3.78.

Solving for $\Delta\zeta$ in equation 3.82 and substituting in equation 3.83, a new equation on q is derived,

$$(NM^{-1}N^T)q = NM^{-1}f \quad (3.87)$$

This is the equation that is going to be solved using the iterative procedure described in Hauguel (1979). This consists of choosing the optimum direction and distance that the solution must move so that the error, $N\Delta\zeta$ reaches an absolute

minimum. If m denotes the iteration number, the solution after each iteration is given by

$$q^{m+1} = q^m + \rho^m W^m \quad (3.88)$$

The new variables in the right hand side are the distance the solution must be moved, ρ and the direction, W . Hauguel (1979) defines a functional J , given by

$$J(q) = \frac{1}{2} q^T (NM^{-1}N^T) q - q^T (NM^{-1}f) \quad (3.89)$$

which is the base for what he calls the descent method (choice of the optimal distance for an arbitrary direction) and the conjugate gradient method (selection of the optimal direction).

The optimal distance ρ is the one for which $J(q^{m+1}) - J(q^m)$ has a zero-derivative. By substituting equation 3.88 in equation 3.89, this is found to be

$$\rho^m = \frac{(W^m)^T N \Delta \zeta^m}{(W^m)^T N M^{-1} N^T W^m} \quad (3.90)$$

Similarly, an optimal direction W can be found by writing

$$W^m = g^m + \mu^{m-1} W^{m-1} \quad (3.91)$$

and finding the value of μ^{m-1} for which the difference $J(q^{m+1}) - J(q^m)$ has a zero-derivative.

This is called the gradient step method because it yields a solution for μ ,

$$\mu^{m-1} = \frac{(\Delta\zeta^m)^T N^T N \Delta\zeta^m}{(\Delta\zeta^{m-1})^T N^T N \Delta\zeta^{m-1}} \quad (3.92)$$

for which W^m and W^{m-1} are conjugate relative to $(NM^{-1}N^T)$, since substituting equation 3.92 into equation 3.91 leads to

$$W^{m-1T} NM^{-1} N^T W^m = 0 \quad (3.93)$$

To make the computation of ρ and μ simpler, a new vector V can be defined as

$$V^m = M^{-1} N^T W^m \quad (3.94)$$

and ρ is now

$$\rho^m = \frac{(W^m)^T N \Delta\zeta^m}{(W^m)^T N V^m} \quad (3.95)$$

Multiplying both sides of equation 3.94 by M , a new equation can be derived that looks similar to equation 3.82:

$$MV^m = N^T W^m \quad (3.96)$$

The full iterative procedure can now be outlined:

1. Use the value of q at the last time step as q^0 .
2. Solve $M\Delta\zeta^0 = f - N^T q^0$.
3. Compute the error $g^0 = \Delta\zeta_1^0 - \Delta\zeta_2^0$.
4. Define the initial direction $W^0 = g^0$.
5. Solve $MV^m = N^T W^m$.
6. Compute $\rho^m = \frac{\sum(\Delta\zeta_1^m - \Delta\zeta_2^m)W^m}{\sum(V_1^m - V_2^m)W^m}$.
7. Advance q , using $q^{m+1} = q^m + \rho^m W^m$.
8. Solve $M\Delta\zeta^{m+1} = f - N^T q^{m+1}$.
9. Compute the new error $g^{m+1} = \Delta\zeta_1^{m+1} - \Delta\zeta_2^{m+1}$ and stop if it falls under a specified control parameter.
10. Compute $\mu^m = \frac{\sum(\Delta\zeta_1^{m+1} - \Delta\zeta_2^{m+1})^2}{\sum(\Delta\zeta_1^m - \Delta\zeta_2^m)^2}$.
11. Define the new direction $W^{m+1} = g^{m+1} + \mu^m W^m$.
12. Increase m and go back to 5.

The two solutions, $\Delta\zeta_1$ and $\Delta\zeta_2$ are averaged point by point, to get the final $\Delta\zeta$ solution. The new values of ζ are given by

$$\zeta^{n+1} = \zeta^n + \Delta\zeta \quad (3.97)$$

The new surface elevation values are the inserted into the discrete form of equations 3.74 and 3.75 to get the new flux values.

$$\begin{aligned}
 U_{i+\frac{1}{2},j}^{\xi^{n+1}} = & \frac{U_{i+\frac{1}{2},j}^{\xi^{***}}}{\beta_{i+\frac{1}{2},j}^{***}} - \frac{gH_{i+\frac{1}{2},j}^n \Delta t}{\beta_{i+\frac{1}{2},j}^{***} A_{i+\frac{1}{2},j}} \left[y_{\eta_{i+\frac{1}{2},j}} \left(y_{\eta_{i+1,j}} \zeta_{i+1,j}^{n+1} - y_{\eta_{i,j}} \zeta_{i,j}^{n+1} \right) \right. \\
 & + x_{\eta_{i+\frac{1}{2},j}} \left(x_{\eta_{i+1,j}} \zeta_{i+1,j}^{n+1} - x_{\eta_{i,j}} \zeta_{i,j}^{n+1} \right) - y_{\eta_{i+\frac{1}{2},j}} \left(y_{\xi_{i+\frac{1}{2},j+\frac{1}{2}}} \zeta_{i+\frac{1}{2},j+\frac{1}{2}}^n \right. \\
 & \left. \left. - y_{\xi_{i+\frac{1}{2},j-\frac{1}{2}}} \zeta_{i+\frac{1}{2},j-\frac{1}{2}}^n \right) - x_{\eta_{i+\frac{1}{2},j}} \left(x_{\xi_{i+\frac{1}{2},j+\frac{1}{2}}} \zeta_{i+\frac{1}{2},j+\frac{1}{2}}^n \right. \right. \\
 & \left. \left. - x_{\xi_{i+\frac{1}{2},j-\frac{1}{2}}} \zeta_{i+\frac{1}{2},j-\frac{1}{2}}^n \right) \right] + \frac{\Delta t}{\beta_{i+\frac{1}{2},j}^{***} \rho} y_{\eta_{i+\frac{1}{2},j}} \tau_{wx_{i+\frac{1}{2},j}} \\
 & - \frac{\Delta t}{\beta_{i+\frac{1}{2},j}^{***} \rho} x_{\eta_{i+\frac{1}{2},j}} \tau_{wy_{i+\frac{1}{2},j}} \quad (3.98)
 \end{aligned}$$

$$\begin{aligned}
 U_{i,j+\frac{1}{2}}^{\eta^{n+1}} = & \frac{U_{i,j+\frac{1}{2}}^{\eta^{***}}}{\beta_{i,j+\frac{1}{2}}^{***}} + \frac{gH_{i,j+\frac{1}{2}}^n \Delta t}{\beta_{i,j+\frac{1}{2}}^{***} A_{i,j+\frac{1}{2}}} \left[y_{\xi_{i,j+\frac{1}{2}}} \left(y_{\eta_{i+\frac{1}{2},j+\frac{1}{2}}} \zeta_{i+\frac{1}{2},j+\frac{1}{2}}^{n+1} \right. \right. \\
 & \left. \left. - y_{\eta_{i-\frac{1}{2},j+\frac{1}{2}}} \zeta_{i-\frac{1}{2},j+\frac{1}{2}}^{n+1} \right) + x_{\xi_{i,j+\frac{1}{2}}} \left(x_{\eta_{i+\frac{1}{2},j+\frac{1}{2}}} \zeta_{i+\frac{1}{2},j+\frac{1}{2}}^{n+1} \right. \right. \\
 & \left. \left. - x_{\eta_{i-\frac{1}{2},j+\frac{1}{2}}} \zeta_{i-\frac{1}{2},j+\frac{1}{2}}^{n+1} \right) - y_{\xi_{i,j+\frac{1}{2}}} \left(y_{\xi_{i,j+1}} \zeta_{i,j+1}^n - y_{\xi_{i,j}} \zeta_{i,j}^n \right) \right. \\
 & \left. \left. - x_{\xi_{i,j+\frac{1}{2}}} \left(x_{\xi_{i,j+1}} \zeta_{i,j+1}^n - x_{\xi_{i,j}} \zeta_{i,j}^n \right) \right] - \frac{\Delta t}{\beta_{i,j+\frac{1}{2}}^{***} \rho} y_{\eta_{i,j+\frac{1}{2}}} \tau_{wx_{i,j+\frac{1}{2}}} \\
 & + \frac{\Delta t}{\beta_{i,j+\frac{1}{2}}^{***} \rho} x_{\eta_{i,j+\frac{1}{2}}} \tau_{wy_{i,j+\frac{1}{2}}} \quad (3.99)
 \end{aligned}$$

3.8 The Boundary Conditions

The present model works only for closed basins, with no-slip and no-flow through boundary condition. Both flux components are taken to be 0 at the boundary, and the surface displacement is taken to be the same as at the nearest cell, or, which is the same, the surface displacement gradient is taken to be 0 at the boundary.

? ainda não assim ?

3.9 Numerical Stability

The complex character of the Navier-Stokes equations and the non-linearity of some of its terms makes it very difficult to formally analyze the numerical stability of the schemes used. As a guideline for the largest admissible time step, however, and since the advection and diffusion terms are solved explicitly, the stability criteria valid for linear equations can be used:

$$\Delta t \leq \frac{\Delta x}{2u} \quad (3.100)$$

$$\Delta t \leq \frac{(\Delta x)^2}{4A_H} \quad (3.101)$$

where the minimum linear dimension of the grid cells and the maximum velocity in the basin should be used.

Since the U^n term in the U^{ξ} Coriolis equation is also treated explicitly, the Coriolis stability condition,

$$\Delta t \leq \frac{1}{f} \quad (3.102)$$

can also be used as an indication. This condition is, in general, much less stringent than 3.100, and it is unlikely to become a limitation on the possible time step.

Finally, the stability condition associated with the propagation step is

$$\Delta t \leq \frac{\Delta x}{\sqrt{2gH}} \quad (3.103)$$

Since the cross-derivative terms in the propagation step are treated explicitly, it was not clear if this condition would effectively impose a limit to the possible time step or not. However, several test cases were run with time steps up to five times higher than this condition would allow, without any stability problems.

Equation 3.100 seems therefore to be, in the usual cases, the best indication of the stability condition for the whole model.

The fact that the time derivatives are approached by forward differences and the spatial derivatives by centered differences leads to first-order accuracy in time and second-order accuracy in space.

CHAPTER 4 APPLICATIONS

After the development of a numerical model, it is necessary to validate it by comparing its results with analytical solutions or with results obtained with well-known models whose accuracy has been, in due time, proved.

In the present case, a number of tests were run with the present model and with the two-dimensional version of the three-dimensional model CH3D, which has been well tested, as presented in, Sheng (1987), Sheng et al. (1988) and Sheng (1989).

4.1 Comparison with Analytical Solution

For the simple case of constant wind over a rectangular basin with flat bottom, if only the pressure and wind terms are retained, the momentum equation in the direction of the wind is reduced to

$$gH \frac{d\zeta}{dx} = \frac{\tau_{wx}}{\rho_0} \quad (4.1)$$

which, when integrated, yields

$$\zeta - \zeta_0 = \frac{\tau_{wx}}{\rho_0 g H} (x - x_0) + C \quad (4.2)$$

(linearized in H)

where the index 0 denotes a known point and C is the constant of integration. To ensure mass conservation, and since the surface elevation gradient is uniform, the

constant of integration is 0 if x_0 is taken to be the center of the basin. Equation 4.2 then becomes

$$\zeta = \frac{\tau_{wz}}{\rho_0 g H} (x - x_0) \quad (4.3)$$

A skewed grid (figure 4.1) was designed for a square basin with $50km \times 50km$ with uniform depth of $3.0m$. The model was run until it reached steady state, for a uniform wind blowing from the west, corresponding to a wind stress of $1dyne/cm^2$ and the results of the simulation were interpolated for a line parallel to the x -axis through the center of the basin. Those results are shown in figure 4.2, together with the analytical results.

4.2 Square Basin with Constant Slope

The same skewed grid as before (figure 4.2) was used, with a uniform bottom slope in the south-north direction. Depth is $7.5m$ at the north end and $2.5m$ at the south end. The Coriolis factor f was taken as $0.00009sec^{-1}$, the eddy viscosity coefficient A_H as $10000cm^2/sec$ and, in modeling the bottom friction, Manning's n was taken as 0.040 . The simulation was run for a constant and uniform wind blowing from the east, with a wind stress $\tau_{wz} = 1dyne/cm^2$, for 2.5 days, with a time-step of $10min$.

The CPU time needed for the computation compared favorably with CH3D (12 min. and 44 sec. against 20 min. and 25 sec.) and the velocity and surface displacement results at the last time step are shown in figures 4.4 and 4.6 for the present model and in figures 4.5 and 4.7 for CH3D. Results at every time-step were recorded at four different points (A through D in figure 4.1) and those results are shown in figures 4.8 and 4.9 for the present model and in figures 4.10 and 4.11 for CH3D.

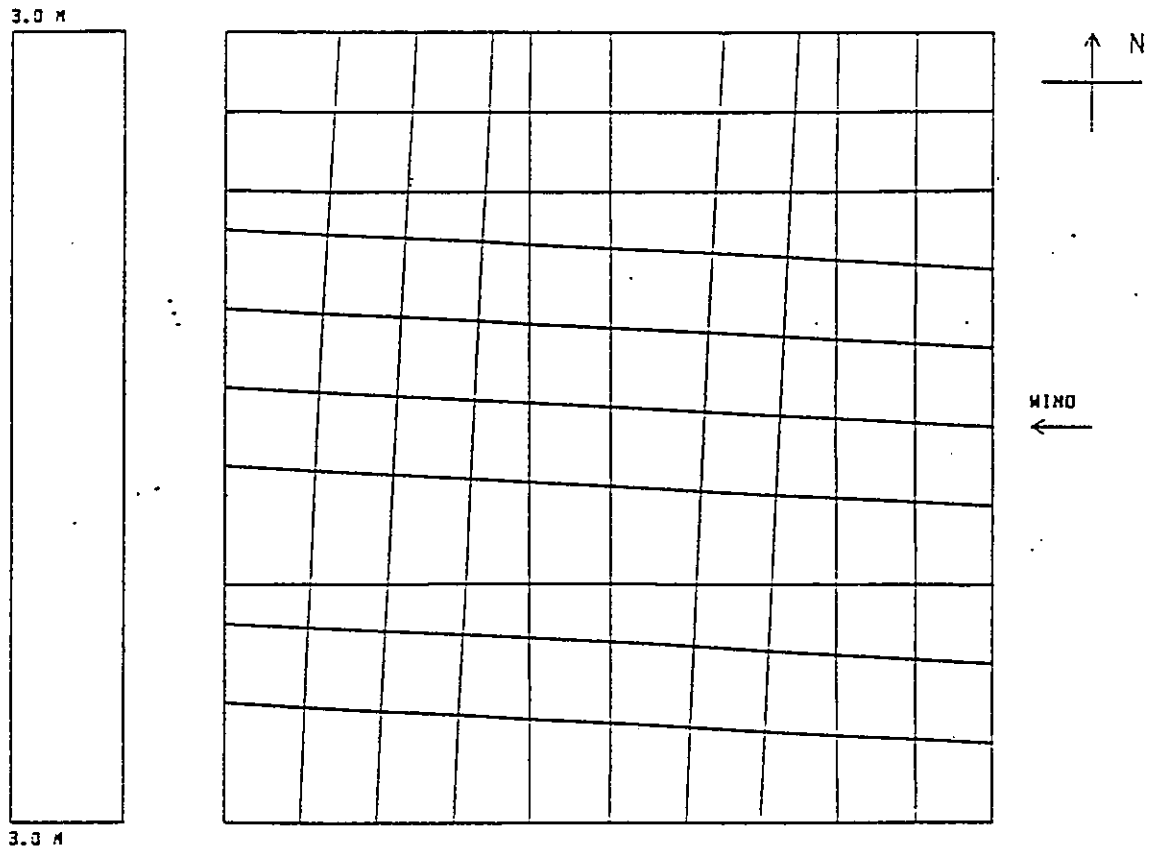


Figure 4.1: Skewed grid for a square basin with uniform depth

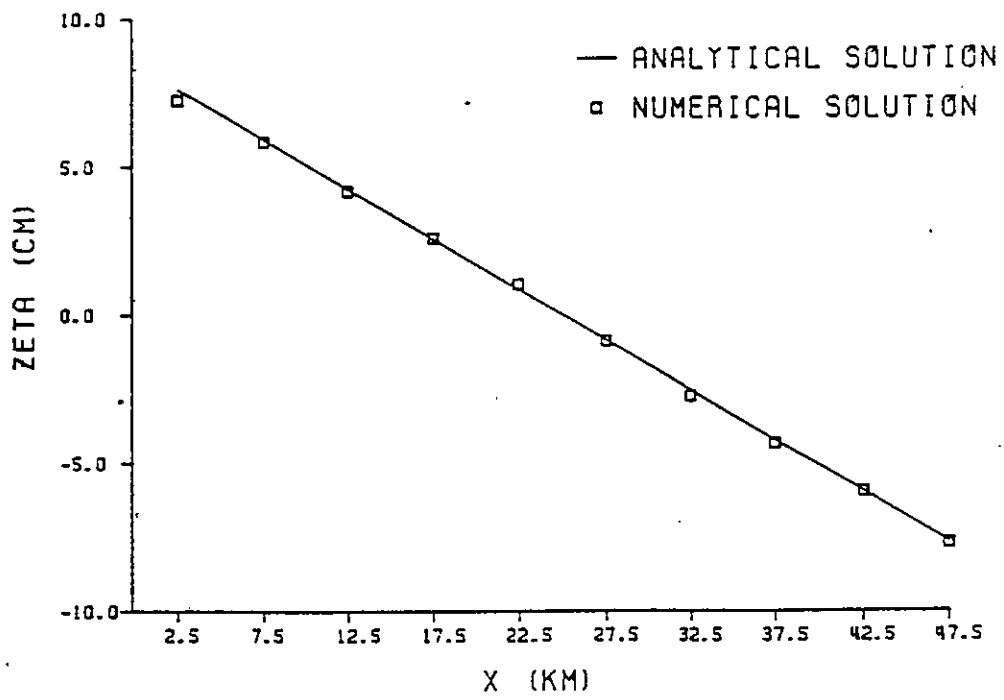


Figure 4.2: Comparison with analytical solution

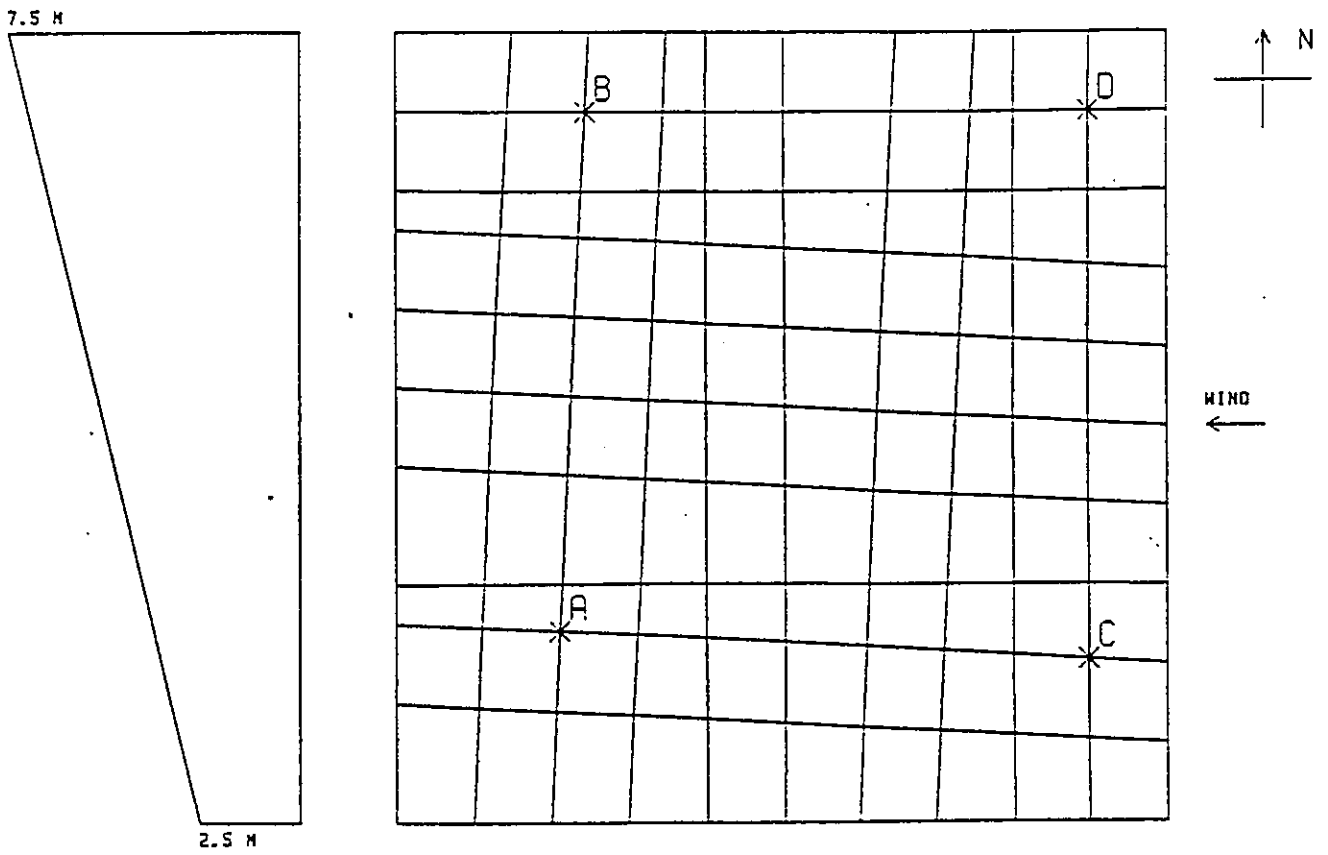


Figure 4.3: Skewed grid for a square basin with uniform bottom slope

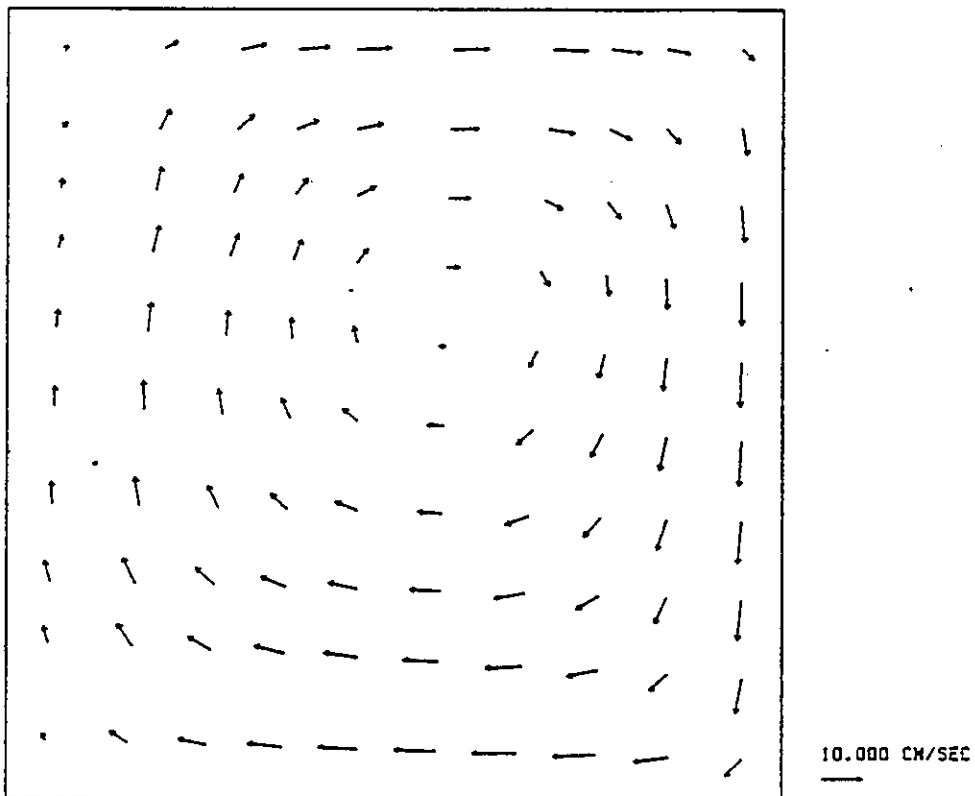


Figure 4.4: Velocity results with constant slope - present model

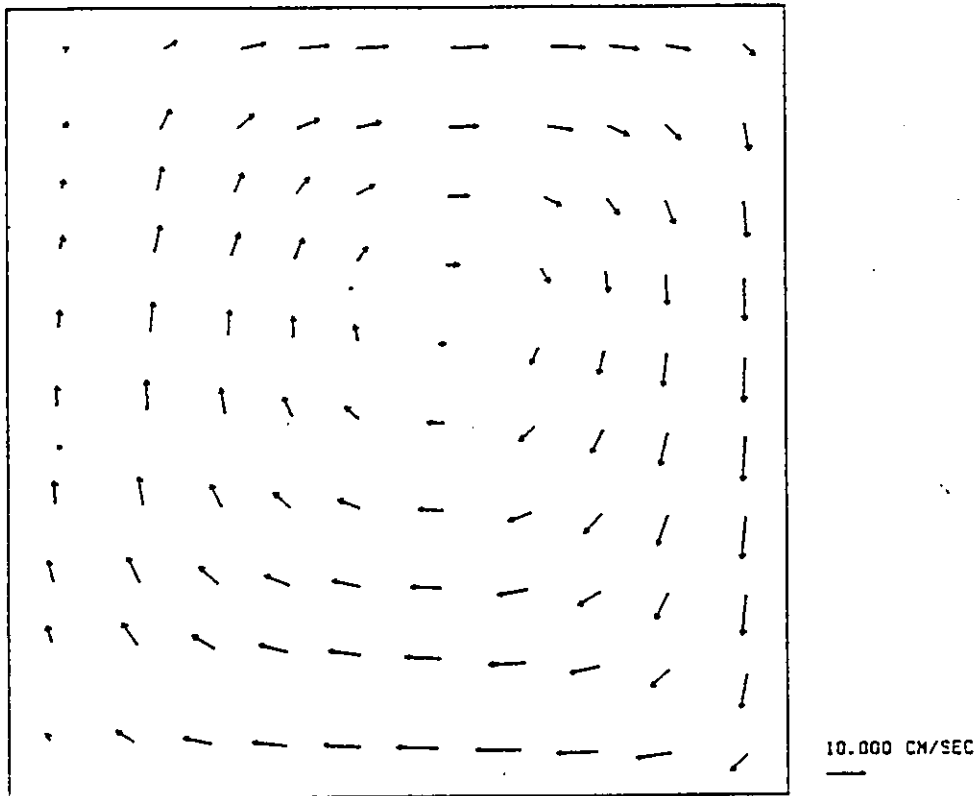


Figure 4.5: Velocity results with constant slope - CH3D

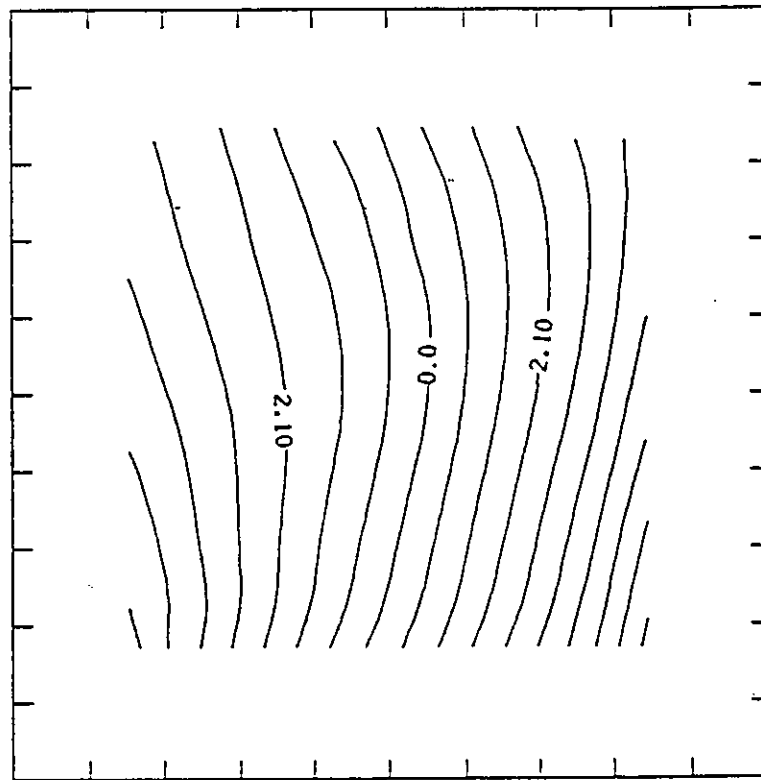


Figure 4.6: Surface elevation with constant slope - present model

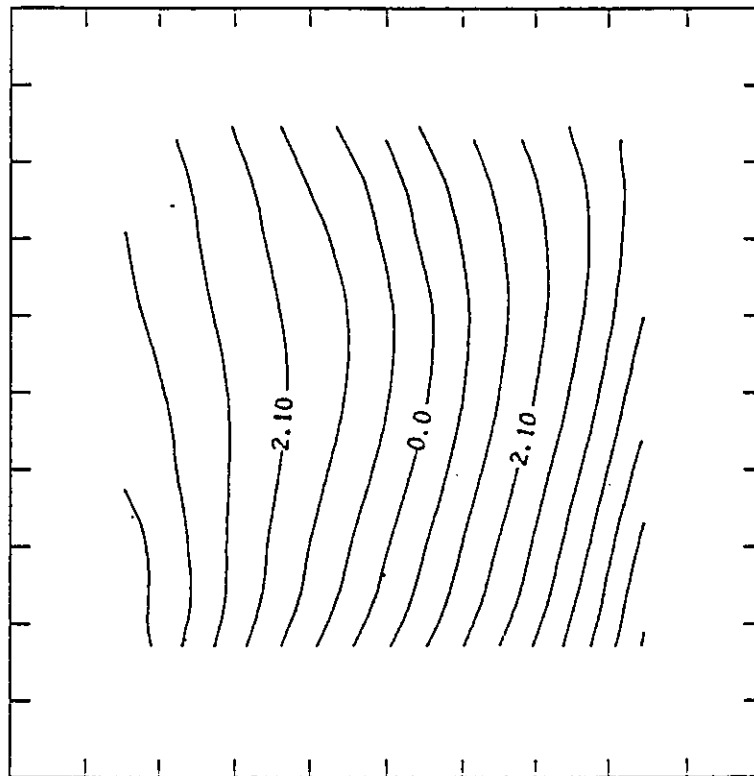


Figure 4.7: Surface elevation with constant slope - CH3D

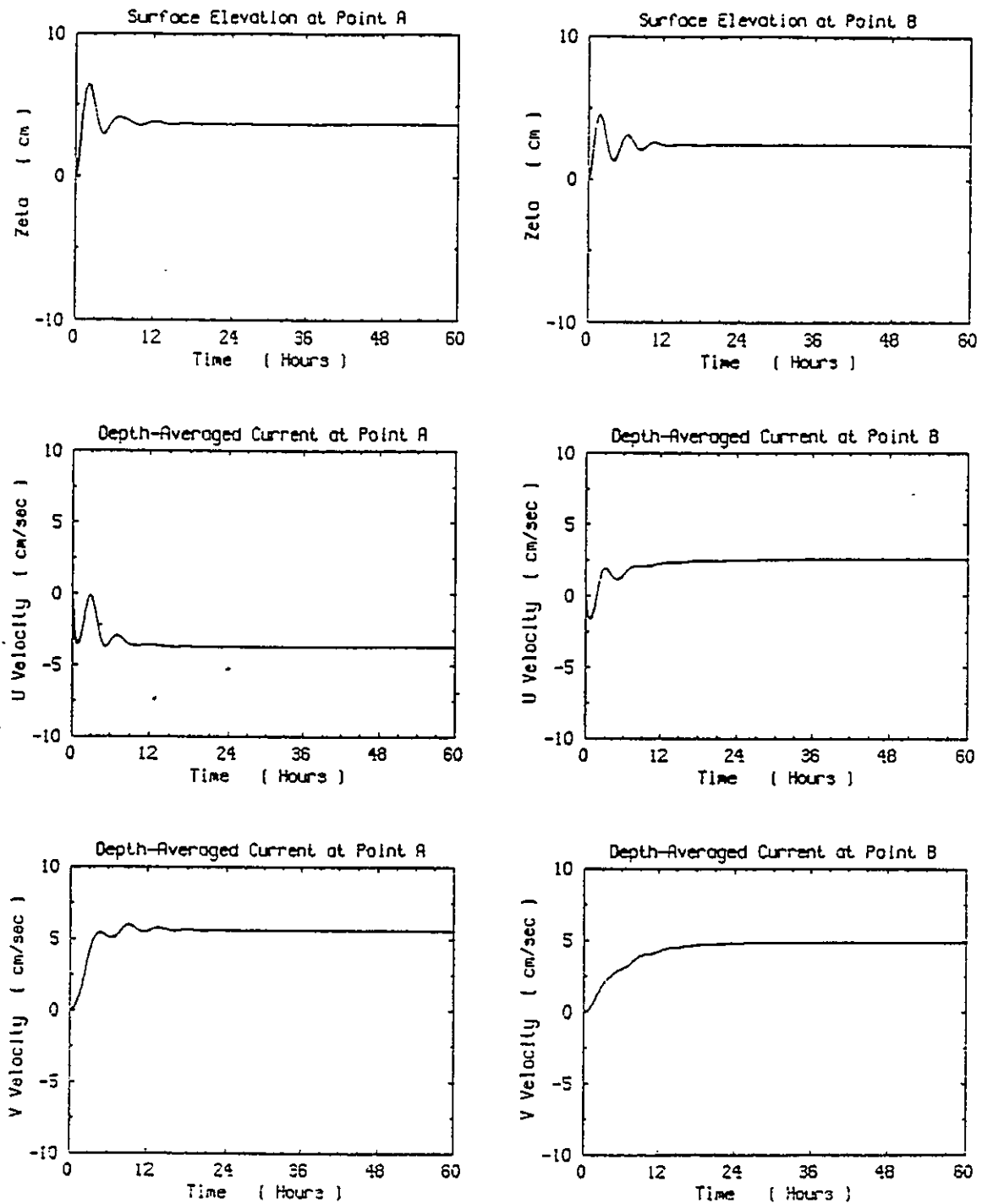


Figure 4.8: Time series results at points A and B - present model

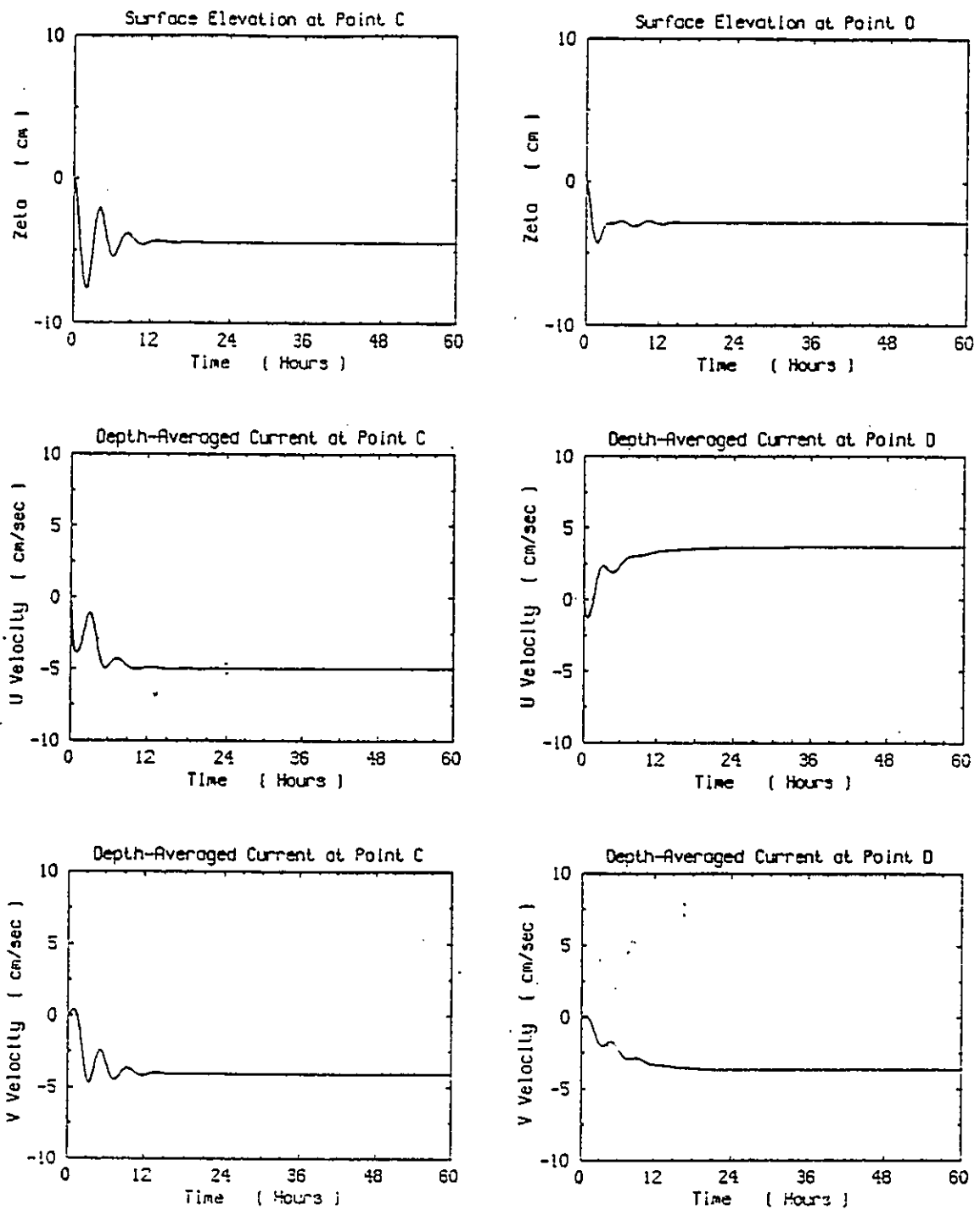


Figure 4.9: Time series results at points C and D - present model

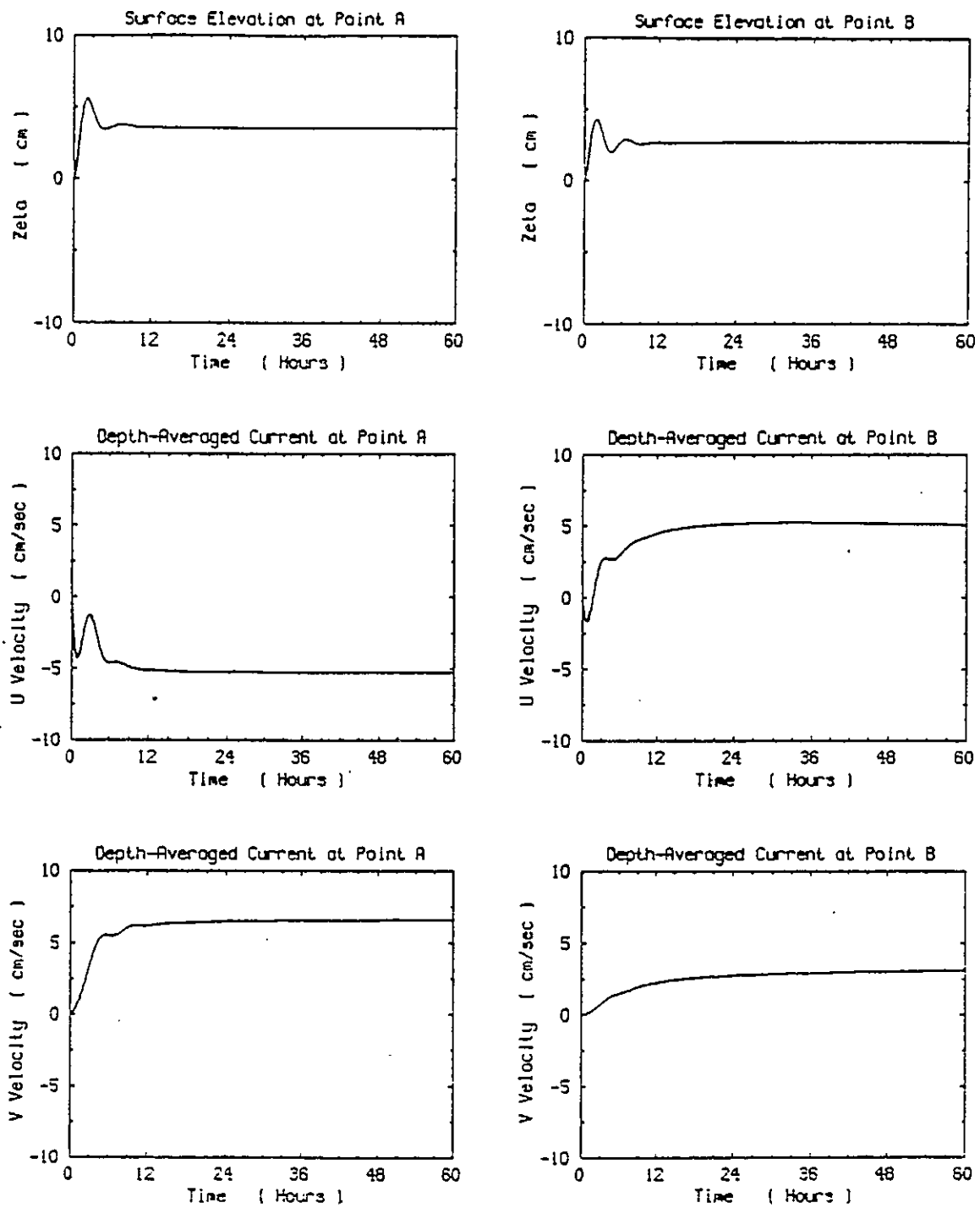


Figure 4.10: Time series results at points A and B - CH3D

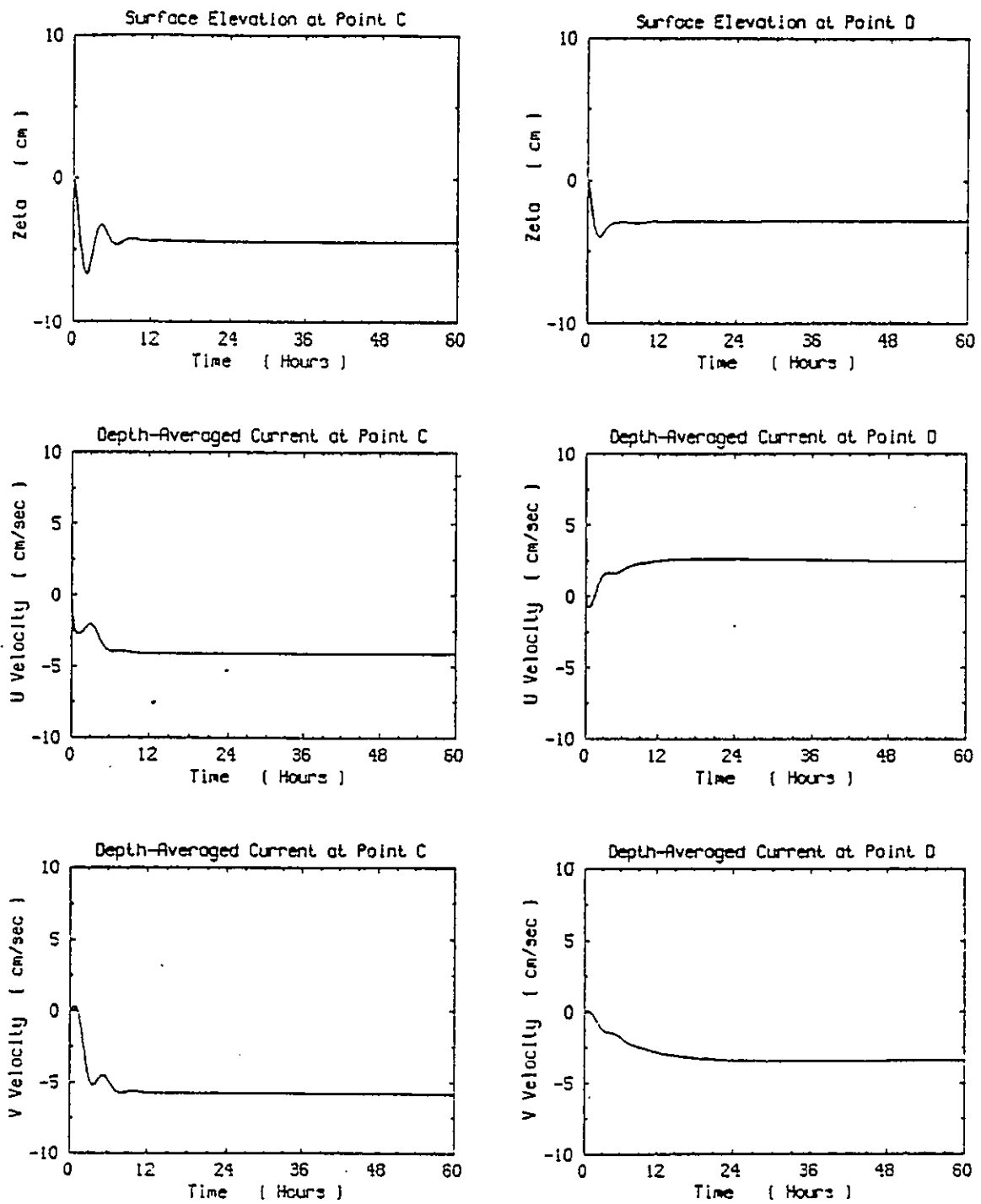


Figure 4.11: Time series results at points C and D - CH3D

The surface displacement results are practically the same for both models, while the velocities computed by the present model are slightly higher than those computed by CH3D. This is consistent with all the other test cases run, and will be discussed in the last chapter.

4.3 Square Basin with V-Shaped Bottom

The same skewed grid (figure 4.12) was used in this problem, with a V-shaped bottom. The deepest part of the basin runs east-west at the center of the basin. Depth is 2.5m at the north and south ends and 5.0m at the center. The Coriolis factor f was taken as 0.00009sec^{-1} , the eddy viscosity coefficient A_H as $10000\text{cm}^2/\text{sec}$ and, in modeling the bottom friction, Manning's n was taken as 0.04. The simulation was run for a constant and uniform wind blowing from the east, with a wind stress $\tau_{wx} = 1\text{dyne}/\text{cm}^2$, for 2.5 days, with a time-step of 10min.

The velocity and surface displacement results at the last time step are shown in figures 4.13 and 4.15 for the present model and in figures 4.14 and 4.16 for CH3D. Results at every time-step were recorded at the same four points and those results are shown in figures 4.17 and 4.18 for the present model and in figures 4.19 and 4.20 for CH3D.

4.4 Lake Okeechobee with Constant Wind

A curvilinear grid (figure 4.21) was designed for Lake Okeechobee, in South Florida. Lake Okeechobee is approximately circular, with an average diameter of more than 50km and depth not exceeding 7m (figure 4.22). At the west end, there is a vast area where depth is less than 1m. The depth values used in the computations were first digitized from a chart, interpolated for the grid nodes and an offset was added to all depth values based on available field data, therefore representing accurately the water level of the lake in the Spring of 1989.

Once again, the Coriolis factor f was taken as 0.00009sec^{-1} , the eddy viscosity coefficient A_H as $10000\text{cm}^2/\text{sec}$ and, in modeling the bottom friction, Manning's n

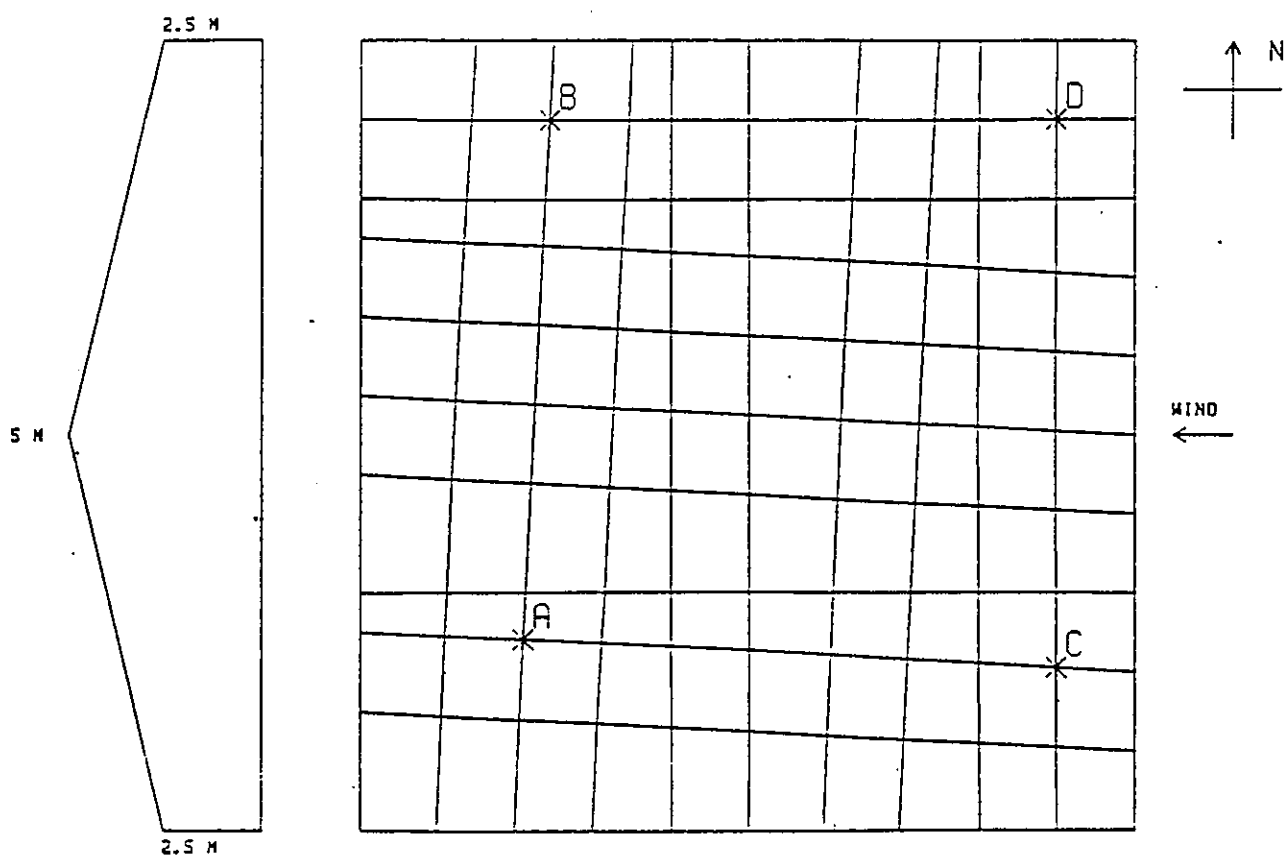


Figure 4.12: Skewed grid for a square basin with V-shaped bottom

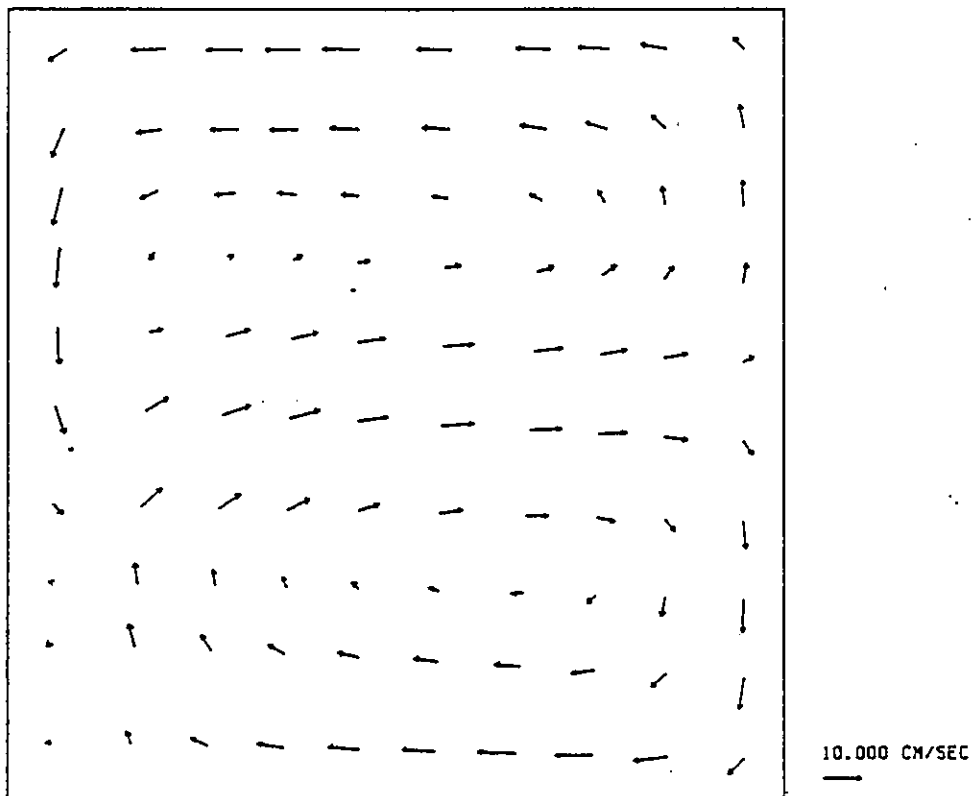


Figure 4.13: Velocity results with V-shaped bottom - present model

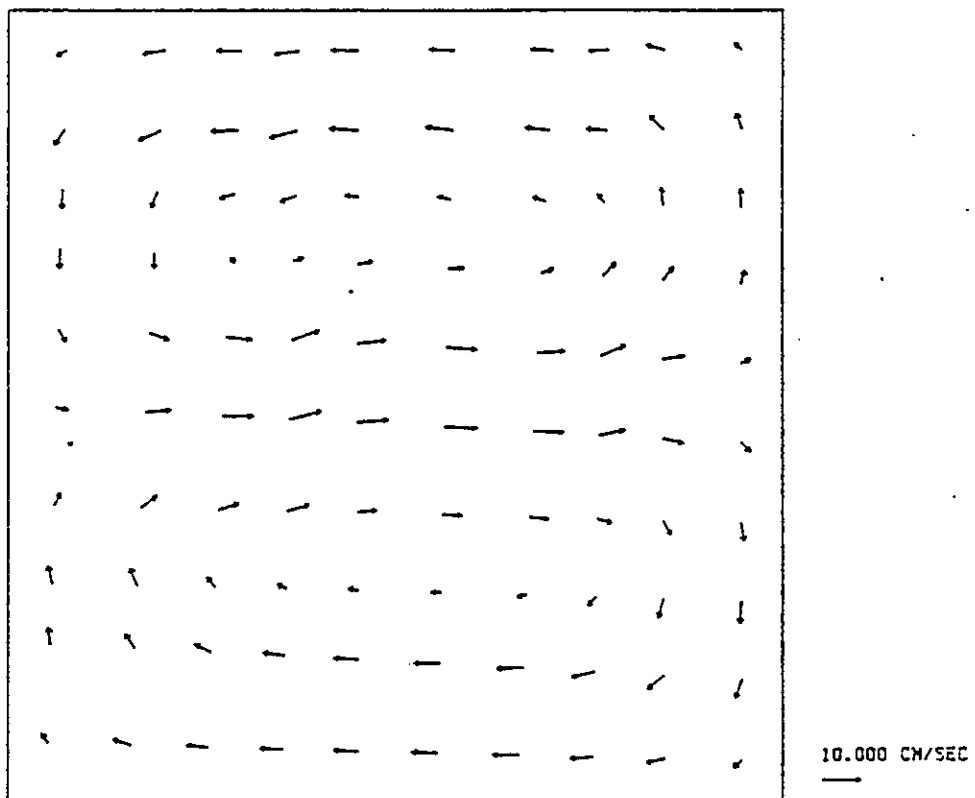


Figure 4.14: Velocity results with V-shaped bottom - CH3D

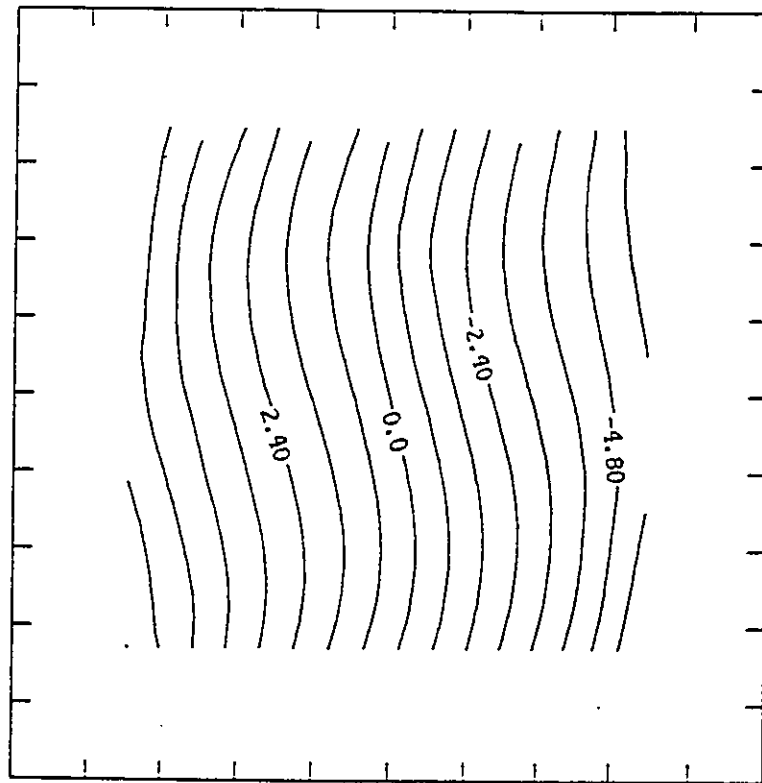


Figure 4.15: Surface elevation with V-shaped bottom - present model

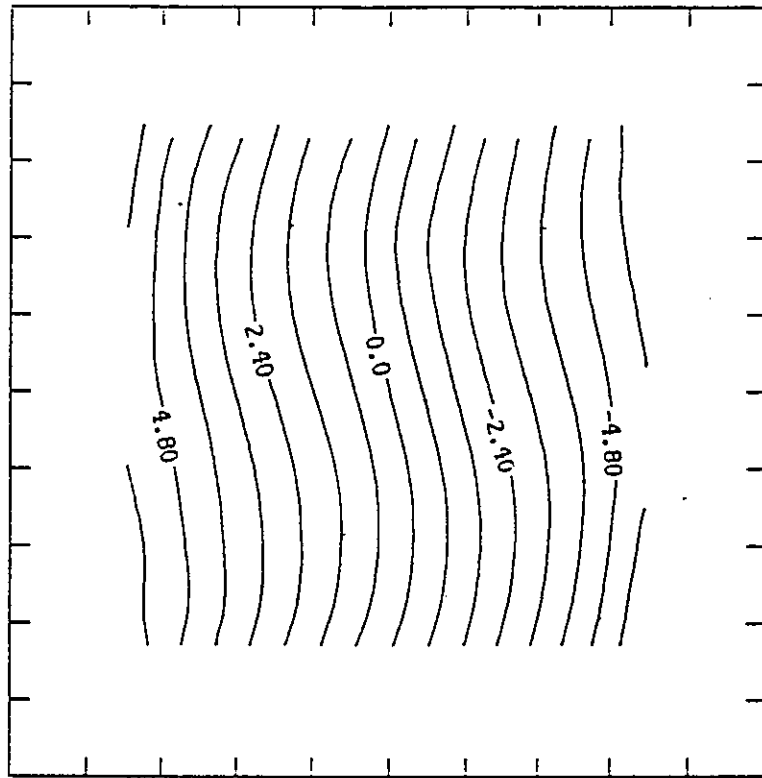


Figure 4.16: Surface elevation with V-shaped bottom - CH3D

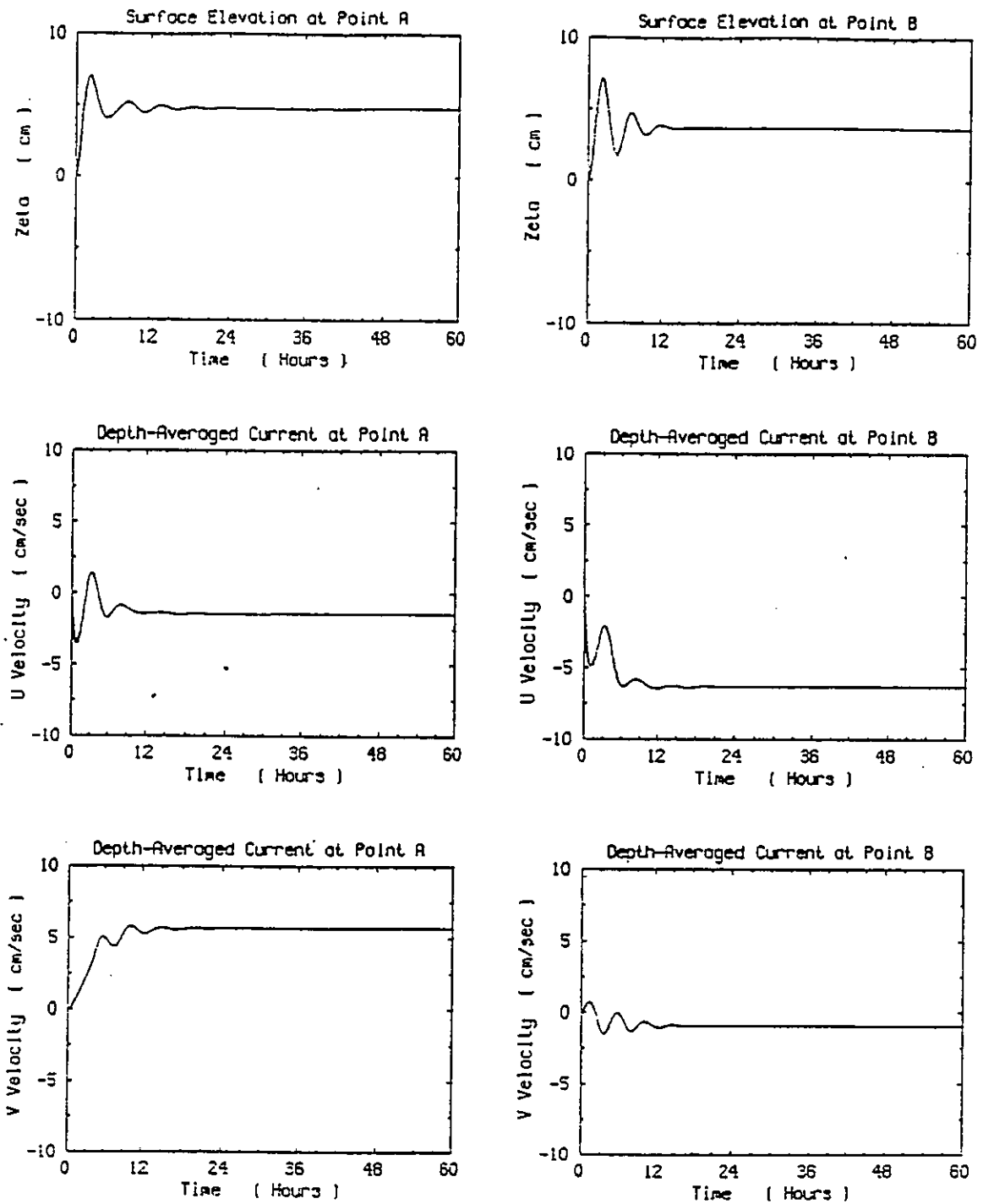


Figure 4.17: Time series results at points A and B - present model

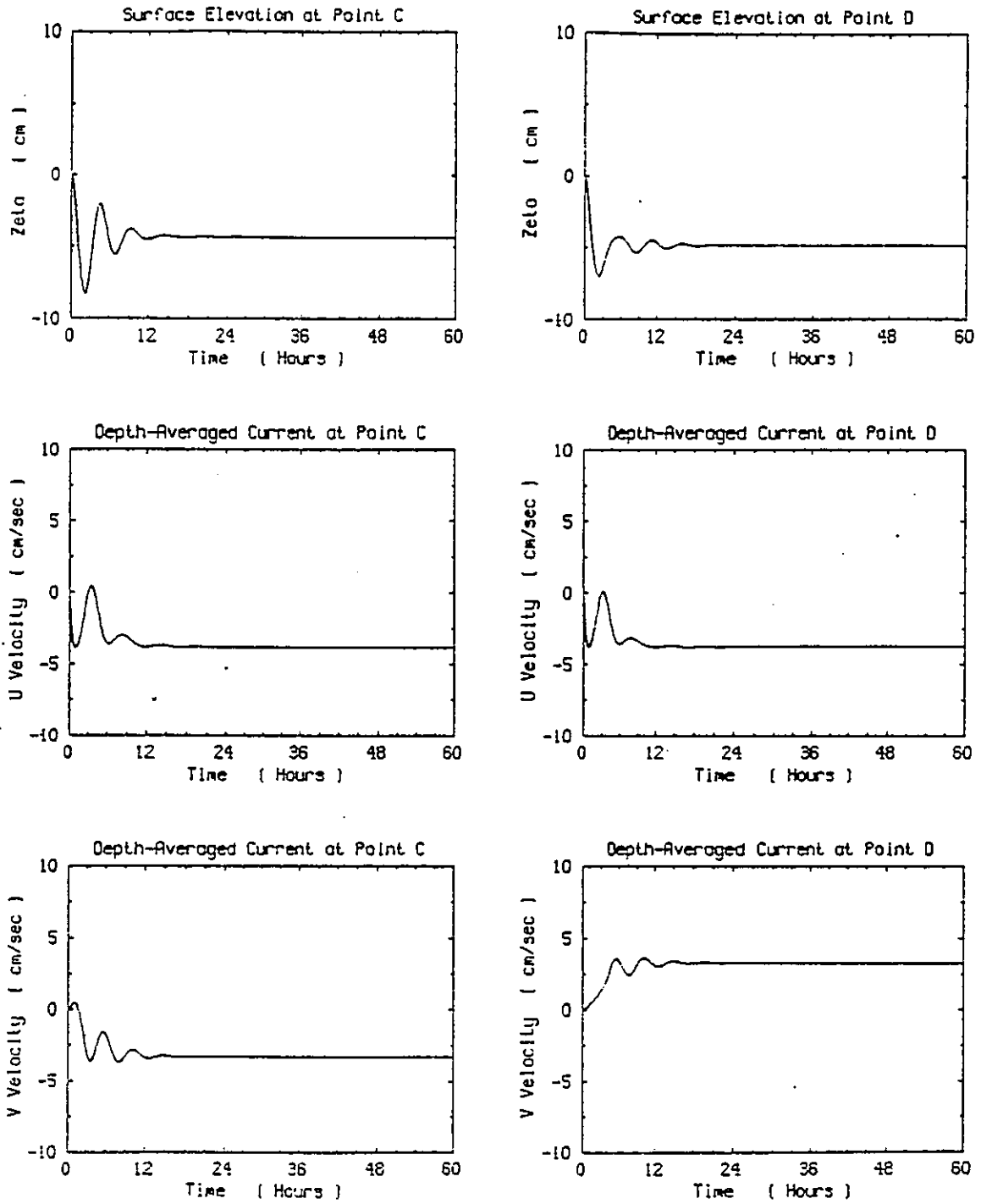


Figure 4.18: Time series results at points C and D - present model

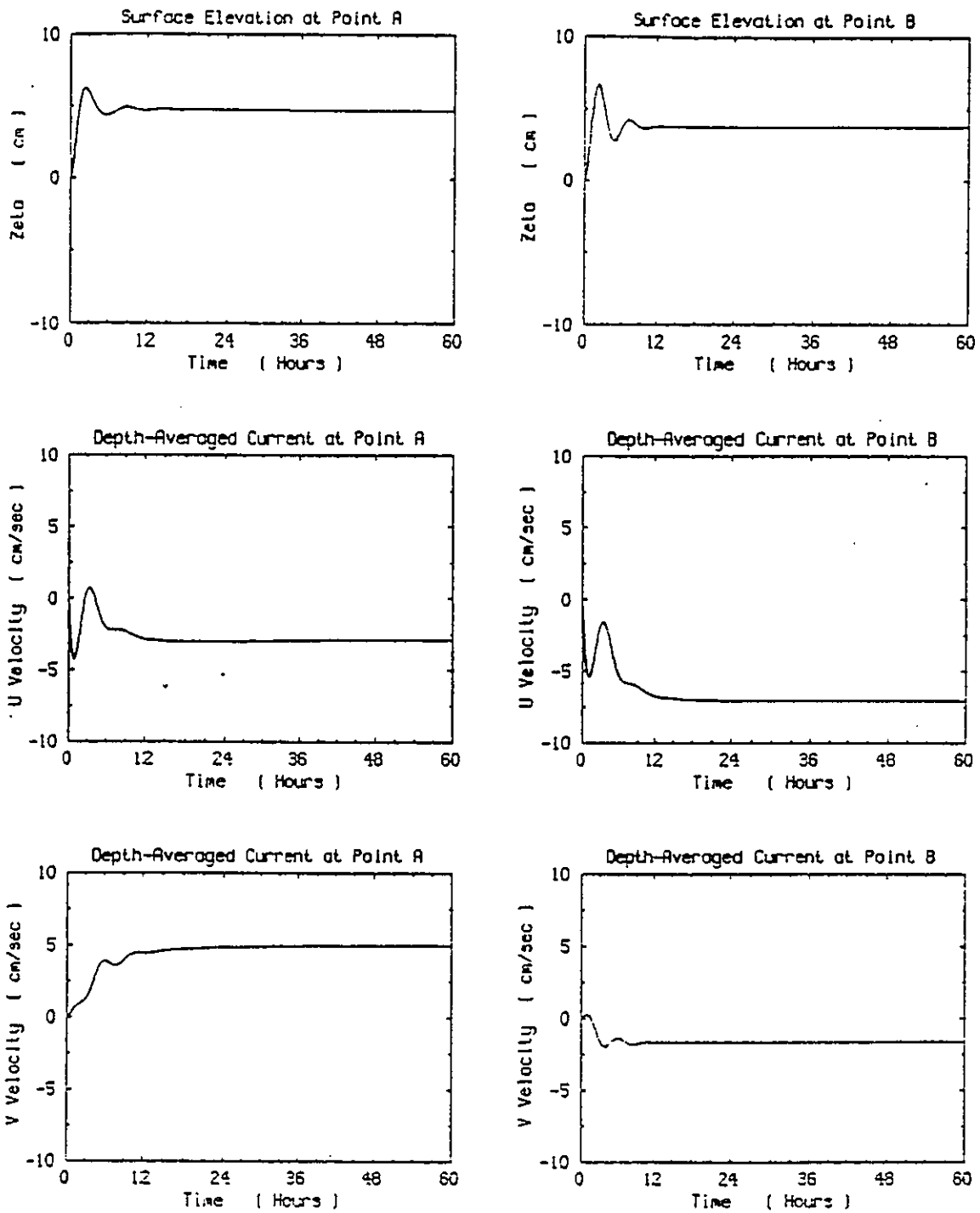


Figure 4.19: Time series results at points A and B - CH3D

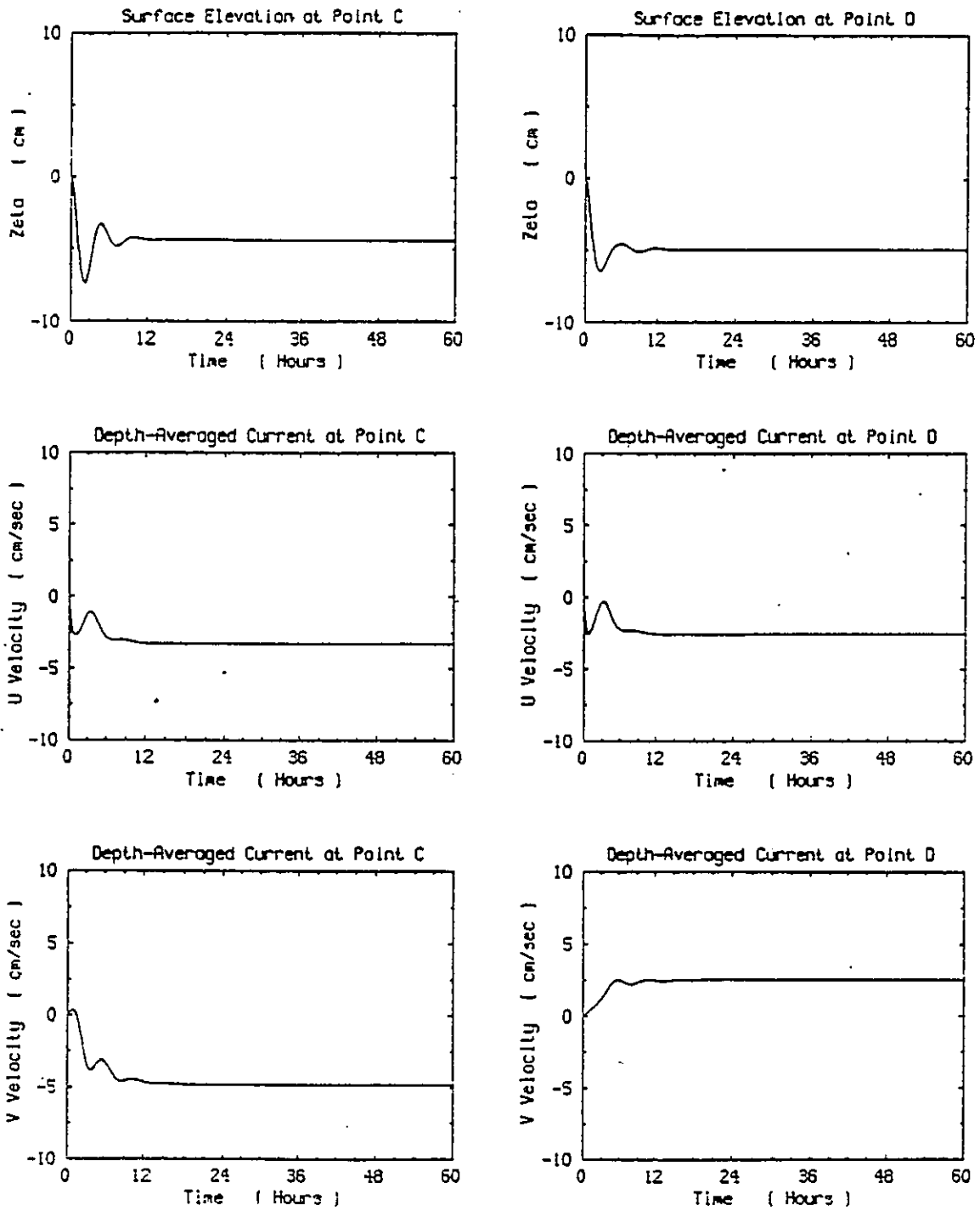


Figure 4.20: Time series results at points C and D - CH3D

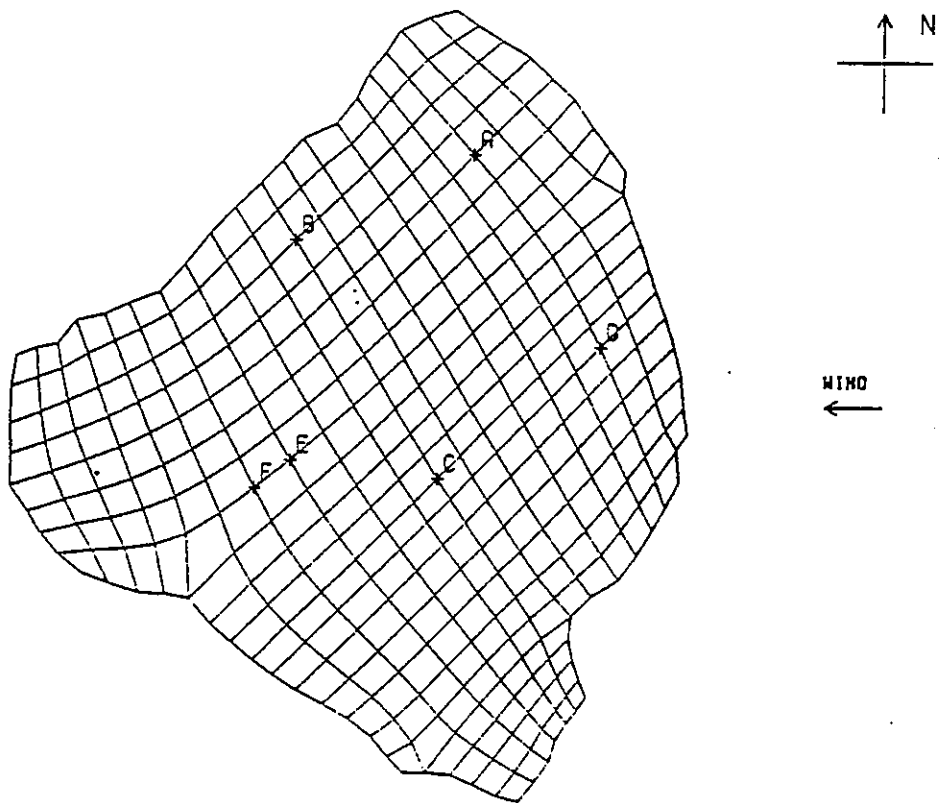


Figure 4.21: Curvilinear grid for Lake Okeechobee



Figure 4.22: Bottom contours for Lake Okeechobee

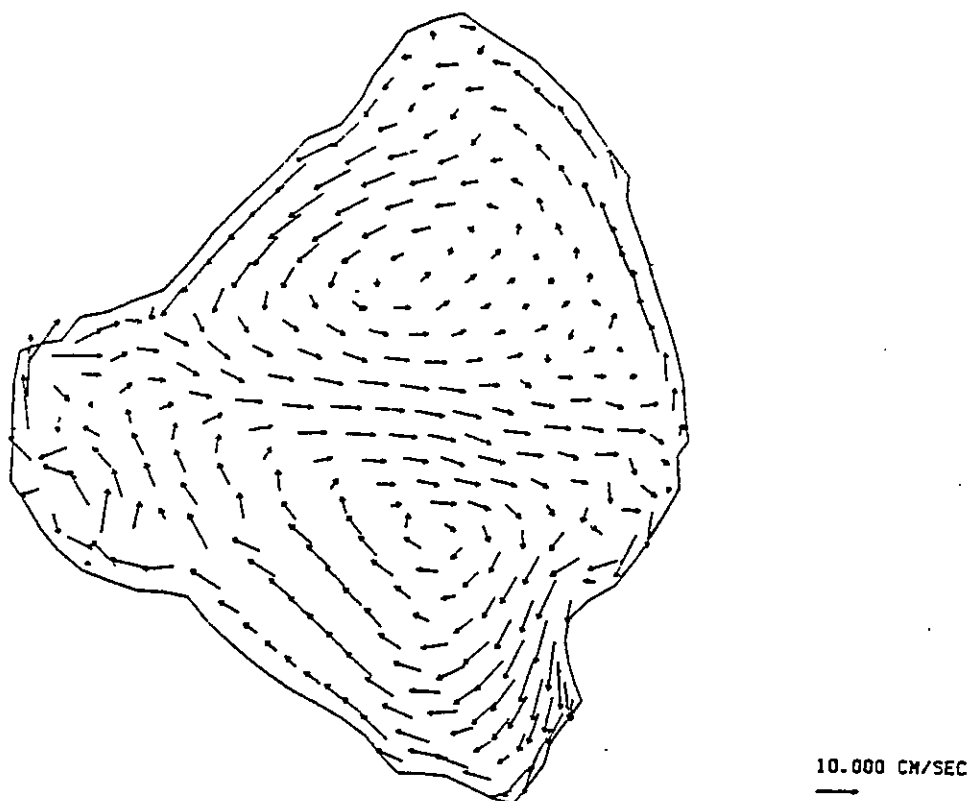


Figure 4.23: Velocity results for Lake Okeechobee - present model

was taken as 0.04. The simulation was run for a constant and uniform wind blowing from the east, with a wind stress $\tau_{wx} = 1 \text{ dyne/cm}^2$, for 2.5 days, with a time-step of 10min.

The velocity and surface displacement results at the last time step are shown in figures 4.23 and 4.25 for the present model and in figures 4.24 and 4.26 for CH3D. Results at every time-step were recorded at six different points (A through E in figure 4.21) and those results are shown in figures 4.27 through 4.29 for the present model and in figures 4.30 through 4.32 for CH3D.

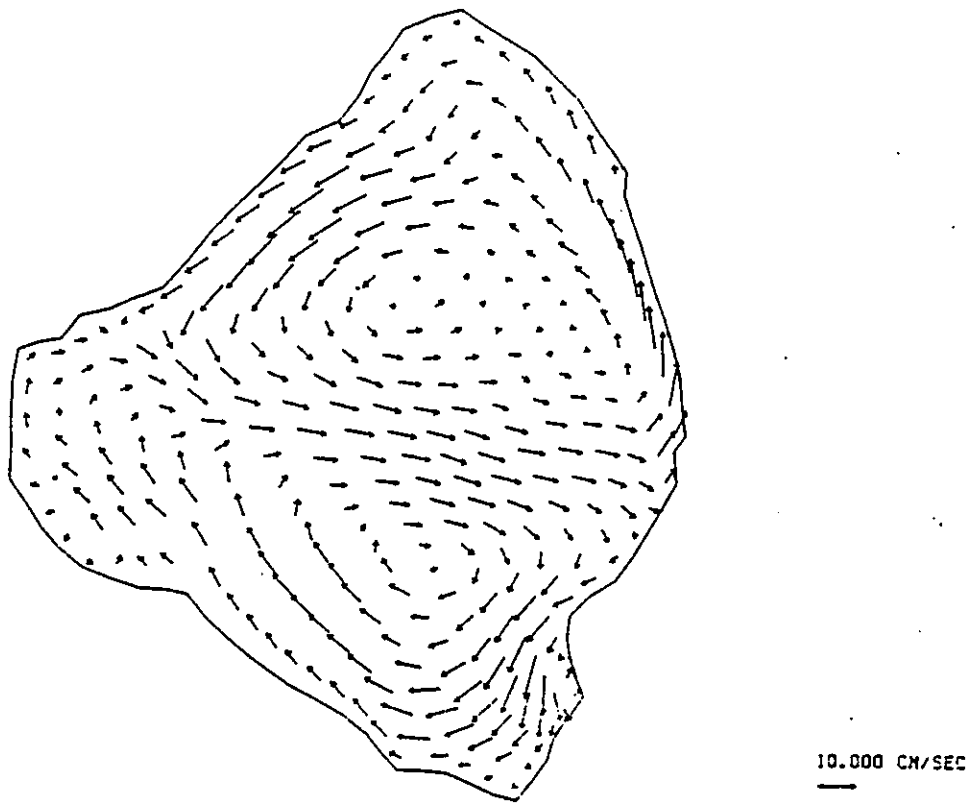


Figure 4.24: Velocity results for Lake Okeechobee - CH3D

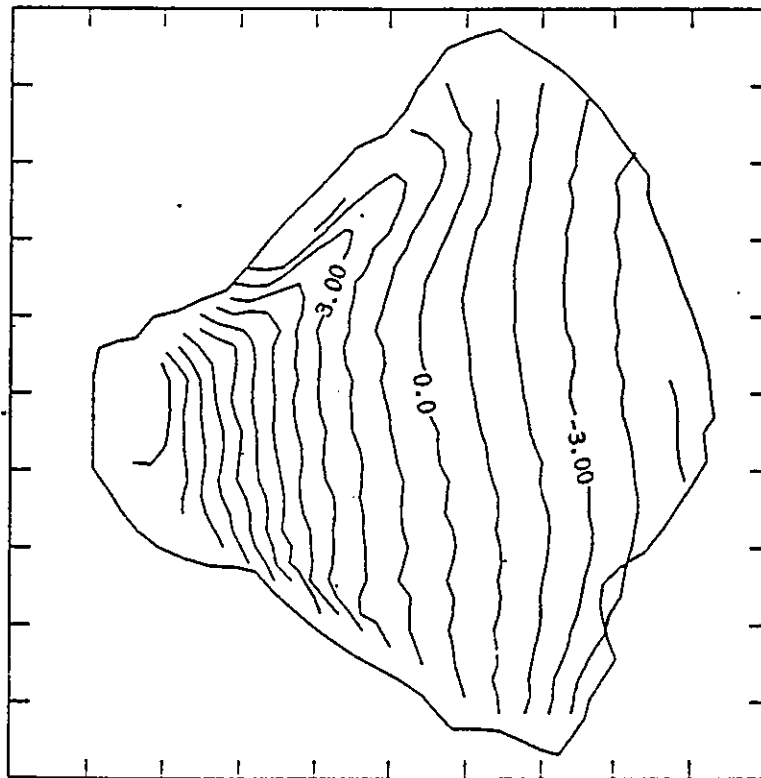


Figure 4.25: Surface elevation for Lake Okeechobee - present model

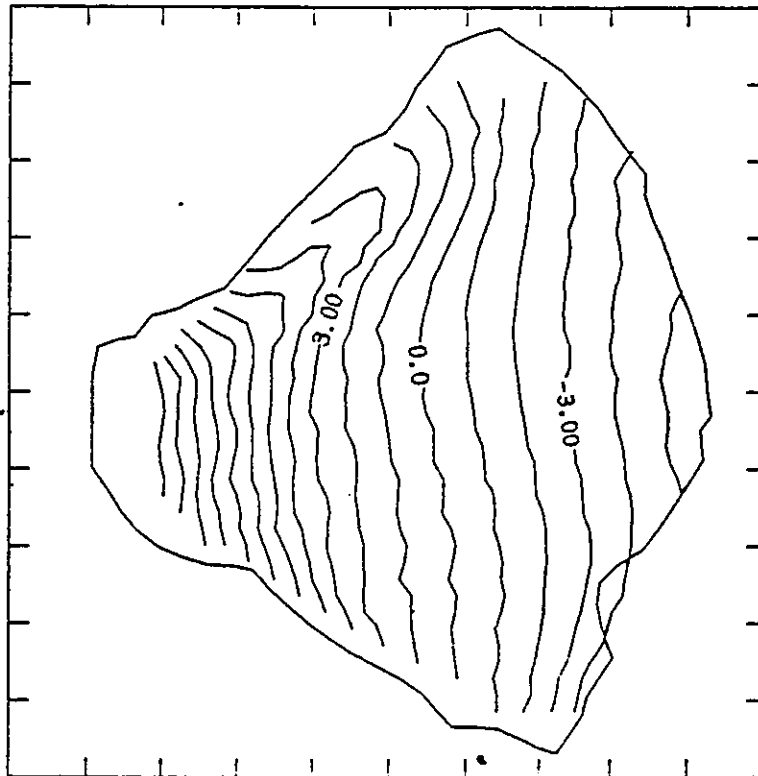


Figure 4.26: Surface elevation for Lake Okeechobee - CH3D

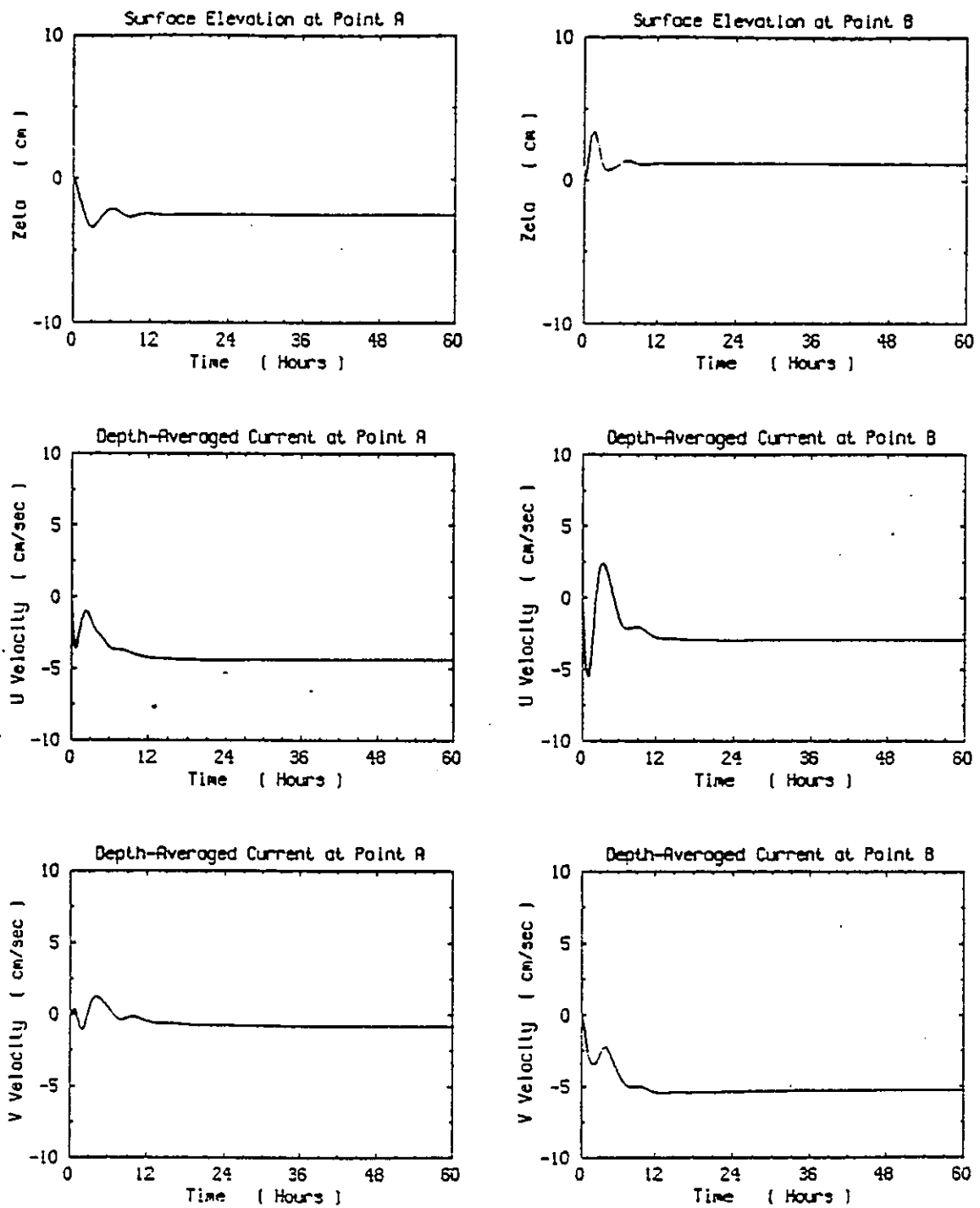


Figure 4.27: Time series results at points A and B - present model

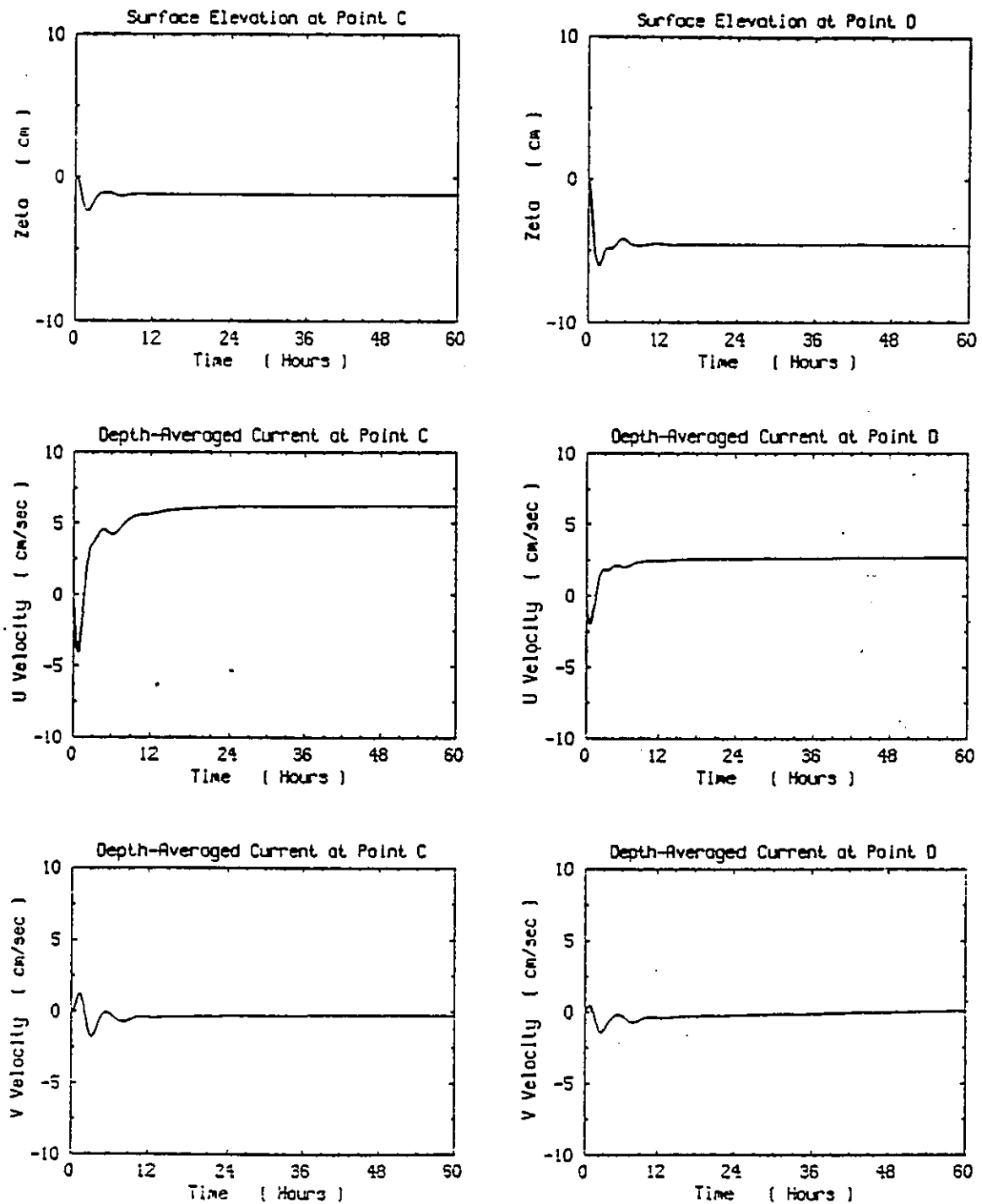


Figure 4.28: Time series results at points C and D - present model

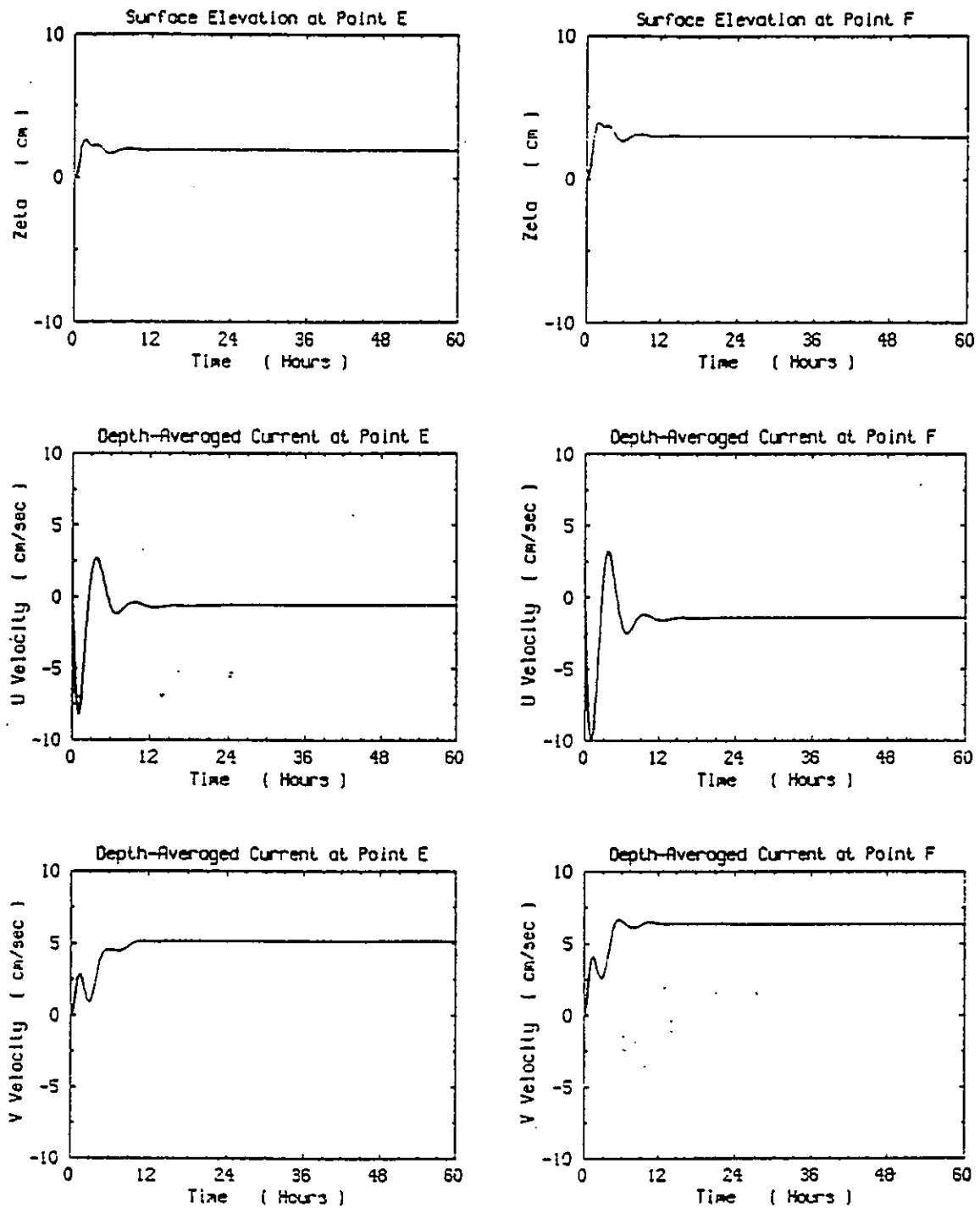


Figure 4.29: Time series results at points E and F - present model

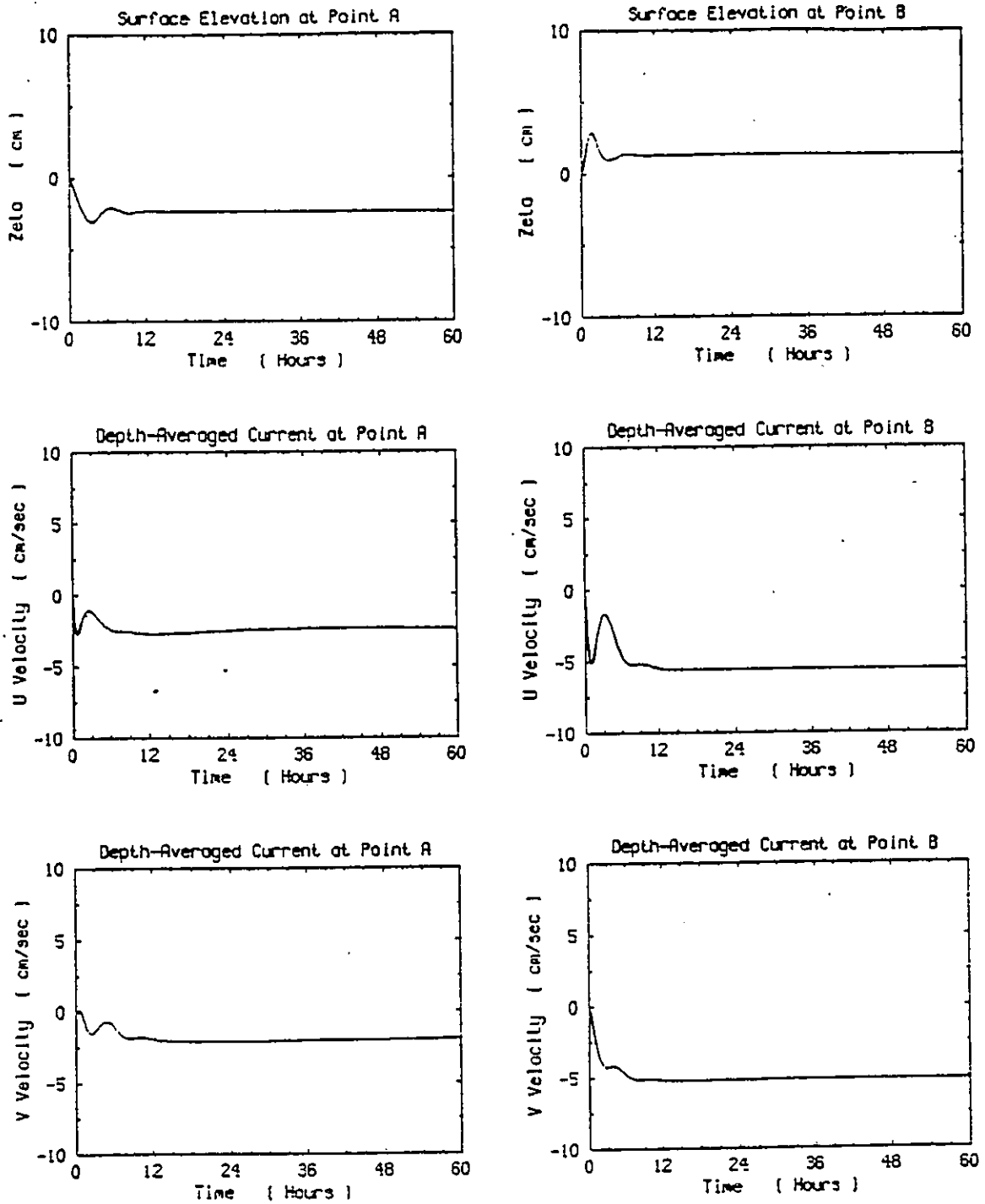


Figure 4.30: Time series results at points A and B - CH3D

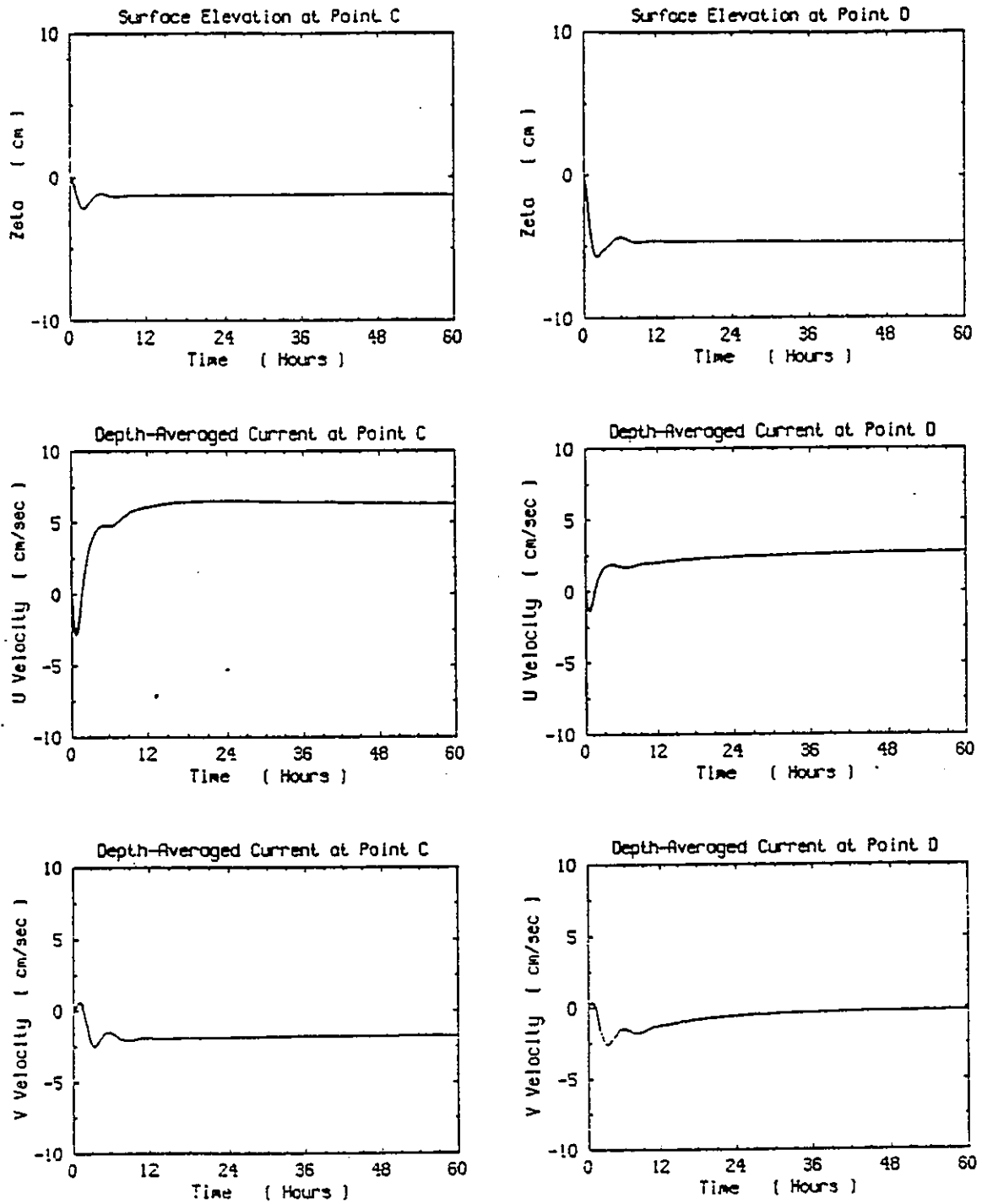


Figure 4.31: Time series results at points C and D - CH3D

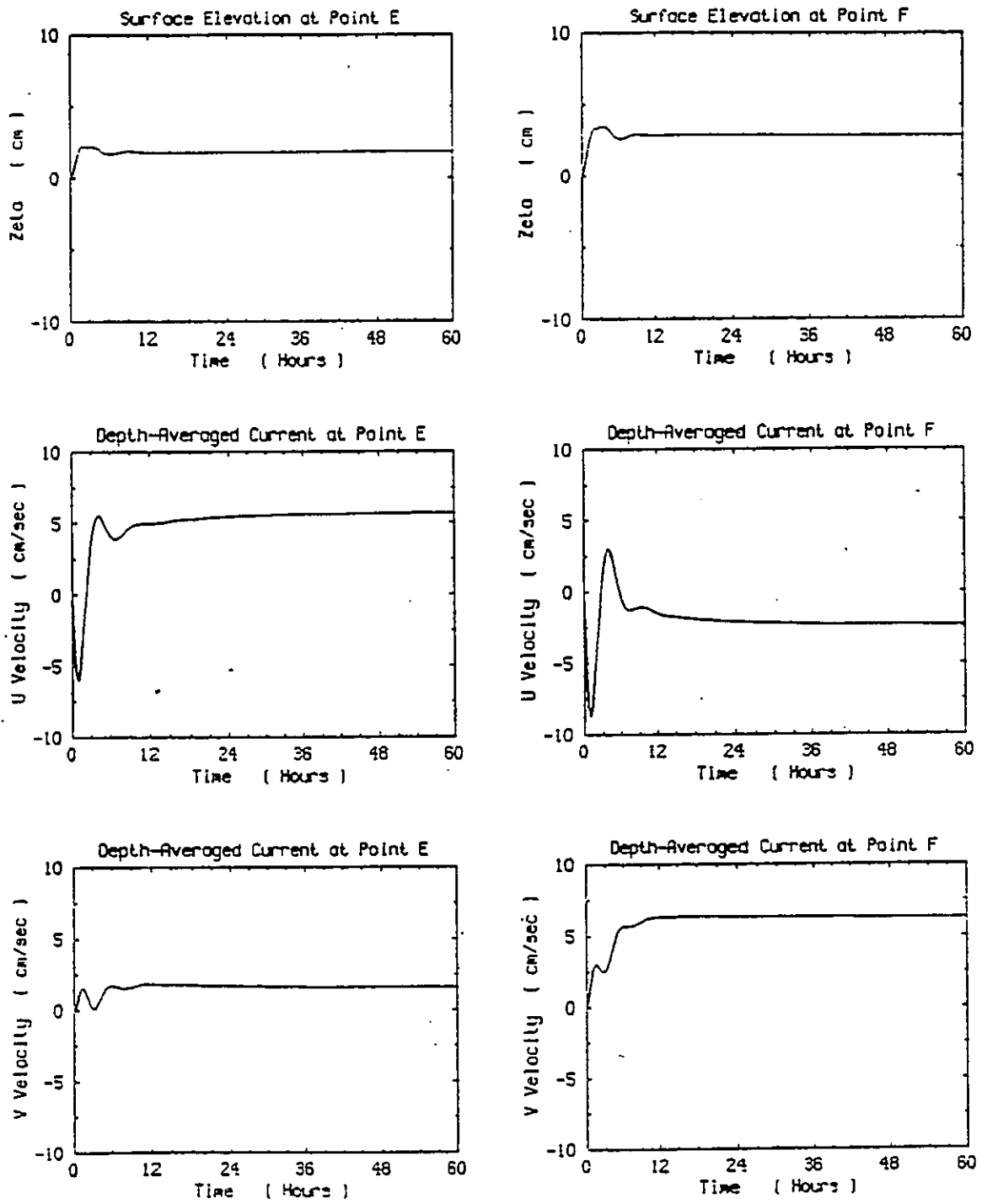


Figure 4.32: Time series results at points E and F - CH3D

4.5 Lake Okeechobee with Sinusoidal Wind

To test the long-term numerical stability of the model, the same problem as before was run, with a uniform wind varying with time. The wind stress was taken to follow a sine wave, of amplitude 1 dyne/cm^2 and period 12 hrs .

The simulation was run for 10 days, and the time-series of the results at the same six points as before are presented in figures 4.33 through 4.35.

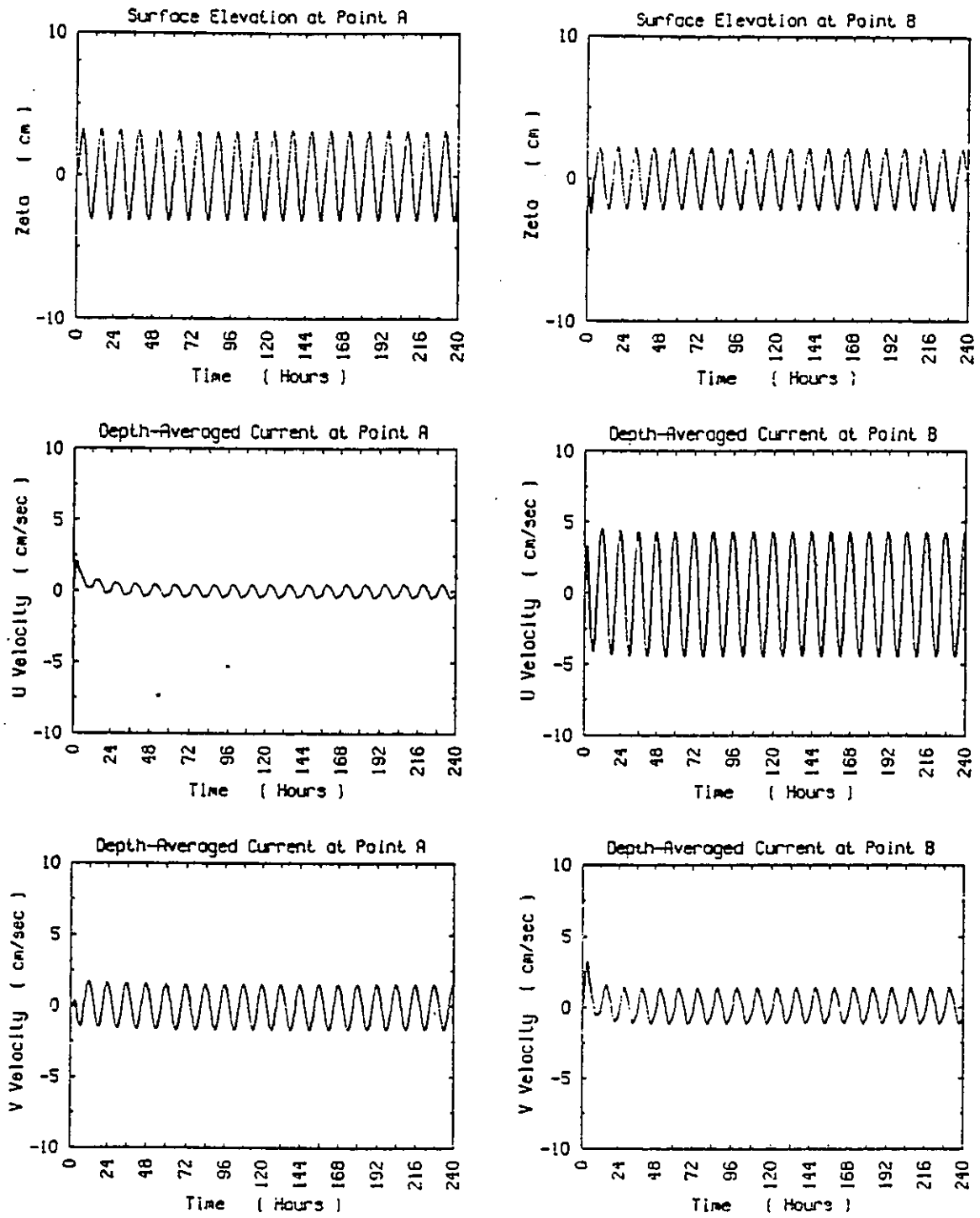


Figure 4.33: Long-term simulation results - points A and B

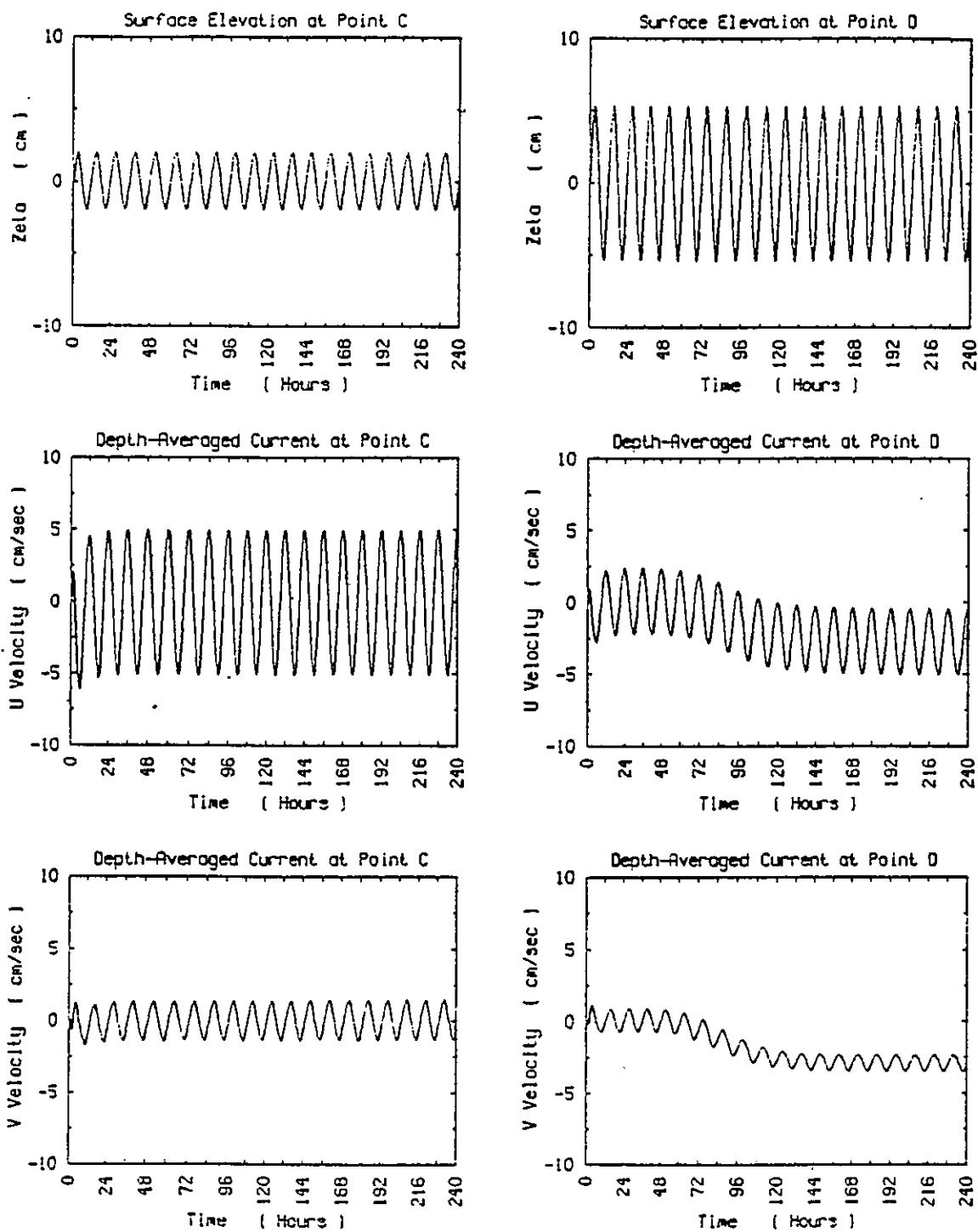


Figure 4.34: Long-term simulation results - points C and D

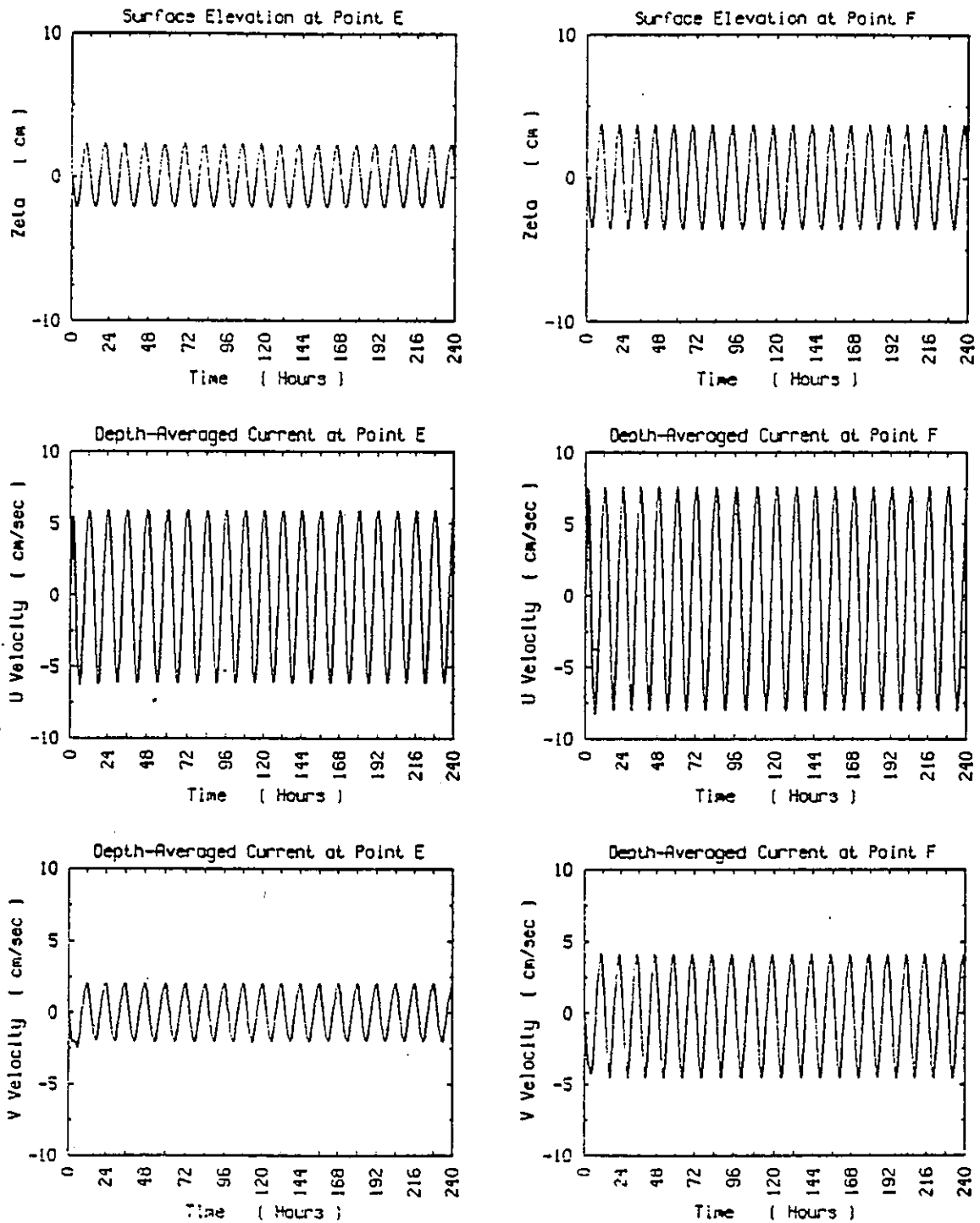


Figure 4.35: Long-term simulation results - points E and F

CHAPTER 5 CONCLUSIONS

The work leading to this thesis was started with the idea that a number of techniques that have been developed for finite difference and finite element models could be successfully applied together with a finite volume approach, therefore combining progress made in different directions in one single model. The time limits involved cut the objectives of this work to a demonstration of the possibilities of the method, instead of a full exploration of those possibilities. Therefore, this chapter is a preview of possible future work more than an analysis of past work.

The advantages that derive from starting the development from the integral form of the conservation equations instead of the differential form of the same equations have been the object of Vinokur (1986) and, therefore, will not be further analyzed here. Being naturally conservative, the resulting equations look considerably simpler than the corresponding finite difference equations, which seems to lead to a considerable economy in terms of computation time. Recent work suggests that a careful combination of cartesian and contravariant velocity components in some terms in the equations might make them simpler. That is one line where future work could bring some developments.

The fractional step method Yanenko (1971), allowing different terms in an equation to be solved using different numerical techniques is a very powerful tool, used before in finite difference models, as in Liu (1988) and in finite element models, as in Baptista (1986). It opens the possibility of avoiding strict stability conditions, by solving implicitly the terms associated with those conditions, allowing, at the same time, other terms in the equations to be solved using simpler techniques, less time

consuming and, therefore, cheaper. It is also possible to use different time steps for different terms in the equations, leading to considerable economy in terms of CPU time.

Using a conjugate gradient method to solve the propagation step involved, as was seen before, the linearization of the cross- derivative terms. It is possible that better ways to deal with the problem can be developed, leading to greater accuracy without losing computational speed.

The more immediate need is, however, the extension of the model to allow for open boundaries, needed to model any estuary or coastal area.

Finally, as was noted in the previous chapter, the velocity results obtained now are consistently higher than those computed by CH3D. This is more evident for smaller depths, as in the westernmost area in Lake Okeechobee. Further research on why this happens is needed and, once again, the possibility to model open boundaries can help, due to the large number of theoretical solutions available for tidal-forced circulation. It should also be noted that, although extreme care was put into writing the computer code, and extensive debugging followed, it should be kept in mind that, as in all new computer codes, it is still possible that errors might remain in the code.

To conclude, the objective of showing the possibilities offered by the joint usage of some of the latest developments in different numerical methods was met. The time limitations implicit in a master's program did not allow for full exploration of some of the features of the model and, therefore, considerable improvements should still be possible. The fact that these first results look promising suggests that further development of the model is advisable.

BIBLIOGRAPHY

- Baptista, A. E. M., "Accurate Numerical Modeling of Advection-Dominated Transport of Passive Scalars - A Contribution," Laboratório Nacional de Engenharia Civil, Lisboa, 1986
- Benqué, J. P., J. A. Cunge, J. Feuillet, A. Hauguel and F. M. Holly, "New Method for Tidal Current Computation," Journal of the Waterway, Port, Coastal and Ocean Division, 108, 1982, pp. 396-417
- Hauguel, A., "Quelques Mots sur la Méthode d'Eclatement d'Opérateur avec Coordination," Report HE042/79.39, Electricité de France, Chatou, 1979
- Leendertse, J. J., "Aspects of a Computational Model for Long Water Wave Propagation," Rept. RH-5299-RR, Rand Corp., 1967
- Liu, Y., "Two-Dimensional Finite Difference Moving Boundary Numerical Model," Master's Thesis, University of Florida, 1988
- ✓ Rosenfeld, M., D. Kwak and M. Vinokur, "A Solution Method for the Unsteady and Incompressible Navier-Stokes Equations in Generalized Coordinate Systems," AIAA 26th Aerospace Sciences Meeting, 1988
- Sheng, Y. P., "On Modeling Three-Dimensional Estuarine and Marine Hydrodynamics," in Three-Dimensional Models of Marine and Estuarine Hydrodynamics, (J. C. G. Nihoul and B. M. Jamart, eds.), Elsevier, Amsterdam, Oxford, New York, Tokyo, 1987, pp. 35-54
- Sheng, Y. P., "Currents and Contaminant Dispersion in the Nearshore Region and Modification by a Jetpost," in Journal of Great Lakes Research, 2, 1976, pp. 402-414
- Sheng, Y. P., "Numerical Modeling of Coastal and Estuarine Processes Using Boundary-Fitted Grids," in River Sedimentation, vol. III, ed. Wang, Shen, Ding, 1986, pp. 1416-1442
- Sheng, Y. P., "Modeling Wind-Induced Mixing and Transport in Estuaries and Lakes," in Estuarine Water Quality Management, ed. W. Michaelis, Springer-Verlag, Berlin, Heidelberg, New York, Tokyo (in the press)
- Sheng, Y. P. and H. L. Butler, "Modeling Coastal Currents and Sediment Transport," in Proc. from the 18th Coastal Engineering Conference, American Society of Civil Engineers, 1982, pp. 1127-1148

- Sheng, Y. P., T. S. Wu and P. F. Wang, "Coastal and Estuarine Hydrodynamic Modeling in Curvilinear Grids," in Proc. from the 21st Coastal Engineering Conference, American Society of Civil Engineers, 1988, pp. 2655-2665
- Spaulding, M. L., "A Vertically Averaged Circulation Model Using Boundary-Fitted Coordinates," in Journal of Physical Oceanography, 14, 1984, pp. 973-982
- Thompson, J. F., Z. U. A. Warsi and C. Wayne Mastin, "Numerical Grid Generation - Foundations and Applications," Elsevier, 1985
- × Vinokur, M., "An Analysis of Finite-Difference and Finite-Volume Formulations of Conservation Laws," Contract Report 177416, NASA, Moffett Field, 1986
- Yanenko, N. N., "The Method of Fractional Steps," Springer-Verlag, New York, Heidelberg, Berlin, 1971

BIOGRAPHICAL SKETCH

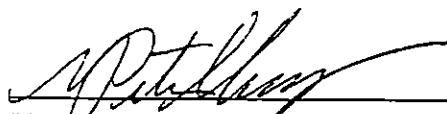
Joaquim José Areias Capitão was born in Coimbra, Portugal, on the 21st of May, 1959.

He got a *Licenciatura* degree in civil engineering (hydraulics) from Universidade Técnica de Lisboa, in December 1982.

He has been working at Laboratório Nacional de Engenharia Civil (LNEC), a government research center in civil engineering in Lisbon, Portugal, since March 1982. He was a trainee at the estuaries division of the hydraulics department from March 1982 to May 1986, a trainee research assistant from May 1986 to June 1987 and a research assistant since June 1987.

After being selected for a Fulbright grant early in 1987, he was admitted to the graduate school of University of Florida, where he has been working for a Master of Science degree at the Coastal and Oceanographic Engineering Department since August 1987.

I certify that I have read this study and that in my opinion it conforms to acceptable standards of scholarly presentation and is fully adequate, in scope and quality, as a thesis for the degree of Master of Science.



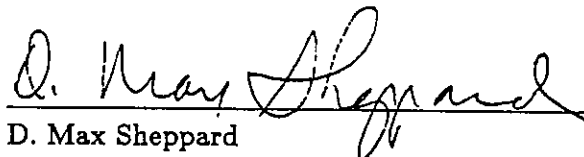
Y. Peter Sheng, Chairman
Professor of Coastal and Oceanographic
Engineering

I certify that I have read this study and that in my opinion it conforms to acceptable standards of scholarly presentation and is fully adequate, in scope and quality, as a thesis for the degree of Master of Science.



Robert G. Dean
Graduate Research Professor of Coastal
and Oceanographic Engineering

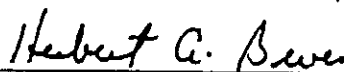
I certify that I have read this study and that in my opinion it conforms to acceptable standards of scholarly presentation and is fully adequate, in scope and quality, as a thesis for the degree of Master of Science.



D. Max Sheppard
Professor of Coastal and Oceanographic
Engineering

This thesis was submitted to the Graduate Faculty of the College of Engineering and to the Graduate School and was accepted as partial fulfillment of the requirements for the degree of Master of Science.

December 1989



for Winfred M. Phillips
Dean, College of Engineering



Madelyn M. Lockhart
Dean, Graduate School